NANYANG TECHNOLOGICAL UNIVERSITY
SINGAPORE

MOLECULAR MODELLING TO INVESTIGATE BIOMASS PYROLYSIS CHEMISTRY

SPANDAN GAUTAM

SCHOOL OF CHEMICAL AND BIOMEDICAL ENGINEERING (SCBE)

2018

MOLECULAR MODELLING TO INVESTIGATE BIOMASS PYROLYSIS CHEMISTRY

SPANDAN GAUTAM

SCHOOL OF CHEMICAL AND BIOMEDICAL ENGINEERING (SCBE)

A thesis submitted to the Nanyang Technological University in partial fulfilment of the requirements for the degree of Master of Engineering (MEng)

2018

ACKNOWLEDGEMENTS

I wish to express my sincere gratitude to my supervisor Prof Samir Hemant Mushrif, for his constant guidance throughout my research. Prof. Samir's enthusiasm, vision, encouragement, and faith motivated me to give my best effort in research and my graduate life. I would also sincerely thank Dr. Jyotsna Arora, Mr. Kartavya Bhola and Dr. Arghya Banerjee who played a crucial role in the shaping of my skills and this research project. It was their timely interventions and advice which gave me a head-on start to my work.

I would also like to thank School of Chemical and Biomedical Engineering, Nanyang Technological University and Ministry of Education, Singapore for giving me an opportunity to pursue my master's by research degree.

I also express my gratitude to other members of Prof. Samir's Research Group, Dr. Jithin John Varghese, Dr. Trinh Quang Thang, Dr. Khursheed Ansari, Mr Ojus Mohan and Dr. Sukriti Gupta for the valuable discussions and inputs regarding my work.

Finally, I would like to thank my parents, family members and friends for their wholehearted support and encouragement throughout my complete journey in SCBE, NTU

Spandan

TABLE OF CONTENTS

TABLE AND FIGURE CAPTIONS

Table

Figure

Appendix

ABSTRACT

Depletion of non-renewable sources has led to efforts in the development of technologies to utilize lignocellulosic biomass as a potential feedstock. One of the promising techniques to convert biomass to fuels is fast pyrolysis. Cellulose, a major component of biomass, is made of the β-D glucose rings attached by a β-1,4 glyosidic bond (C-O-C). Cleavage of the glycosidic bond is the first and an important reaction step in the decomposition of cellulose during fast pyrolysis. Experimental studies have shown that cellulose fragmentation undergoes two distinct cleavages - high activation barrier, possibly associated mid/intra-chain cleavage and low activation barrier, possibly associated end-chain scission. However, fundamental understanding and mechanistic insights into the two distinct kinetic regimes is completely lacking. Hence, in this study, the mechanistic and kinetic differences in mid and end-chain glycosidic bond cleavages in a condensed phase environment using periodic boundary conditions is investigated by mimicking the condensed environment observed experimentally during cellulose fragmentation. The activation barriers for different end and mid-chain scission mechanisms were calculated using cellotetraose as model compound and are also compared with those for cellulose and cellobioise. The end-chain scission enthalpic activation barriers are calculatedwere found to be lower than the mid-chain scission barriers by ~18.7 kcal mol^{-1}, ~6.5 kcal mol^{-1} and ~5.1 kcal mol^{-1} for transglycosylation, glycosylation and ring contraction mechanisms for cellotetraose, respectively. This is in excellent agreement with the reported experimental studies showing different kinetic parameters regimes for different scission mechanisms. The

difference between the end and mid chain scissions was attributed to the inter and intra molecular interactions that govern the relative stabilisation of the transition state. These interactions were interpreted using Reduced Density Gradient (RDG) plots. Energy decomposition analysis shows that the intermolecular interaction stabilizes end-chain scission, while mid-chain cleavage transition state is stabilized by intramolecular interactions. The magnitude of intermolecular interactions for end-chain cleavage was observed to be higher than intra-molecular interactions of mid-chain cleavage, leading to a more stable end-chain fragmentation transition state and lower C-O-C bond scission barriers. This observation was consistent when compared with cellobiose and cellulose glycosidic bond breaking. To the best of our knowledge, this is the first study providing mechanistic insights into end and mid-chain glycosidic bond cleavage and the need to incorporate intermolecular interactions while simulating pyrolysis reaction mechanisms using DFT.

1. INTRODUCTION

Fossil fuel depletion and impact of greenhouse gas on environment are pushing the development of alternate technologies for energy generation. Biomass can be used as one of the renewable energy sources and has huge potential to contribute towards increasing global energy needs. It is the only alternative resource which can be converted into fuel, electricity, and value-added chemicals.

1.1 Biomass and its composition

Biomass is a solid fuel consisting of carbon, oxygen and hydrogen. Lignocellulosic biomass is an alternate source of carbon. Both, herbaceous and woody biomass can be classified as lignocellulosic biomass. The physical structure and chemical composition of biomass is highly irregular. consists of carbohydrate polymers like cellulose (35 – 50%), hemicelluloses (20 – 35%), and aromatic polymers i.e. lignin (15 – 30%). It also comprises of small percentage of other compounds such as proteins and minerals (5 – 10%).[1] These polymers can coexist in varied relative composition with each other in a hetro-matrix to different degrees.

Cellulose is the most abundant organic polymer on earth, it is made up of a linear chain of glucose monomers linked by β 1,4 glycosidic bonds. The chemical structure of cellulose is shown in Figure 1.1. Degree of polymerization (DP) is one of the most important structural properties of cellulose, which can range from 100s to 10,000 in real biomass.[2]

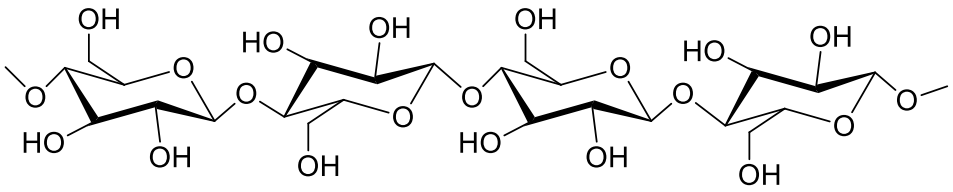

Figure 1.1 Structure of Cellulose

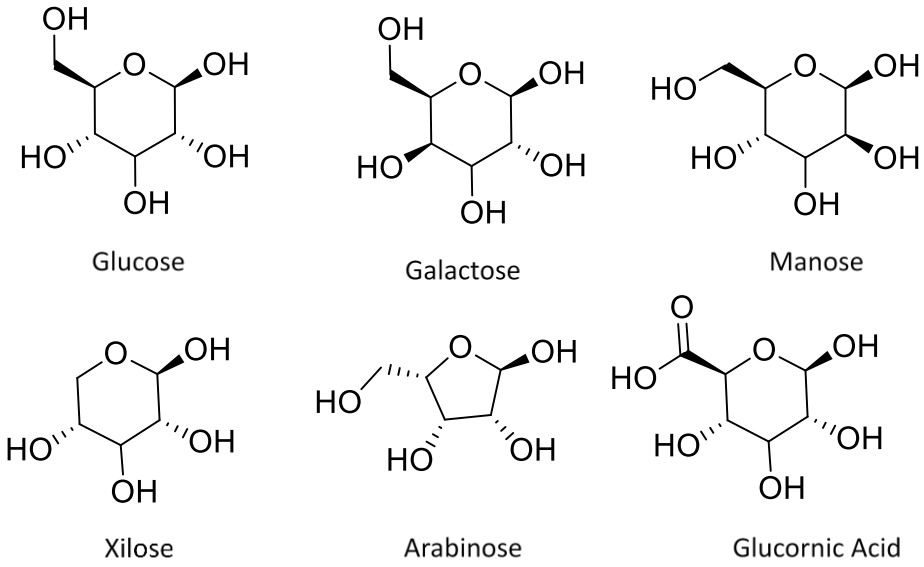

Figure 1.2 Major components of Hemicellulose

Second major constituent of biomass is hemicellulose, which is a group of complex carbohydrates consisting of different sugar units (D-xylose, L-arabinose, D-mannose, 4-O-methy-l-glucuronic, D-galactose, D-galacturonic, D-glucose and D-glucuronic acids), arranged in different proportions and with different substituents. The chemical structures of these monomer constituents are shown in Figure 1.2 Unlike cellulose, hemicellulose mainly consists of pentose sugars and has a lower DP (50-300). The source of hemicellulose can strongly influence the relative composition of sugars. For example, the relative amounts of xylan and glucomannans completely switch between hard and soft wood derived hemicelluloses. Hardwood hemicelluloses are rich in xylan (and contain

small amounts of glucomannan), whereas softwood hemicelluloses are rich in galactoglucomannan (and small amount of xylan).[2] The third major component of lignocellulosic biomass is lignin in which phenyl propane monomers are linked by an ether bond (monomers of lignin, are shown in Figure 1.3). Lignin is water insoluble and optically inactive.

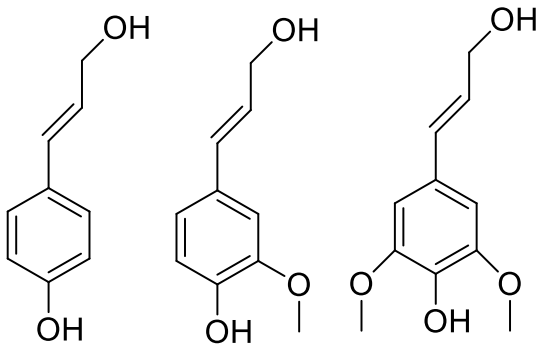

Figure 1.3 Monomers of Lignin

1.2 Biomass conversion technologies

Biomass can be converted into different useful products using biochemical and thermochemical pathways. Biochemical conversion comprises of technologies such as anaerobic digestion and fermentation. In biochemical conversion processes biomass is broken down into small molecules by bacteria. This conversion process is less energy intensive but has a large conversion time when compared with other thermochemical processes.[3]

In thermochemical conversion processes biomass is subjected to external heat at high temperatures, it is decomposed into a mixture of compounds of lower

molecular weight. The three-major biomass thermochemical conversion processes are combustion, gasification, and pyrolysis.

- Combustion is the thermal decomposition of biomass in the presence of oxygen at very high temperatures of 1000-1400^0 C. Major products constitute hydrogen (H_2), carbon dioxide (CO_2). Heat is also generated during combustion.[4]
- Gasification is the thermal decomposition of biomass at high temperatures of 400-900^{0}C with controlled oxygen supply. Syn gas, a mixture of carbon monoxide (CO), hydrogen (H_2), carbon dioxide (CO_2) and light hydrocarbons is the major product of the gasification process.[5]
- Pyrolysis is the thermochemical decomposition in complete absence of oxygen at temperatures range of 300-900^{0}C. Products of pyrolysis are fuel gas, bio-oil, and bio-char.[6-7]

It has been shown that the profitability of a bio-fuels based power plants can increase by 30% due to transportation costs alone. Hence, it is important to combine the handling and transportation of biomass and its processing, unlike petroleum fuels, where the crude is transported from multiple distant locations to a central processing facility. Pyrolysis, on that front, is the only biomass processing technology which offers this unique advantage of setting up processing plants at multiple geographic locations to convert biomass to bio–oil, which later can be stored/transported for the end use or for the upgradation in a to value added chemicals and fuels. [8-10] Additionally, an economical comparison of multiple biomass conversion processes like pyrolysis, gasification and biochemical conversion, has shown that pyrolysis has the lowest operating and capital cost.[11] The bio-oil is a mixture of compounds having varied calorific

which can be potentially stored and transported. It can be further upgraded to value added chemical and transportation fuels. Based on the operating conditions pyrolysis can be classified as shown in Table 1.1.[12]

Table 1.1 Classification of different pyrolysis according to major products and operating temperature conditions

Pyrolysis	**Flash**	**Fast**	**Slow**
Temperature	Over 950^0 C	Around 500^0 C	Less than 300^0 C
Major product	Gas	Liquid	Char

1.3 Fast pyrolysis

Fast pyrolysis a thermal decomposition of biomass carried out at high heat transfer rate, producing bio-oil as its major product. Whereas, slow pyrolysis is carried out at lower temperatures, around 450^0 C and the major product obtained is char.[13] Fast pyrolysis is a promising approach for production of renewable fuels and value-added chemicals from lignocellulosic biomass. Fast pyrolysis of biomass produces higher percentages of vapours and aerosols which are condensed to give dark brown liquid called bio-oil. The calorific value of this bio-oil is higher than that of conventional fuel oil.[12] The bio-oil produced can be potentially transported and used as fuels making fast pyrolysis a promising technology, The underlying principles of fast pyrolysis and the reactor configurations have been studied by various authors.[14] Biomass must be dried to less than 10% moisture and grinded to a particle size of less than 3 mm. Biomass particles are fed to the reactor to decompose into vapours and char. Cyclone

separators are used to separate char. Vapours are condensed to bio-oil. The sequence of steps in fast pyrolysis process are shown in Figure 1.4.

The criteria for fast pyrolysis to produce maximum bio-oil are

- Controlled reaction temperatures around 400-500°C
- Short vapor residence time (preferably in milliseconds)
- Inert atmosphere
- Rapid cooling of volatiles

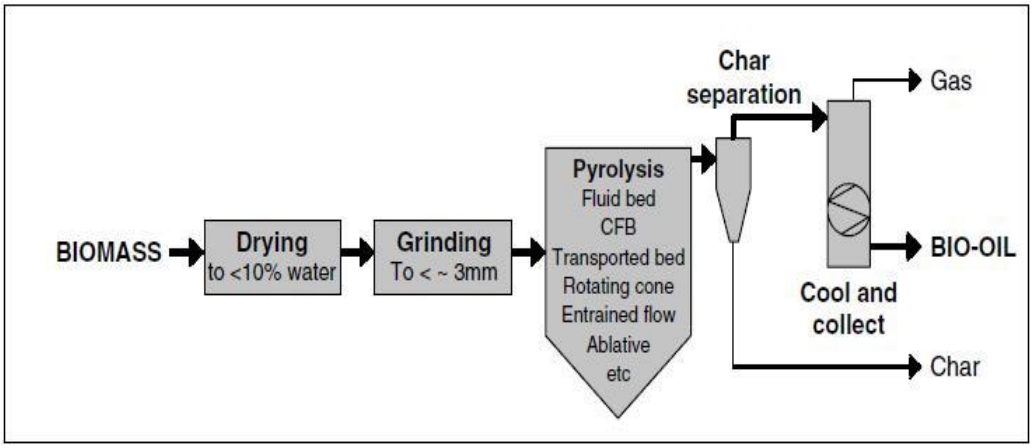

Figure 1.4 Schematic of Fast Pyrolysis process from Biomass to Bio-oil

Bio-oil is a complex mixture of many compounds which can be classified into four main categories namely, an-hydro-sugars, furan and pyran ring derivatives, light oxygenates, phenolic family of compounds and permanent gases. These compounds are oxygen rich and hence need to be catalytically upgraded to be used as fuels. Cellulose being a major component of biomass have been extensively used to study fast biomass pyrolysis process. Experimental studies have shown that cellulose pyrolysis produces levoglucosan (LGA) as a major product along with furans and other low molecular weight compounds like glycolaldehyde, formaldehyde and formic acid.[6] Increasing yields of permanent

gases such as CO, CH_4 and H_2 are linked to decreasing yields of bio-oil components like LGA, glycolaldehyde and furfural.

The quality and quantity of bio-oil is not only dependent on the type of feedstock but also varies significantly with operating conditions and reactor design. Operating temperature, residence times, cooling rates and particle size greatly affect the product distribution (percentage of bio-oil and the char to bio-oil ratio). Since bio-oil is a direct product of reactions that happen in the condensed particle phase, its quality and quantity are governed by those reactions. However, reaction chemistry, kinetics and transport effects are inter-related, and they are significantly affected/altered by operating conditions of the reactor and by the reactor design. Despite of numerous studies in the field of pyrolysis, understanding of condensed phase pyrolysis reactions remains limited. Most of the research reports, hypothesize molecular reaction schemes, which are either based on the reaction mechanism knowledge in the aqueous phase biomass processing technology or based on the experimentally observed effect of operating conditions on the macroscopic product distribution. Though existing pyrolysis technology is considered economical, its commercialisation largely depends on the optimisation and process designing. Developing a foundation of process designing and operating conditions, in turn requires developing of kinetic models and detailed understanding of the underlying chemistry and its associated kinetic parameters. Determining the primary and secondary reaction pathways in pyrolysis remains a challenge for experimental and theoretical researchers.

1.4 Kinetics Models

Kilzer and Broido proposed a pathway for cellulose pyrolysis based on the data obtained by thermo-gravimetric analysis (TGA) and mass spectrometric thermal analysis (MTA), which is shown in Fig 1.5 a. They interpreted that pyrolysis of cellulose includes three distinct steps knowns as dehydration, depolymerization and decomposition steps.[15] Another popular model proposed by Broido-Shafizadeh is shown in Fig 1.5b. It is also based on an irreversible process, forming an intermediate product which is converted to either condensable volatiles (bio-oil) or chars and gases. The subsequent conversion of char to other product is no longer considered in this reaction model. Further selectively choosing between the increased yield of char and gases is not possible from this model, neither we can vary the ratios of char to volatile gas production. This model would also serve inappropriate at high temperatures, where volatiles could be converted to char and gases.[16]

There are several other lumped models in the literature for cellulose pyrolysis. One such model is shown in Figure 1.5c in which active cellulose is disintegrated into condensable products and LGA.[17] Some kinetic models have predicted glucose as intermediate for the formation of pyrolysis products. However, glucose has shown to follow an entirely different reaction mechanism pathway when compared to cellulose.[18]

These lumped kinetic models have failed to predict product specifications and are unable to selectively form individual products, they are also unable to decide on the composition of the bio-oil. These models lack the influence of transport conditions on product distribution and their prediction capability is very limited.

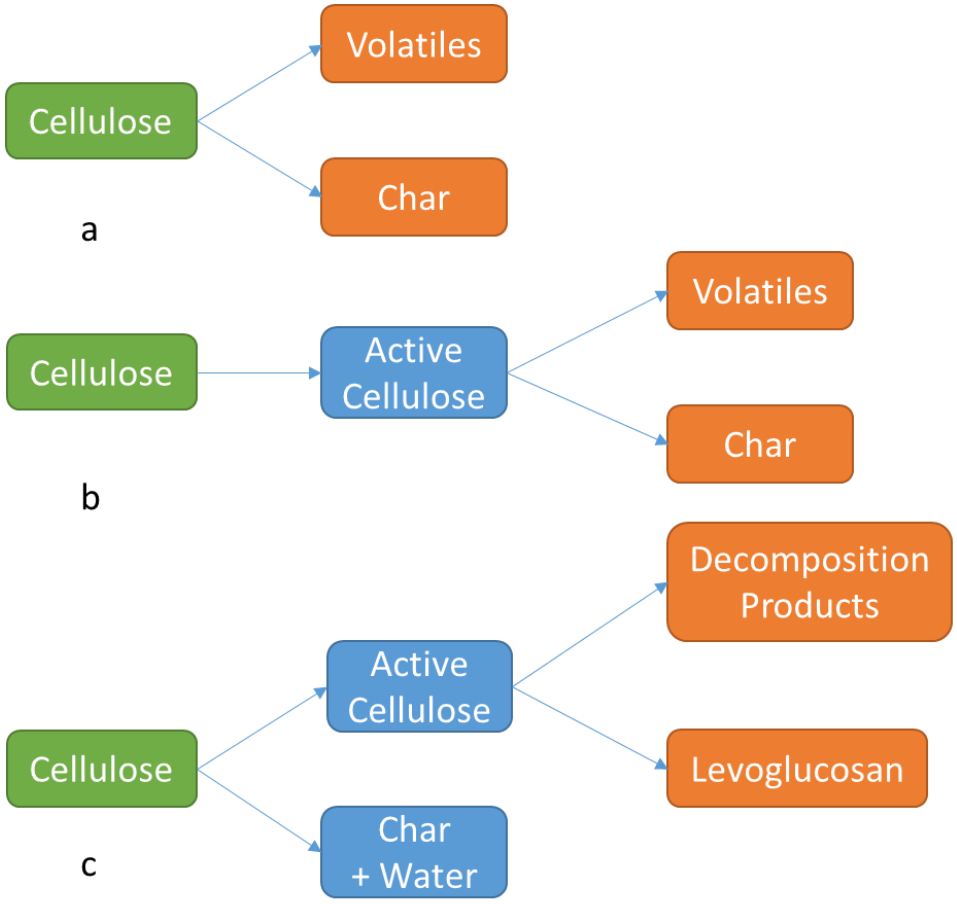

Figure 1.5 Proposed kinetic models of cellulose pyrolysis proposed in literature.

We require a reaction-transport model containing detailed information of reaction kinetics, heat and mass transfer which will allow engineers to optimally design and operate pyrolysis reactors from first principles, instead of relying on the conventional trial and error approach. We need to a model which can correctly predict the decomposition of the feed particle into all the volatile products and char. The model should include all the reaction chemistry details and transport effects based on experimental operating conditions and feed properties These lumped kinetic models are unable to predict the product specification and therefore act as a limitation in usefulness as tools for process and reactor design.

Understanding the pyrolysis condensed phase chemistry is an important step towards the commercialisation of the process. It is the chemistry of the pyrolysis

which determines the bio-oil quality and economy of the process. Hence, to build a detailed micro-kinetic model providing mechanistic insights, it is required to understand each elementary step and the associated kinetic parameters.[19]

Isolated experimental investigation into pyrolysis reactions and kinetics is extremely difficult due to several factors such as fast reactions (milliseconds), short residence times, high temperatures and transport limitations. Hence, purely experimental studies cannot be extensively used to study the reaction pathways and develop these kinetic models, a combined experimental and theoretical studies can be implemented to investigate the process and designing parameters. We can apply quantum mechanical based multiscale modelling methodology to discover multiple reaction pathways for the formation of experimentally identified primary and secondary products during pyrolysis. This will help us to compute the energetics and kinetics associated with these pathways. The coming sections talk about the recent discoveries experimental studies as well as computational studies for cellulose pyrolysis.

1.5 Recent discoveries in Experimental studies of cellulose pyrolysis

Mettler et. al. developed a novel thin film pyrolysis experiment to nullify the transport effects present. The research showed that glucose and cellulose generate very different product distribution on pyrolysis. Therefore, glucose cannot be considered as a surrogate of cellulose to study cellulose pyrolysis. α-cyclodextrin was for the first time proposed as a surrogate molecule of cellulose.

For past few decades, two alternative global mechanisms of cellulose chemistry have been debated, in the first mechanism crystalline cellulose undergoes intra/mid-chain cleavage to form oligomers, which further disintegrate to form monomeric products. In the second pathway, cellulose can directly undergo end-chain cleavage to from monomeric products. These two-different cellulosic decompositions have been shown in Figure 1.6.

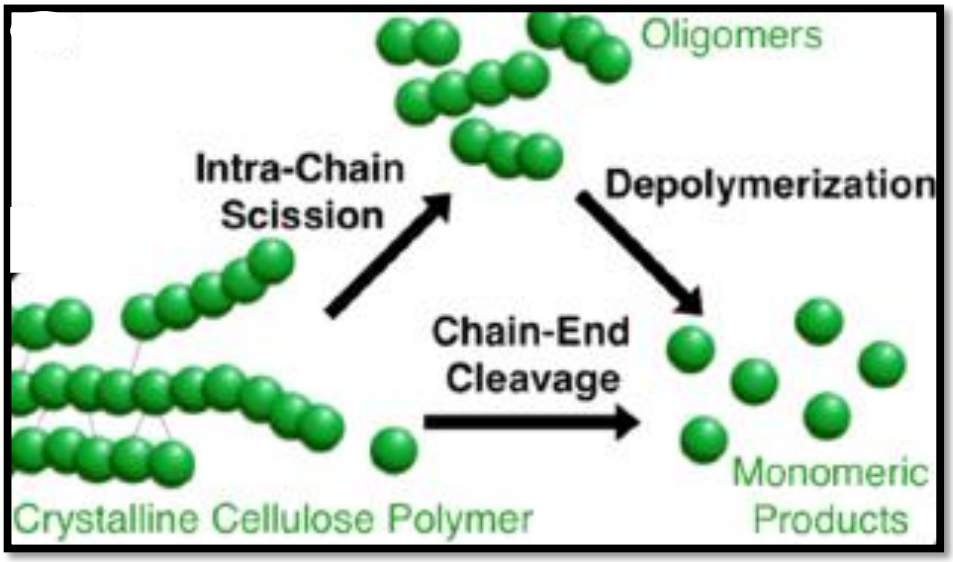

Figure 1.6 Direct and In-direct pathways of Cellulose decomposition (Intra/Mid-Chain and End-chain scission of glycosidic bond

(Krumm, C. *et al*. *Chemistry of Materials* 2016)

Recent experimental studies propose two different mechanism for cellulose decomposition, in the first mechanism cellulose converts into an un-identified reaction intermediate before forming volatiles. In the second model a single step conversion to volatiles is observed, it has been observed that cellulose melts between 450°C to 500°C to form an intermediate called liquid (active) cellulose. Photography of a cellulose film at 550°C forming liquid intermediate before vapouring has been shown in Figure 1.7. For temperatures below 450°C, cellulose is observed to decompose without undergoing melting. To understand

this different pathway of cellulose pyrolysis, a direct and indirect mechanism involving chain end and mid-chain cleavages respectively have been proposed.

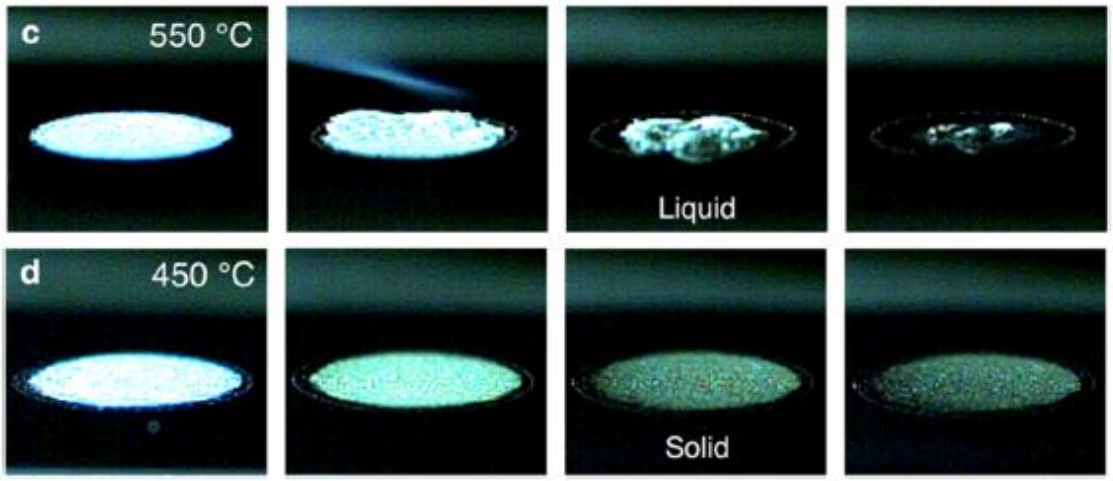

Figure 1.7 Cellulose film forming liquid intermediate at 550°C (c) whereas it reacts without melting at 450°C (d)

(Krumm, C. *et al*. *Chemistry of Materials* 2016)

There has always been a lack of experimental methodology to identify hundreds of volatile compounds which evolves concurrently within timescale of few milliseconds, this was one of the biggest challenges to confirm the two pathways of cellulose pyrolysis. To address these challenges, Krumm et. al developed a reactor known as Pulse Heated Analysis of Solid Reactions (PHASR). This reactor system can heat and cool reaction samples on milliseconds time scale bases. It was proposed by them that at low temperatures, initiation by glycosidic bond cleavage is slow and the formation of products predominantly follow the end chain mechanism. In contrast, at higher temperatures cellulose undergo rapid intra/mid-chain scission and small species are formed.

Experiments were performed using thin film of cellulose to avoid heat and mass transfer artefacts. Sample thickness of various sizes were taken, and it was observed that measured rates decreased monotonically at larger thickness, indicative that the transport effects (heat and mass transfer) can no longer be

ignored. As depicted in Figure 1.8, rate of cyclodextrin consumption and furans formation was observed, furan formation (which contribute to around 7-8% product distribution) follows first order kinetics at 500°C; the furans formation rate from cyclodextrin consumption (slope in Figure 1.8C) decreases until active sites in surrogate is fully consumed. However, formation rate of furan at 450 °C follows apparent zero order kinetics; the rate of formation of furan(s) was found to be independent of the conversion of cellulose conversion (slope Figure 1.8E). The transition in kinetics between 450 and 500 °C is correlated to simple glycosidic bond cellulose fragmentation mechanisms A constant formation rate of furan rate is analogous with a fixed supply of active sites in cellulose; this is depicted in Figure 1.8E, for end-chain depolymerization a constant supply of sites for chain ends cleavage is available for reaction as individual products are formed. On the other part, as the reaction progress beyond reactive melting point of 467 °C, an observed reduction in the furans formation rate (Figure 1.8C) with time is unvarying with the fast consumption of the cellulose active sites for reaction. The mid-chain or "random" scission breaks the plentiful intermonomer glycosidic bonds in cellulose.

The mechanisms of mid-chain versus end-chain cleavage were confirmed by measuring the differential formation rate of furan products by varying chain length of cellulose chains also β-(1,4)-cellodextrin reactants (Figure 1.8 D,F). At higher temperatures of 550 °C, all cellodextrins exhibit the same rate of formation of the product (furan) per unit mass and is independent of chain size; cellulose shows similar formation rate of furan and is only two times slower despite of cellulose being longer than cellodextrins by a magnitude of two orders.

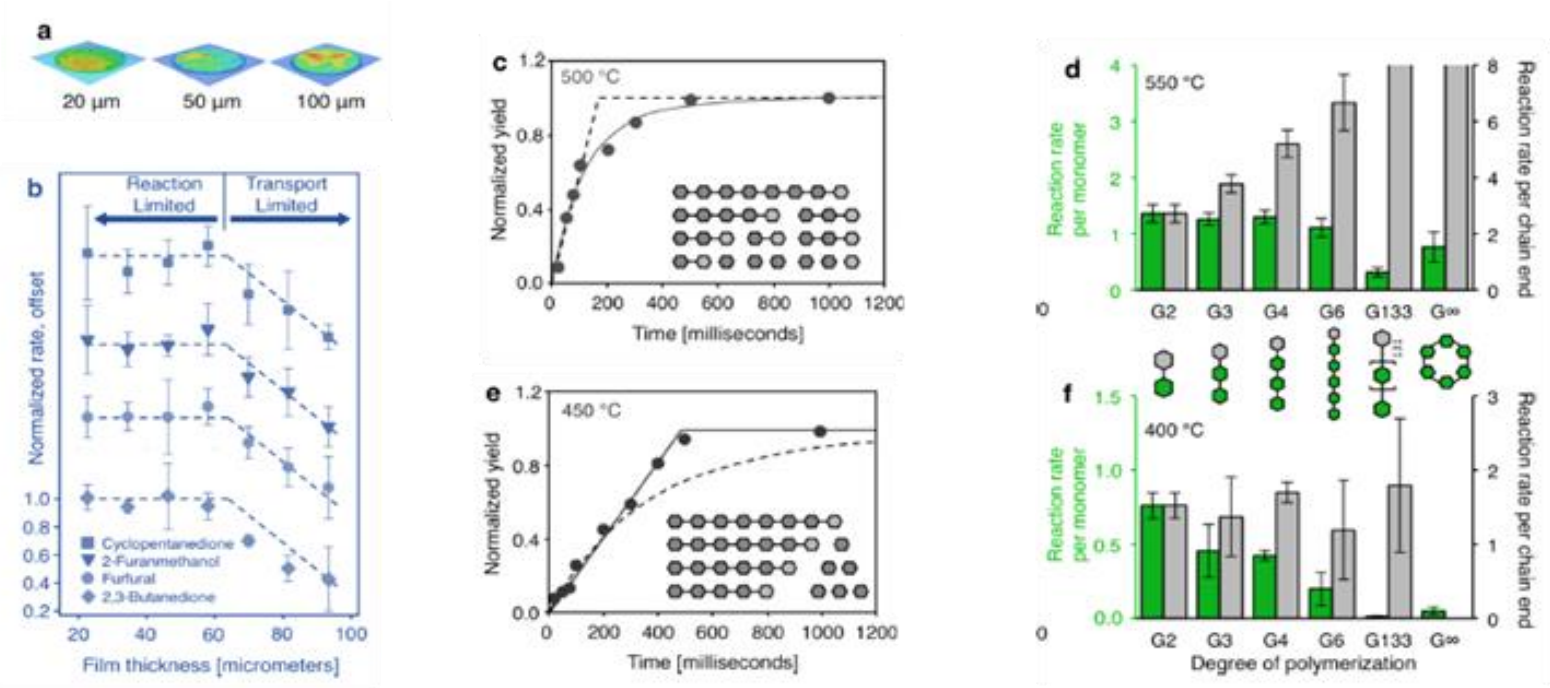

Figure 1.8 PHASR kinetics: end-chain and intrachain fragmentation mechanisms of cellulose. (A) Variable cellulose film thickness characterized by optical profilometry. (B) Differential kinetics of product formation from cellulose at 500 °C for variable film thickness. (C) Time-resolved, normalized yield of eight furan products shows apparent first-order kinetics at high temperature with first-order (solid line) and zero-order (dashed line) kinetic models. (D) Differential furans product formation rate per monomer (green bars) or per chain end (gray bars) from cellodextrins (G2−G6), cellulose (G133), and α-cyclodextrin indicates the midchain scission mechanism dominates at 550 °C. Reaction rates per chain end are defined as (mol furans)/(mol reactant × s) and reaction rates per mol monomer are defined as (mol furans)/(mol. glucan monomer in reactant × s). (E) Time-resolved, normalized yield of eight furan products exhibits apparent zero-order kinetics at low temperature with zero-order (solid line) and first-order (dashed line) kinetic models. (F) Differential furan product formation rate per monomer (green bars) or per chain end (gray bars) from cellodextrins (G2-G6), cellulose, and α-cyclodextrin indicates the chain-end mechanism dominates at 400 °C.

(Krumm, C. *et al*. *Chemistry of Materials* 2016)

However, at 400 °C, the rate of furan formation was found to be same for all cellodextrins only when it is normalized by the concentration of active polymer sites, confirming that the product formation occurs only as an end-chain scission in cellulose.[20] Cheng et. al. calculated the kinetic parameters for glycosidic bond fragmentation by measuring the time resolved conversion of cyclodextrin. It was shown for the first time that there exist two different kinetic regimes corresponding to two different reaction mechanisms (Figure 1.9).

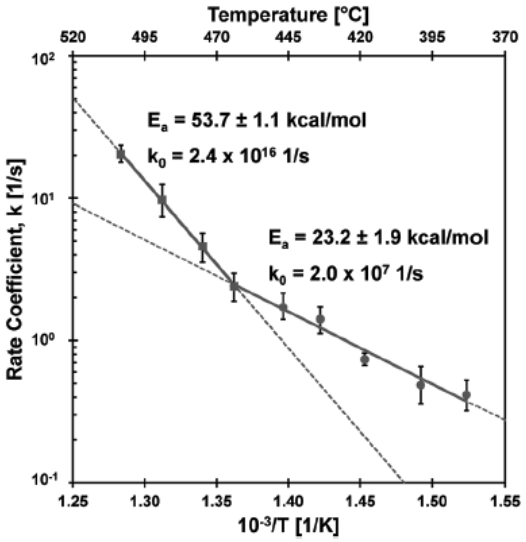

Figure 1.9 Kinetics of glycosidic bond cleavage. The conversion of reactant exhibits a distinct change in kinetic regimes at 467 °C, indicative of a change in the mechanism of glycosidic bond cleavage

(Zhu, C. *et al.* . *Reaction Chemistry & Engineering* 2017)

A slow mechanism occurs at temperatures below reactive melting point (T = 467°C) and corresponds to the lower activation energy (23.2 kcal/mol). However, at higher temperature a high activation barrier mechanism (53.7 kcal/mol) dominates the slow mechanism. The temperature of 467°C is known as the reactive melting temperatures across which transition of kinetic regimes takes place.[21]

1.6 Discoveries in DFT studies of Cellulose pyrolysis

Cleavage of the glycosidic bond is found to be key step in the cellulose depolymerisation reaction. Researchers have applied the quantum mechanical based multiscale modelling methodology to discover reaction pathways associated with cleavage of glycosidic bond for the formation of experimentally identified primary and secondary products, during pyrolysis. They have computed the energetics and kinetics associated with these pathways.[18-19, 22-25] Simulating cellulose molecule is a concern because of its highly complex structure and very high degree of polymerization, therefore dimer and trimer model compounds such as glucose, methyl-cellobiose, cellobiose, cellotetraose, cellohexaose and cyclodextrin have been used to investigate the glycosidic bond breaking reaction pathways of pyrolysis for cellulose. Levoglucosan is one of the major product obtained by cellulose pyrolysis. Several mechanisms have been proposed in literature for formation of levoglucosan from cellubiose which are heterolytic, homolytic, free radical, ionic, and concerted mechanism.[19, 24] Broadbelt et. al. used methyl-cellobiose as a model surrogate for cellulose and investigated multiple formation pathways of levoglucosan incorporating radical formation, ion formation and concerted reaction way. A methyl group was added on the non-reducing end of the chain to emulate the effect of the rest of cellulose chain. Their density functional theory calculations suggested that kinetics favours the concerted glycosidic cellulose fragmentation mechanism over the conventional reported radical or ionic mechanisms.[19]

Mettler et. al. identified α-cyclodextrin as a surrogate molecule of cellulose and his first principles molecular dynamics simulations showed that glycosidic bond cleavage occurs via homolytic cleavage, giving furan as its major product without

formation of glucose as its intermediates.[18] It was also highlighted for the first time that cellulose glycosidic bond breaking chemistry does not involve formation of glucose as an intermediate.

Agarwal. et. al. in their molecular dynamics calculations to mimic solid cellulose used a simulation cell which comprised of two-unit of cellulose β chain, having periodic boundary conditions repeated in three dimensions. Car Parrinello Molecular Dynamics (CPMD) - metadynamics simulations were implemented by varying sets of collective variables to model cellulose depolymerisation pathways. They observed that, at lower temperatures of 327 °C, cellulose fragmentation reaction occurred dominantly via ring contraction mechanism forming a precursor to furan compounds known as gluco-furanose ring. They also highlighted this step as an important key process for formation of liquid step intermediate. At 600 °C, formation of precursor to LGA was observed to be the most kinetically favoured step.[23] Zhang et. al. also investigated the reaction mechanism and kinetics of LGA and formaldehyde formation from pyrolysis of cellulose. The work highlights that LGA is a major primary product obtained from cellulose pyrolysis, it is either formed as an intermediate which further break into furans/ pyrans or is present as a final product. Three mechanisms namely free-radical, glucose intermediate mechanism and end-scission mechanism have been studied for the formation of LGA. The formation mechanism of active LGA and formaldehyde was also investigated using the density functional theory (DFT) methodology.[26] Zhang. Y. et. al. in his work investigated ten chemical reaction pathways of glycosidic bond breaking using cellobiose model compound, providing the reaction barrier of all the pathways proposed.[22] Takashi H., et al computed the reaction barrier for LGA formation

considering the hydrogen bonding network. They were first to highlight the importance of incorporating the inter-molecular hydrogen bonding in DFT calculation. They obtained activation barriers comparable to that of the experimental value.[27]

Majority of these computational simulations were done using glucose or cellobiose as its model compounds in a non-periodic environment. These calculations have failed to predict the condensed phase chemistry as observed experimentally. Moreover, the use of single glucose and cellobiose molecule has failed to mimic the complex nature of cellulosic structure with intensive inter and intramolecular interaction. In addition, cellobiose with only one glycosidic bond cannot be used to study both the end and mid-chain scissions. The experimentally reported value of 23.2 KJ/mol corresponding to low temperature cellulose decomposition have also not been computationally obtained using these surrogates. Therefore, we hypothesize that it is important to incorporate the inter and intra molecular interactions in our calculations. These interactions are present in the form of covalent and non-covalent (NCI) interactions within the three-dimensional structure. The coming section talks about these interactions in detail.

1.7 Covalent and Non-Covalent interactions

Inter and intra molecular interactions within a three-dimensional molecular structure is controlled by electrostatic, covalent and non-covalent interactions. Covalent bonds are defined by the lewis structure whereas non-covalent interactions (NCI) are present within voids of the bonding and anti-bonding structures.[28] NCI comprises a wide range of bonding and anti-bonding

interactions like vander waals interactions, hydrogen bonding, dipole-dipole interactions, and steric repulsions. They are the inter and intra molecular interactions present within the system because of bond breaking/ formation or the geometry of the system.[28] NCI are largely depend on the geometry of the system in used and are very less affected by the methodology and basis set used in the high performance computational calculations.[29] NCI develops a force field where interactions occurs between the chemical species without sharing of electrons. Covalent interactions on the other hand are electron sharing interactions forming bonds, these interactions are much stronger than the non-covalent interactions.

These interactions play a major role in stabilizing or destabilizing the molecular structures. Therefore, largely affecting the activation barrier of the reaction mechanisms. There are several methodologies defined in literature to understand these covalent, non-covalent and electrostatic interactions. Some of the current methods to identify these interactions are defined in section 2.5 under methodology chapter of the thesis. Section 3.2 of the results and discussions chapter talks about the various interactions observed in our three-dimensional system and its influence on the activation barriers of end-chain and mid-chain glycosidic bond scission.

1.8 Aims and Objectives of the thesis

It is now established that there exist two different regimes of cellulose fragmentation corresponding to end-chain and mid-chain scission. The experimentally reported value of 23.2 KJ/mol corresponding to low temperature cellulose decomposition have also not been computationally obtained using any

cellulose surrogates. Moreover, most of the density functional theory-based calculations investigating activation barriers of glycosidic bond breaking mechanisms have been performed in a non-periodic gas phase environment, contrary to the actual condensed phase. There is also an absence of the mechanistic insights for end and mid-chain scission activation barriers in the literature. It is important to investigate the mechanistic insights of end-chain and mid-chain scission barriers in a condensed phase environment, as observed during the formation of active cellulose intermediate. In accordance with these discussed gaps, the thesis aims to achieve the following: -

1) Compute energetics of glycosidic bond breaking mechanisms (both end-chain and mid chain cleavage) in a condensed phase environment.
2) Providing mechanistic and kinetic differences in mid and end-chain glycosidic bond scissions in a condensed phase system. The activation barrier was calculated using cellotetraose as model compounds.
3) Comparing cellulose fragmentation energetics using different model compounds of biomass namely cellobiose and cellulose as an extension of the study. Cellulose fragmentation is a mid-chain cleavage, on the other hand cellobiose decomposition is both end and mid-chain cleavage due to only one glycosidic bond.

2. METHODOLOGY

This chapter talks about the detailed methodology used in this thesis work. Section 2.1 describes the fundamentals of molecular modelling and its governing equations. It also highlights the two different molecular modelling methods, namely the newton law's-based force field method and schrödinger equation-based quantum methods. Section 2.2 lays the foundation of Density Functional Theory (DFT) and its governing principles. All the simulations performed for this work is based on DFT. Section 2.3 highlights the major approximations used in DFT and its advantages over the other. The section on Computational methodology (Section 2.4) lists in the function, correction factors, crystal structure and box sizes, K-points used for our system in consideration. The last section 2.5 describes the physics of Reduced Density Gradient plots and its rationale behind using as a tool to interpret non-covalent interactions.

2.1 Molecular Modelling

Theoretical methods and computational techniques used to explain the behaviour of molecules and molecular systems are termed as molecular modelling methods. Atomic and molecular level phenomena that are challenging to be explored using experimental methods can be studied theoretically using molecular modelling. There are two different ways of modelling the molecules based on the consideration of fundamental particle.[30] In electronic structure (ESM) or ab initio method, charged components namely nuclei and electrons are the fundamental particles, whereas in force field method or molecular mechanics (MM) the

electrons and nuclei combine as effective atoms constitute the fundamental particles. The calculation of potential energy in ESM and MM is based on the interaction between charged species (nuclei and electron) and parametric function of atomic coordinates respectively. Newton's laws of motions are only valid in the MM approach. In the ESM approach, the positively charged nuclei and the negatively charged electrons are the fundamental particles and the interaction between these charged particles give rise to the potential energy. This method is called electronic structure calculation or *ab initio* method. In Quantum mechanics, energy of a system is calculated using Schrödinger equation, a second order partial differential equation. It is also known as a wave equation which serves as a mathematical model of the movement of waves. It can describe the spatial and temporal evolution of the wave function of a particle in each potential. The time independent Schrödinger equation is given by

$$H\psi = E\psi \qquad (2.1)$$

where H is the Hamiltonian operator, ψ is the wave function and E the energy of the system.

Two prominent approaches in quantum mechanics are wave function approach and electron density approach (Figure 2.1). Wave function approach is an accurate method but is highly computational expensive. Wave function derived from electronic structure theory contains all the information about the system. Every single electron has four coordinates which includes the spin, for larger molecules system the number of electrons (N) increases thereby increasing the coordinates 4N times. Schrödinger equation can exactly be solved for hydrogen atom only. For a many-electron system, approximations are needed to find a solution.

On the other hand in an electron density approach, all ground state properties of the system are determined by electron density. This approach is called Density Functional Theory (DFT) and was proposed by Pierre Hohenberg and Walter Kohn in 1964.[31-32] They proved that all the information of the system is contained in the electron density, a simple function of three coordinates. In DFT, the total ground state energy of a many-electron system is a function of the density. Therefore, if the electron density functional is known we can calculate the total energy of our system.

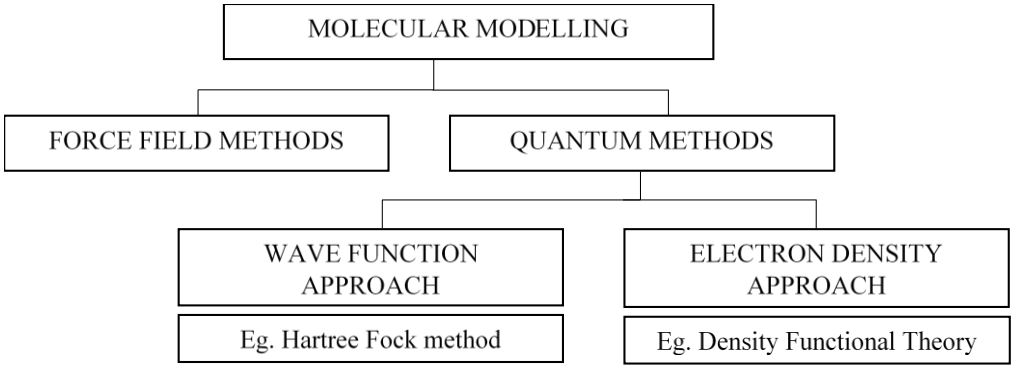

Figure 2.1 Molecular modelling methodologies – Force Field and Quantum methods

2.2 Density Functional Theory (DFT)

It is possible to calculate the ground state density for a given potential through wave function. However, Kohn and Hohenberg showed that an inverse mapping exists between external potential and ground state density. Based on this idea Kohn and Hohenberg proposed two fundamental theorems in DFT. First theorem is a proof for the existence of a relation between wave function and electron density of the system. It states that the ground-state energy obtained from Schrödinger's equation is a unique functional of the electron density.[33]

$$E = E[\rho(r)] \qquad (2.2)$$

where E is the ground state energy and ρ(r) is the electron density.

However, it doesn't convey the exact methodology to get the density. The second theorem shows that the density obeys the variational principle, it states that the electron density that minimizes the energy of the overall functional is the true electron density corresponding to the full solution of the Schrödinger equation.[33]

$$E[\rho(r)] > E[\rho_0(r)] \quad (2.3)$$

The energy functional can be represented as:

$$E[\rho(r)] = T[\rho(r)] + E_{ne}[\rho(r)] + E_{ee}[\rho(r)] + E_{ion}[\rho(r)] + E_{xc}[\rho(r)] \quad (2.4)$$

where $E[\rho(r)]$ is the total energy of the system, $T[\rho(r)]$ is the kinetic energy, $E_{ne}[\rho(r)]$ is the coulomb interaction between electron and nuclei, $E_{ee}[\rho(r)]$ is the coulomb interaction between electrons, $E_{ion}[\rho(r)]$ is the coulomb interaction between pair of nuclei and $E_{xc}[n(r)]$ is the exchange correlation energy.

The electron density can be varied until energy obtained from the functional is minimized. Kohn Sham self-consistent field approach solved the problem of finding trial density and determining energy from trial densities. Kohn Sham proposed a novel approach by taking a fictitious system of non-interacting electrons, where ground state density is the same density as that of a real electron interacting system. In Kohn Sham formulation, the energy is calculated using series of one electron Kohn-sham (KS) equations:

$$\varepsilon_i \emptyset_i(r) = \left[-\frac{\nabla^2}{2} + V_{KS}(r)\right] \emptyset_i(r) \quad (2.5)$$

where the first term on the right of equation 2.5, represents the kinetic energy of the electron, $\emptyset_i(r)$are the KS single-particle orbitals, ε_i are the KS eigenvalues, ρ is the electron density and V_{KS} is defined as

$$V_{KS}(r) = V(r) + V_H(r) + V_{XC}(r) \quad (2.6)$$

$$V_H(r) = e^2 \int \frac{n(r')}{|r - r'|} d^3r' \quad (2.7)$$

$$V_{XC}(r) = \frac{\partial E_{XC}}{\partial n(r)} \quad (2.8)$$

Where $V(r)$ and $V_H(r)$, and $V_{XC}(r)$ are the external potential of electron-nuclei interaction, the of electron-electron coulomb interaction potential (Hartree potential), and exchange-corelation potential respectively. $E_{XC}(r)$ represents the exchange-corelation energy. The only unknown term in the energy functional is the exchange correlation energy. It's the net difference between the energy of the interacting (real) system and the non-interacting (pseudo) system. In other words, the exchange-correlation energy encapsulates the quantum mechanical exchange and correlation effects. It is the correction for unphysical electronic self-interaction columbic energy as well as the difference in kinetic energy between non-interacting system and real system. Therefore, to solve the Kohn - Sham equation, we should specify the exchange correlation energy part as accurately as possible. The existence of exchange correlation functional is guaranteed but unfortunately its true form is not known.[33]

2.3 Exchange-Correlation functional

The selection of appropriate functional, based on the system under consideration, is crucial in DFT calculations for minimizing the errors and computational cost in calculation. Many approximations are available for the exchange-correlation functional. Two commonly employed approximations are local density approximation (LDA) and generalized gradient approximation (GGA).

2.3.1 Local Density Approximation (LDA)

LDA is associated with DFT calculations where the value of energy density at some position r, can be computed exclusively from the value of density at that position i.e. the local value of density. Most of the LDA functionals are derived from the considerations of uniform electron gas. LDA is the uniform electron gas exchange and correlation functional that are employed for molecular calculations. It can be extended to spin-polarized calculations also. The exchange-correlation functional with LDA can be expressed as:

$$E_{xc}[\rho(r)] = \int \rho(r)\varepsilon_{xc}[\rho(r)]dr \qquad (2.9)$$

where ϵ_{xc} is the energy density and $\rho(r)$ is the electron density. Eq. 2.9 shows the functional dependence of exchange-correlation functional on density expressed as an interaction between density and an energy density that is itself dependent on electron density. Energy density, ϵ_{xc} is treated as a sum of individual exchange and correlation contribution. LDA can give incorrect results when the electron density is non-uniform and changes drastically. In such cases the gradient in density should also be taken into taken consideration.

2.3.2 Generalized Gradient Approximation (GGA)

LDA has limitations of the assumption of electron density being uniform, which is not the case in a real scenario. GGA exchange correlational functional goes beyond the absolute value of the density at a spatial point and also includes the change in density at that point. The inclusion of the gradient in the LDA formulation thus provides a better estimate of the exchange-correlation term by including the extent of change in local density. GGA functionals thus depend on both the density and its gradient.[33] Most GGA functionals are constructed with

the correction being a term added to the LDA functional. The exchange-correlation functional with GGA can be expressed as:

$$E_{xc}[\rho(r)] = \int \rho(r)\varepsilon_{xc}[\rho(r)]F_x(s)dr \quad (2.10)$$

where $F_x(s)$ is called enhancement factor and s is the reduced density gradient given as $|\nabla\rho(r)|/2k_F\rho(r)$ in which k_F is the local Fermi wave vector. The enhancement factor accounts for the deviation of LDA from GGA by considering the variation of density. Based on the description of enhancement factor there are different GGA functionals. Many GGA functionals are inadequate for the description of dispersion interactions (non-local electron-electron correlation). Hence many schemes are developed to incorporate van der Walls interaction and thereby improving the energies of dispersion bonded systems.

2.4 Computational Methodology – Density Functional Theory

All simulations for the current work are performed in periodic boundary conditions using VASP [34] (Vienna ab initio simulation program) with plane wave implementation of Density functional theory.[31, 34] We have used the GGA[35] with Perdew – Burke – Ernzerhof (PBE) exchange correlation function and projected augmented wave method (PAW)[36-37] within DFT to describe inner core valence interaction with a plane wave cut-off energy of 450 eV. To correctly describe the vander waals interactions, the widely accepted DFT-D3 method with Becke-Jonson damping correction factor is incorporated.[38-39] The Nudged elastic bond (NEB) scheme was used to identify the transition state (TS) for glycosidic bond cleavage using different model compounds and are subsequently fully optimised.[40] Vibrational frequency analysis is used to confirm the nature of TS.

Strict energy convergence criteria of 10^{-6} eV was employed to ensure high level of accuracy. The crystal structures of cellotetraose[41], cellulose[42] and cellobiose[43] were modelled. A 3 x 3 x 1 monkhorst pack k-point mesh for cellotetraose, 1 x 1 x 3 for cellobiose and 3 x 3 x 3 for cellulose were used to sample the brillouin zone. With respect to the statistical thermodynamics we calculated the enthalpic and entropic translational, rotational and vibrational corrections factors.[44] The respective molecular partition function was used to calculate the corrections. Since electronic energies are computed at 0 K, zero-point vibrational energy (ZPE) are added to these energies. Cellotetraose has 3 glycosidic bonds present and is chosen as model compound because it can be used to study both end-chain and mid-chain scission. On the other hand, cellobiose has single glycosidic bond which can behave both as a mid and end-chain. cellulose is an infinite chain length molecule and can be used to study the mid-chain scission activation barrier. The crystalline geometry of cellotetraose, cellobiose and cellulose with a network of inter and intra molecular interactions is optimised at high convergence and is the thermodynamically most stable conformer.[41-43]

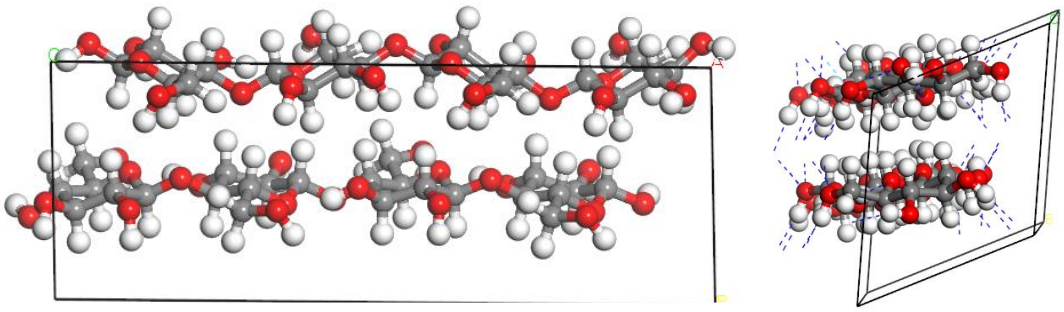

Figure 2.2 Cellotetraose crystal structure in front view and side view. A unit cell contains 2 chains of cellotetraose. The violet dotted line in side view shows the inter and intra molecular hydrogen bonding network. Red indicates oxygen atom, white is the hydrogen atom and grey is a carbon atom. The dotted lines are the inter and intra molecular interactions

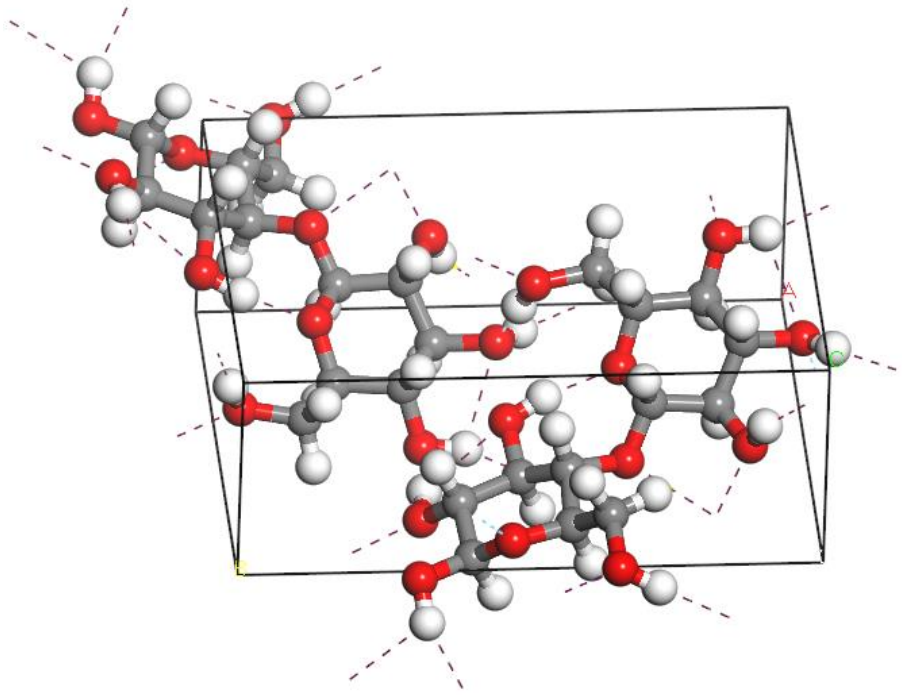

Figure 2.3 Cellobiose crystal structure in front view. A unit cell contains 2 chains of cellobiose. Red indicates an oxygen atom, white is a hydrogen atom, grey is carbon atom. Dotted lines are inter and intra molecular interactions

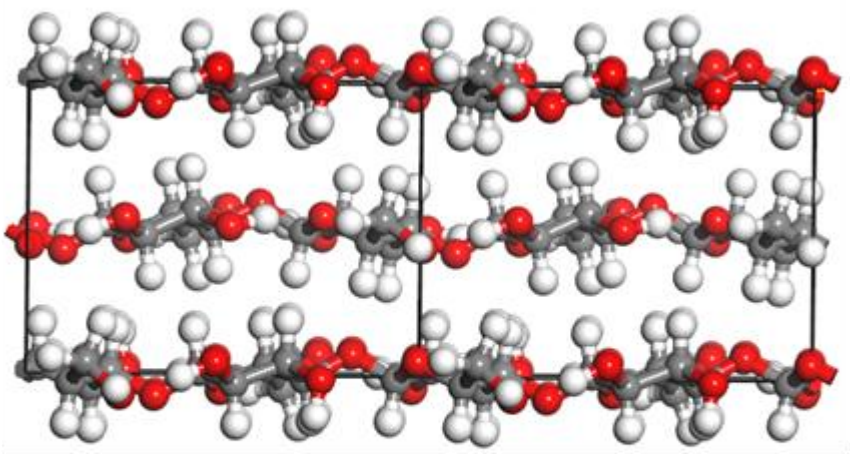

Figure 2.4 Cellulose crystal structure in front view. Red indicates an oxygen atom, white is a hydrogen atom, grey is carbon atom. Dotted lines are inter and intra molecular interactions

2.5 Computational Methodology - Reduced Density Gradient plots

There are several methods defined to analyse covalent interactions. The quantum-mechanical models like electron localisation function (ELF) and Bader's quantum theory of atom-in-molecules (AIM) are well established methods to identify covalent interactions by visualising the electronic density,[45-46] NCI are analysed using electronic density and its derivatives known as reduced density gradient(s). The reduced density gradient is one of the fundamental dimensionless quantity in density functional theory which is used to describe the deviation in electronic density from a homogenous distribution s(r).

$$S(r) = \frac{1}{2(3\pi^2)^{\frac{1}{3}}} \frac{|\nabla\rho(r)|}{\rho(r)^{\frac{4}{3}}} \qquad (2.11)$$

In an isolated system which is far from nucleus, both the numerator and denominator attains small values, however the denominator approaches zero faster than the gradient and the value of s(r) approaches infinity at very low densities. In regions closer to nuclei i.e. higher density regions the denominator increases at a greater rate in comparison to the gradient, making values of s(r) decreasing at a steady rate. The bonding and non-bonding interactions can be visualised when s(r) is plotted verses ρ. Whenever an interference between atomic orbitals occurs, a spike in the s(r) plot is observed. These spikes correspond to an interaction and can be mapped back into the real space. The sign of the second eigenvalue of the Hessian electron density matrix is used to differentiate between attractive (bonding) and repulsive (non-bonding) interactions. Bonding interactions can be identified by the negative sign of $\lambda 2$,

Conversely, if atoms are in nonbonded contact, $\lambda 2 > 0$. Large negative values of sign($\lambda_2(r)\rho(r)$) is bonding interactions such as hydrogen bonding, bond formation interactions. If the sign($\lambda_2(r)\rho(r)$) is large positive, the interaction indicates non-bonding such as ring or chain repulsions. Values which are near zero corresponds to weak vander waals interaction.[28]

A multifunctional wave analyser named Multiwfn is used to study the non-covalent interactions in our system, through Reduced Density Gradient (RDG) plots. Multiwfn superimposes the density of free state of atoms for calculating the RDG, also known as pro-molecular approximation. The density of free stated atoms are taken from in-built data of Multiwfn calculated using B3LYP/6-31G. It serves a good tool to study the inhomogeneous low electronic density areas using RDG plots. As the NCI are characterised by low density values, the iso-surfaces are constructed at low gradients ($s < 0.4$ a.u.) around the molecular structure in real space.

3. RESULTS AND DISCUSSION

This chapter discusses glycosidic bond breaking mechanisms involved in biomass pyrolysis process and explains the difference in activation barriers for end-chain and mid-chain cleavage. The section 3.1 describes the glycosidic bond breaking mechanism namely transglycosylation, glycosylation and ring contraction. Activation barriers for these mechanisms are discussed and compared with literature. Section 3.2 of this chapter discusses the non-covalent interactions present in the three-dimensional geometry of our system (initial state, transition state) and its usage in determining the difference between the end-chain and mid-chain activation barriers. We also define a methodology called energy decomposition analysis in section 3.3 to explain the difference in activation barriers for end-chain and mid-chain cleavage by quantifying these non-covalent interactions. Finally, the present study is extended for different surrogate molecules, namely cellulose and cellobiose in the section 3.4 of this chapter.

3.1 Glycosidic bond breaking mechanisms

Glycosidic C-O-C bond breaking is considered to be the first step of depolymerisation during cellulose pyrolysis. Fragmentation of β 1,4 glycosidic bond results in the formation of products like levoglucosan (LGA) and furans.[47] These compounds are the major products obtained during thin-film pyrolysis experiments using different cellodextrins (DP 2-6).[48] The glycosidic bond breaking reactions can be characterised into three main groups (i) Transglycosylation (ii) Ring Contraction and (iii) Glycosylation (*cf* Figure 3.1).

These reactions contribute around 60-70% of the products, forming anhydrosugars and precursors to furans and pyrans.

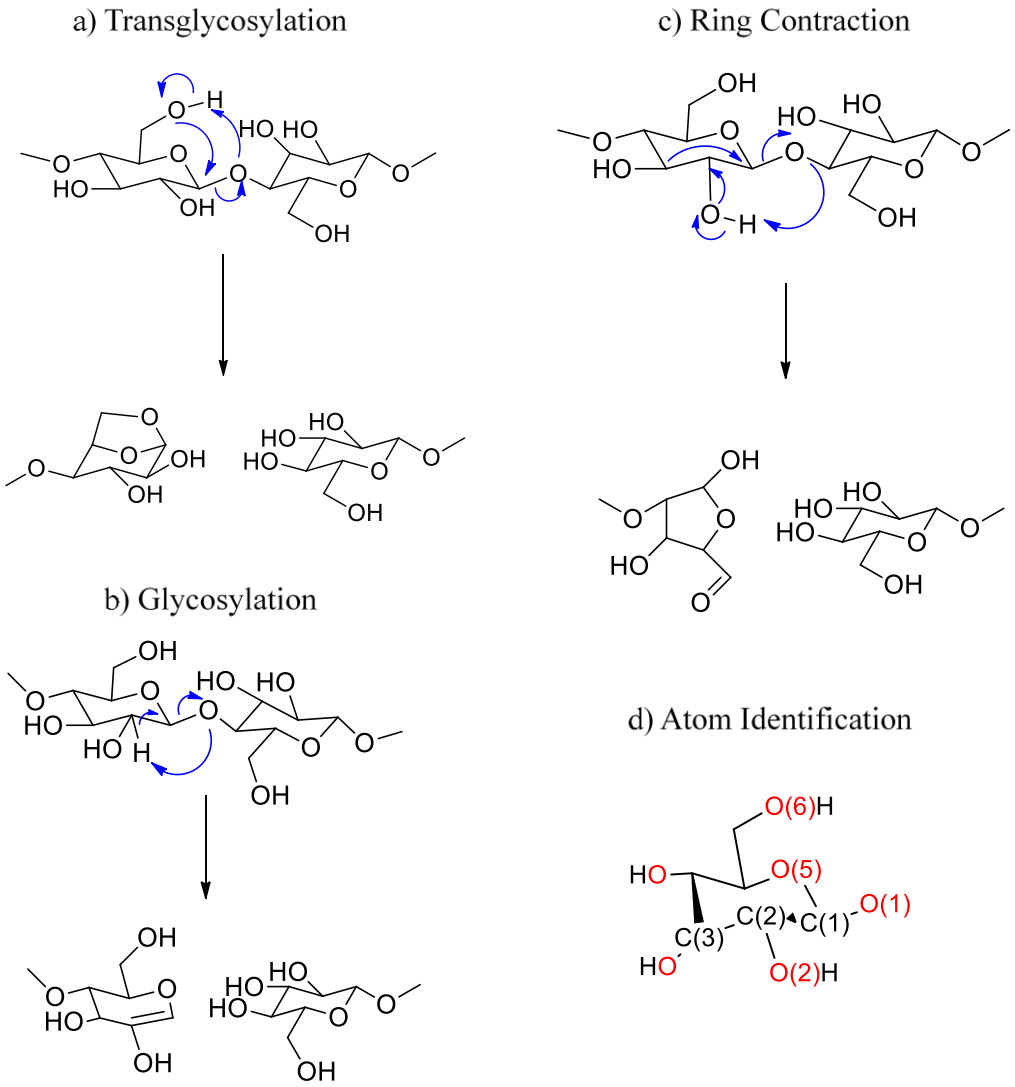

Figure 3.1 Glycosidic bond breaking mechanisms. Proposed bond movements for concerted mechanism a) Transglycosylation b) Glycosylation c) Ring Contraction. The atom identification numbers are shown in d.

Transglycosylation, is a concerted mechanism forming a dominant product in cellulose pyrolysis called levoglucosan. In transglycosylation, O(6) hydrogen is abstracted by the glycosidic oxygen O(1) followed by concerted O(6) addition to C(1) with breaking of the glycosidic bond. The electron and bond movements of this reaction are shown in Figure 3.1.a. The second reaction is glycosylation, also a concerted mechanism, involving breaking of the glycosidic bond to form 1,2

anhydroglucose and depolymerised cellulose chain. The glycosylation reaction mechanism is shown in Figure 3.1.b. The C(2) hydrogen is abstracted by the glycosidic oxygen to form a pyran ring. The third glycosidic bond breaking reaction showing depolymerisation is the ring contraction, which results in the formation of precursor to 5-hydroxymethly-furfural via a concerted mechanism. In this reaction, the O(2) hydrogen is abstracted by the glycosidic oxygen O(1),C(2)-C(3) bond breaks and the ring contraction occurs in a concerted manner to give a (precursor to) furanic compound (Figure 3.1.c). Activation barriers of the above discussed reactions are computed for both end-chain and mid-chain scission using cellotetraose (having three C-O-C glycosidic bonds) as a surrogate molecule. The enthalpic activation barriers for end-chain and mid-chain scission for transglycosylation reaction are 39.9 and 58.6 kcal/mol, respectively as seen in Figure 3.2. The structure of the transitions states are given in Appendix A and are labelled as A and B.

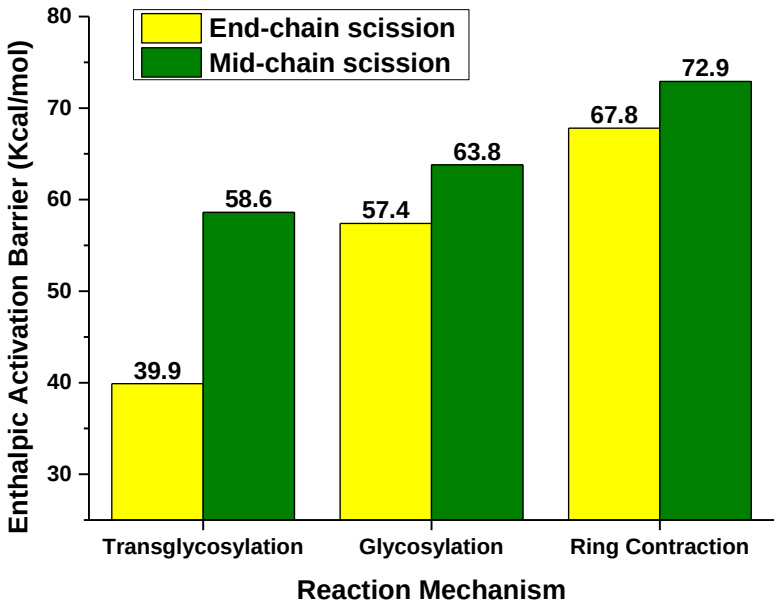

Figure 3.2 Activation barriers of glycosidic bond breaking using cellotetraose as a model compound. The end-chain scission barrier is lower than mid-chain scission barrier for all the reactions

Agarwal et.al. calculated the activation barrier for (precursor to) LGA formation to be 36 kcal/mol at 600°C, using CPMD simulations.[23] The system into consideration was cellulose 1β containing cellobiose units. Direct comparison to the results is not possible because the reported reaction is a two-step mechanism which forms the precursor of LGA and does not account for product formation. Moreover, CPMD accounts for accurate temperature and entropy effects. We on the other hand, calculated the entropy of our system by vibrational frequency analysis using partition functions of the statistical thermodynamics[44] and harmonic oscillator approximation, which tends to overestimate the thermochemical data as it is unable to account for anharmonicities.

Mayes et.al, using cellobiose as a model compound, showed that the concerted mechanism for LGA formation exhibits the lowest barrier of 55.2 kcal/mol over heterolytic and homolytic cleavage of C-O bond.[19] The points to comparison are first, our concerted transglycosyation mechanism also has the lowest barrier as seen by them. Second, our model system, with cellotetraose in a periodic environment, can show end and mid glycosidic bond scission to produce LGA, of which end-chain scission shows the enthalpic activation barrier 39.8 kcal/mol, lower than reported by Mayes and Broadbelt.[19] Further, Krumm et al reported the existence of two different pathways for cellulose fragmentation with respect to the change in pyrolysis temperature[20] and labelled them as end-chain and mid-chain scissions. Recently, Zhu et al, reported two different experimental kinetic activation barriers of 53.7 kcal/mol and 23.2 kcal.mol for cellulose decomposition corresponding to different temperatures.[21] On comparing our computational results with these experimental studies,[21] the following point is noteworthy. The activation barriers of 39.9 kcal/mol and 58.6 kcal/mol for LGA

formation using cellotetraose by end-chain and mid-chain cleavage, respectively, follows the same trend as seen in the experimental results. On comparing the computational results with experiments, mid-chain cleavage barrier of 58.6 kcal/mol for LGA formation is found to be near experimentally reported 53.7 kcal/mol for high temperatures corresponding to mid-chain cleavage. Direct comparison is not possible, as the computed activation barriers are enthalpic with approximations, and we need to correctly consider the temperature effects which then can be compared with the experimental values. Nonetheless, the present study supports the experimentally determined two different kinetic regimes for glycosidic bond cleavage and further explaining that the change in product distribution has been attributed to different types of cleavage observed for cellulose decomposition.

In glycosylation, the enthalpic activation barriers for end-chain and mid-chain scissions are 57.4 and 63.8 kcal/mol respectively, as seen in Figure 3.2. The structure of the transitions states are shown as E and F in Appendix A. Assary and Curtiss reported 59.1 kcal/mol as the activation barrier for the glycosylation mechanism using a higher level method MP2/6-311G++(3df,3pd)//B3LYP/6-31+G(2df,p) and cellobiose as a surrogate, showing excellent agreement with the experimental value of 58 kcal/mol required to form active cellulose.[24, 49] The value reported by Assary and Curtiss lies within the range of the end-chain and mid-chain values calculated in this study. For the ring contraction mechanism, the enthalpic activation barriers for end-chain and mid-chain scission are 67.8 and 73 kcal/mol (Figure 3.2). The structure of the transitions states are given as I and J in Appendix A. Agarwal et al. reported 49 kcal/mol as the activation barrier for precursor to HMF via ring contraction at 600°C. Direct comparison to our

results is not possible because of the same reason discussed for transglycosylation mechanism, the reported mechanism is a two-step process and CPMD accounts for accurate temperature and entropy effects. Moreover, cellobiose was used as a model compound which cannot be used to study mid and end chain cleavage.

The enthalpic activation barriers of all the above discussed mechanisms for end-chain and mid-chain glycosidic bond scission using cellotetraose as a surrogate compound are found to be in the range of 40-73 kcal/mol. The end-chain scission activation barrier of glycosidic bond breaking is always found to be lower than that of mid-chain scission. A consistency in this trend is seen for all the three-reactions, namely, transglycosylation, glycosylation and ring contraction. This observation can be linked to the existence of two different kinetic regimes of cellulose pyrolysis at different temperatures.[20] The major contribution towards the difference in activation barrier is enthalpic. The entropic contribution for all the reactions was found to be in the range of 3-6 cal/mol and is calculated by vibrational frequencies using harmonic oscillator approximation and partition functions of the statistical thermodynamics.[44] Going by the magnitude of these values, the entropic contribution is found to be similar for both end-chain and mid-chain activation barriers. Molecular dynamics (MD) simulations is an effective methodology to accurately determine the temperature effects and entropic contribution. The MD determined entropy is expected to further reduce free energy barriers, but major difference between end-chain and mid-chain entropy is not expected.

The activation barriers reported in this thesis are purely enthalpic as MD simulations are out of the thesis scope and partition functions determined entropy is found to be similar for both types of scissions. Additionally, the enthalpic

difference observed can be attributed to differences in the inter and intramolecular interactions present in the geometry of the system. These inter and intramolecular interactions are controlled by covalent and non-covalent interactions, a detailed study on these interactions is done in the consequent sections of this thesis.

3.2 Non-Covalent interactions

Section 1.7 of the introduction chapter emphasized the importance of non-covalent interactions (NCI) in a molecular structure (a three-dimensional geometry) and its effect in stabilizing or de-stabilizing the molecular structure. The reduced density gradient plots (RDG) (explained in section 2.5 of the methodology chapter) are used to identify the NCI present in the system. Figure 3.3 shows the RDG for end-chain scission transition state of transglycosylation reaction. Each spike, designated with a red dot on the RDG plot, corresponds to an interaction.

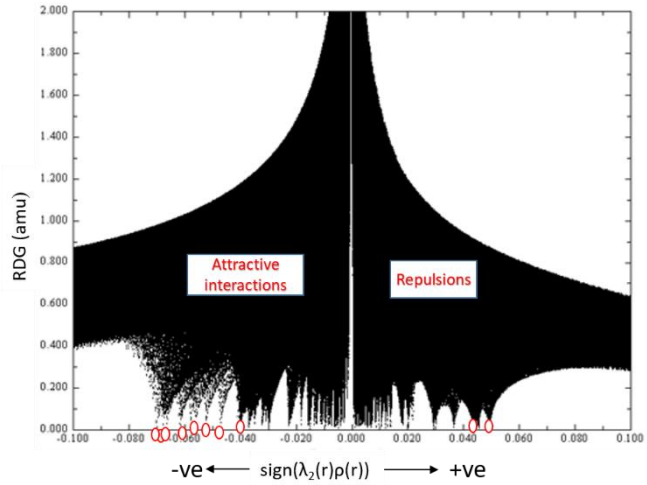

Figure 3.3 Reduced density gradient plots (Identifying Non-covalent interactions) in end-chain scission transition state of transglycosylation mechanism. The spikes in the -ve part shows bonding interactions whereas spikes corresponding to +ve part shows non-bonding interactions.

The spikes on the negative *x* axis are indicative of attractive or bonding interactions, whereas spikes on the positive *x* axis are non-bonding or repulsive interactions. The strength of an interaction is determined by the corresponding absolute value of the electronic density.[28] On visualising these spikes in real space for transglycosylation TS, the bonding or attractive interactions constitute the C-O-C glyosidic bond breaking interaction, O(6)-C(1) bond formation interaction (Figure 3.1.a) and inter/ intramolecular hydrogen bonding interactions within the same ring or with neighbouring chains. The ring and chain repulsions constitute the non-bonding or repulsive interactions. All these interactions constitute the NCI and are shown in Figure 3.4 below.

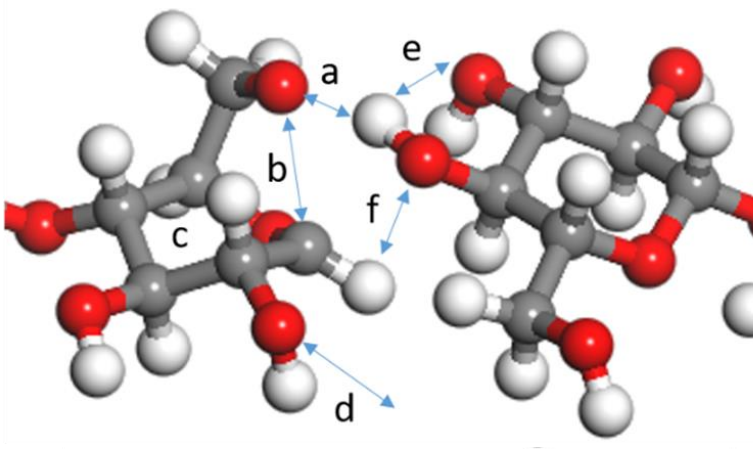

a) Interaction on account of O-H breaking (H-bonding)
b) Interaction due O-C bond formation
c) Steric repulsion in the ring
d) Intermolecular hydrogen bonding between chains
e) Intramolecular hydrogen bonding within the chain
f) Interaction on account of C-O glycosidic bond breaking

Figure 3.4 Non-covalent interactions present in end-chain scission transition state of transglycosylation. Red indicate oxygen atom, grey is carbon and white is a hydrogen atom

These interactions contribute towards the stability of a transition state. Hence, it is important to analyse the respective RDG plots for both end-chain and mid-chain transition state. The next section discusses the differences between the two RDG plots and its usage as a tool to explain differences in the activation barriers.

Additionally, a new approach known as energy decomposition analysis is defined and used to quantify these interactions.

3.3 Energy decomposition analysis

With respect to the glycosidic bond breaking reactions investigated in this thesis, maximum difference between the end-chain and mid-chain activation barrier is observed for the transglycosylation reaction, hence we choose this mechanism to explain our basis of analysis and methodology. The RDG plots of end and mid-chain scission transition state of tranglyosylation reaction are plotted in Figure 3.5 to get an insight about the respective bonding and non-bonding interactions. On comparing the two RDG plots (shown in Figure 3.5a and 3.5b), it is observed that mid-chain scission RDG (Figure 3,5b) has only one spike crossing -0.07 a.u. mark. On the other hand, end-chain scission RDG plot (Figure 3.5a) has multiple spikes after the -0.07 a.u. electronic density mark. The spikes on the positive side of RDG plots for both the scissions are found to be of similar strength and magnitude. Thus, the presence of a larger number of negative value spikes are found in end-chain scission transition state which corresponds to large electronic density (indicating strong bonding interaction). This leads to further stabilization of the end-chain transition state and hence lowering of the activation barrier for C-O-C glycosidic bond breaking is observed. On visualising the spikes of RDG plot in real space, the interactions observed can be divided into two main categories namely intermolecular and intramolecular interactions as shown in Table 3.1.

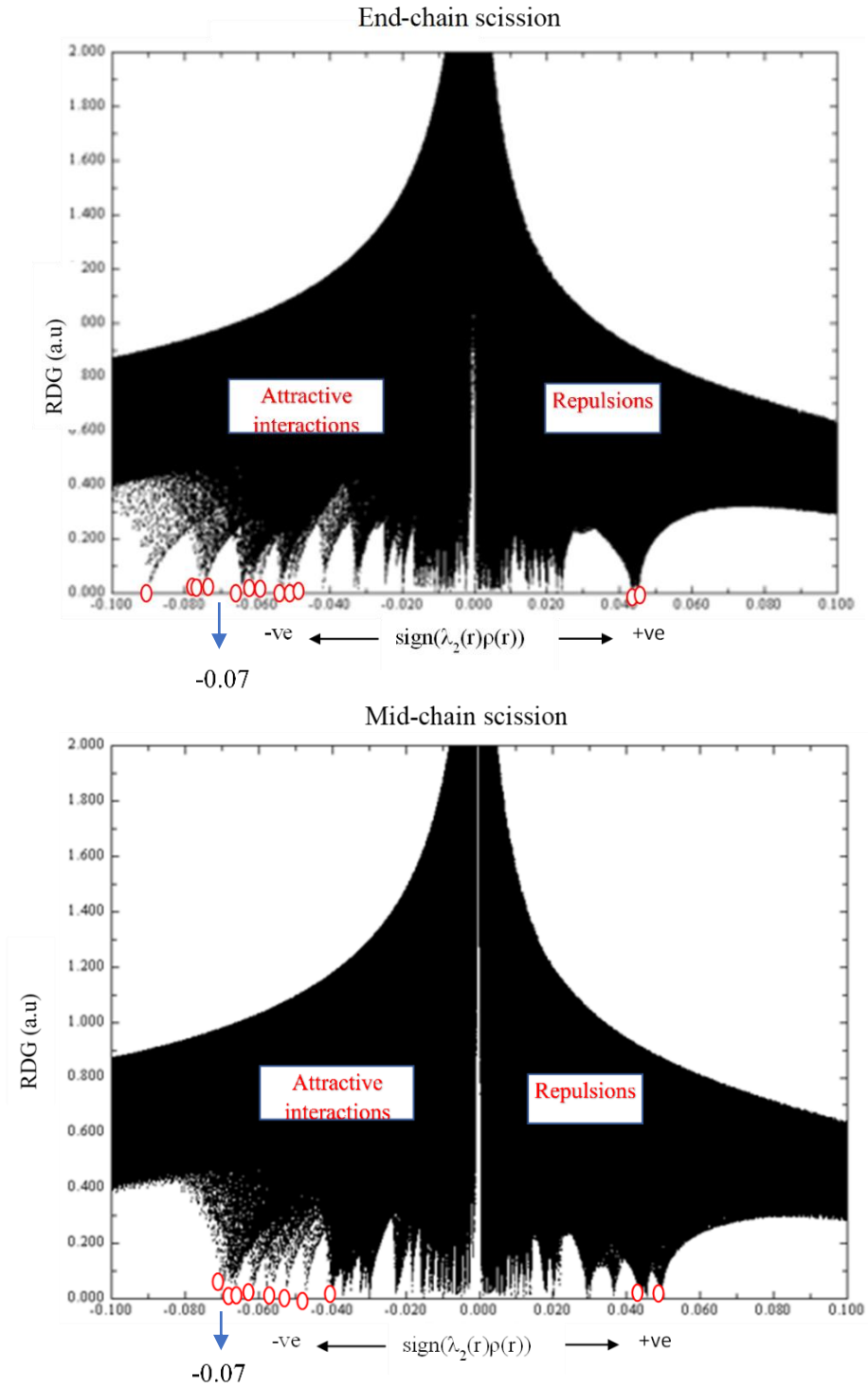

Figure 3.5 Comparing reduced density gradient plots for a) End-chain TS and b) Mid-chain scission TS of the Transglycosylation mechanism

The strongest interaction beyond -0.08 a.u mark in the end-chain RDG plot corresponds to a strong intermolecular hydrogen bonding with the neighbouring chain. These inter and intramolecular interactions present in the end and mid-

chain transition states are responsible for the difference in the activation barriers. Therefore, it is important to quantify these interactions and investigate their roles in the stability of respective transition states. For which, we define an energy decomposition analysis.

Table 3.1 Classification of different interactions observed in the end-chain and mid-chain scission transition states of transglycosylation mechanism

Intermolecular interactions	**Intramolecular interactions**
Intermolecular hydrogen bonding between chains	Intramolecular hydrogen bonding within the chain
	Interaction on account of C-O glycosidic bond breaking
Steric repulsion between chains	Interaction due O-C bond formation and Interaction because of O-H breaking (H-bonding)
	Steric repulsion in the ring

The energy decomposition analysis is used to calculate the change in inter-molecular and intra-molecular interactions of end-chain and mid-chain transition states with respect to its initial state. In this method, the two chains present in the transition state periodic cell, namely the scission chain and non-scission chain (1 and 2 respectively) are isolated such that the effect of neighbouring atoms and inter-molecular interactions are nullified. The diagrammatic representation is given in Figure 3.6. The single point energy calculations of the isolated chains (E1, E2 for end-chain and M1, M2 for mid-chain) are performed to evaluate their isolated electronic energies. During the single point calculation of the isolated chains, the box size is optimized and kept the same as that of the transition state so that there is no change in the electronic energy due to change in box size.

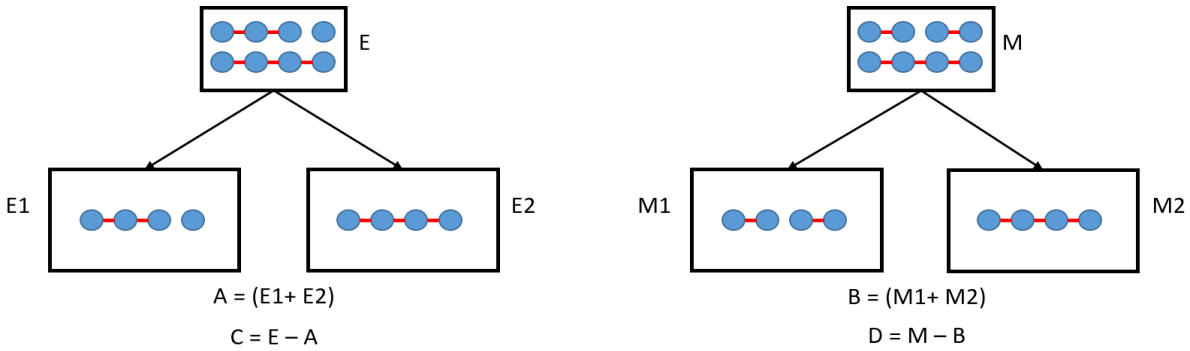

Figure 3.6 Schematic for Energy Decomposition Analysis

E – End-chain scission transition state, E1 – Scission chain, E2 – Non-scission chain, M - Mid-chain scission transition state, M1- Scission Chain, M2- Non-scission chain, C - Intermolecular interaction in E, D - Intermolecular interaction in M, Net Intra-molecular interactions = (A – B), Net Inter-molecular interactions = (C – D)

The single point energies of isolated scission chain and non-scission chain are added (E1+E2) and then the sum (A for end-chain and B for mid-chain) is subtracted from the transition state electronic energy to give intermolecular interactions present in the respective scission (C and D). The difference between these individual intermolecular interactions (C and D) gives us the net difference in intermolecular interactions between mid-chain and end-chain scission transition state (C-D).

On the other hand, when the sum of isolated single point energy values of mid chain (B) and end chain transition state (A) are subtracted (A-B), the net difference in the intramolecular interactions between the two scissions is obtained. In this calculation, the effect of intermolecular interactions is negated, and we get the net difference in intramolecular interactions of mid-chain and end-chain scission transition state. This energy decomposition analysis is performed for transglycosylation, glycosylation and ring contraction mechanisms and the effect of these interactions on the activation barriers is analysed. It can be seen from Figure 3.7 that the net difference in the intermolecular interactions is higher than the difference in intramolecular interactions for three reactions. The net

intermolecular interactions (majorly comprising of intermolecular hydrogen bonding; table 3.1) are found to dominate the end-chain scission for all the three glycosidic decomposition reactions, thus stabilizing the end-chain transition state. On the other hand, the transition state of mid-chain scission is stabilized more by the intramolecular interactions (such as intra-H bonding, bond breaking and bond formation interactions). Overall the magnitude of net intermolecular interaction is higher than the net intramolecular interactions, making intermolecular interactions the governing factor for stabilising the TS. Further, as the intermolecular interactions are found to dominate the end-chain scission, it stabilizes the transition state and further lowers the activation barrier.

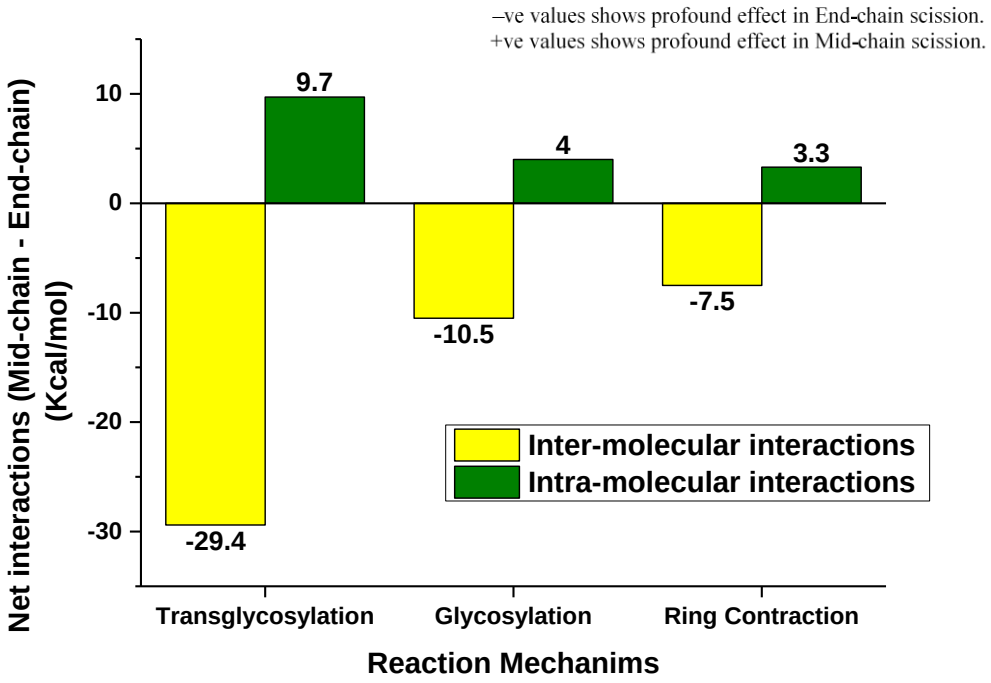

Figure 3.7 Net (midchain – endchain) inter and intra-molecular interactions. Intermolecular interactions dominate in end-chain scission, intramolecular interactions dominate in mid-chain scission. Sign only represent whether intermolecular of intramolecular, absolute values depict the actual strength of the interaction,

For the transglycosylation mechanism, it was earlier seen in the end-chain scission RDG plot (Figure 3.5a) that there exists a spike beyond -0.08 a.u

corresponding to a strong intermolecular hydrogen bonding and multiple other bonding spikes between -0.07 a.u and -0.08 a.u. The bonding spikes beyond -0.07 a.u was only one in the mid-chain scission RDG plot (Figure 3.5b). This suggests that there exist strong intermolecular interactions in end-chain scission transition state. On further analysing the quantified values of net intermolecular and intramolecular interactions for the tranglycosylation reaction (Figure 3.7), it is further confirmed that the intermolecular interactions are the governing factor. This dominating effect of intermolecular interactions in stabilising the transition state suggests the need to incorporate periodicity and condensed phase environment while simulating cellulose pyrolysis reactions, which on the other hand are not considered and are currently lacking in quantum mechanical calculations.

3.4 Extension of the study using cellulose and cellobiose as model compounds

The smallest subunit of cellulose having single glycosidic bond is the glucan dimer called cellobiose. As discussed in the introduction chapter cellobiose and its associated family have been extensively used as surrogate molecules to study cellulose pyrolysis reaction mechanisms in a gas phase environment.[19, 22, 24] Cellobiose fragmentation has characteristics both of end-chain and mid-chain scission (end-mid scission), while cellulose which have multiple glycosidic bonds can be used to investigate mid-chain scission activation barrier. Hence, it is also important to study the glycosidic bond cleavage of cellulose and cellobiose using their crystal structures in a condensed phase environment, which however,

is currently lacking in the literature. Therefore, glycosidic bond breaking activation barriers for transglycosylation, glycosylation and ring contraction reaction are calculated and the results are shown in Figure 3.8. The structures of the transitions states are given as C, D, G, H, K and L in Appendix A. It can be seen from Figure 3.8 that the activation barrier for cellobiose end-mid glycosidic fragmentation is lower than the mid-chain scission in cellulose for all the discussed reactions by 18.3 kcal/mol for tranglycosylation, 5.4 kcal/mol for glycosylation, 5.2 kcal/mol for ring contraction.

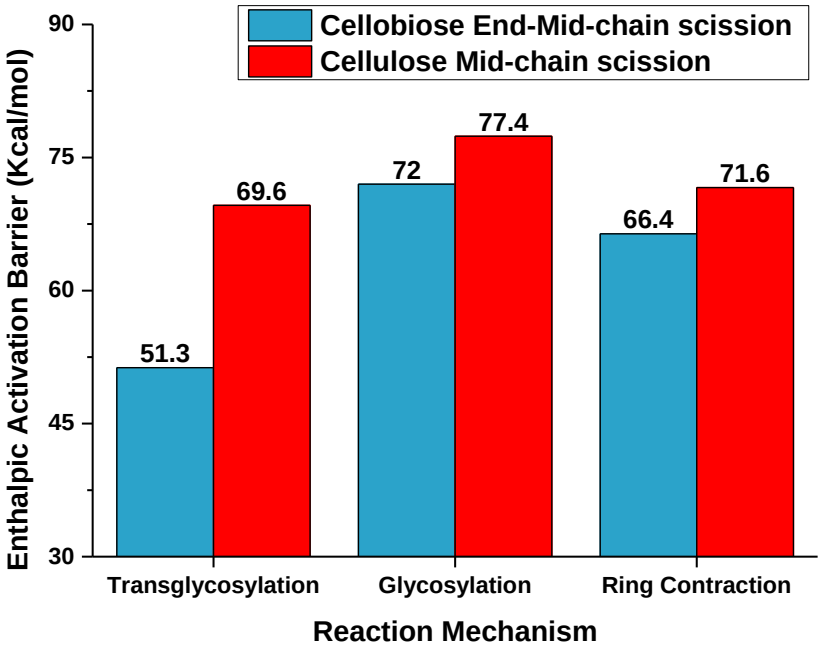

Figure 3.8 Activation barriers of glycosidic bond breaking in cellobiose and cellulose.

To quantify this difference in the activation barriers in Figure 3.8, it is important to obtain insights about the attractive and repulsive interactions present in the system. As, the maximum difference in the activation barriers of 18.3 kcal/mol is seen between cellobiose and cellulose decomposition for the LGA formation reaction mechanism, we choose the transglycosylation reaction to explain these results. The RDG of cellobiose and cellulose transition states for the

transglycosylation reaction (Figure 3.9). shows the presence of only one spike beyond -0.07 a.u. mark in the cellobiose RDG plot (Figure 3.9a). whereas, two spikes are seen in the cellulose RDG plot (Figure 3.9b).

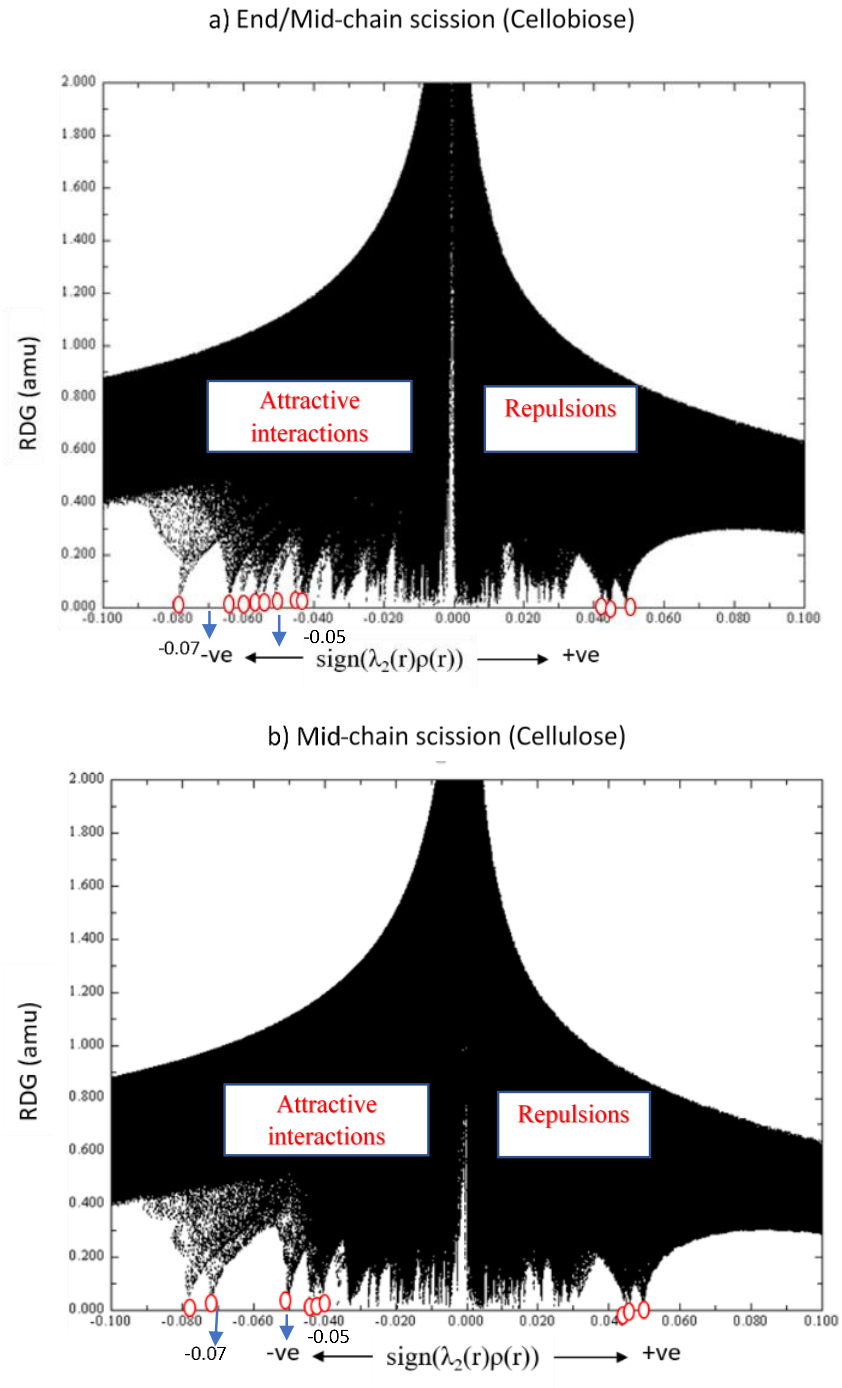

Figure 3.9 Comparing reduced density gradient plots for a) cellobiose end-mid-chain and b) cellulose mid-chain glycosidic bond scission for transglycosylation reaction

Further comparison of the spikes beyond the -0.05 a.u. electronic density mark shows a larger number of spikes in the cellobiose RDG plot as opposed to the presence of only one spike beyond -0.07 a.u. mark.

Therefore, a direct comparison of the two RDG plots is unable to explain the difference in activation barrier. In addition, directly comparing the transition states of cellobiose and cellulose scission is also not valid (which is true for cellotetraose) because of the different initial states of cellobiose and cellulose. Loerbroks et. al. also highlighted that cellobiose and cellulose crystal structure (initial state) have an intense network of hydrogen bonding which, makes it cumbersome to undergo conformational changes to activate the glycosidic bond.[50] Hence, it is important to understand the change in inter and intramolecular interactions in the transition states with respect to different initial states. The energy decomposition analysis, as discussed in section 3.3, is performed to quantify these interactions.

The change in the intermolecular interactions of the transition states with respect to the corresponding initial states is plotted in Figure 3.10. For the transglycosylation reaction, a larger decrease in the intermolecular interactions is seen for cellulose scission than cellobiose, while for the other two reactions, the increase in intermolecular interactions is higher for cellobiose glycosidic bond breaking. This concludes that cellobiose transition state has a higher number of strong intermolecular interactions when compared to cellulose transition state and hence its activation barrier is lowered. Even though a decrease in the intermolecular interactions is observed for transglycosylation reaction contrary to the increase in network for ring contraction and glycosylation, the lowest

barrier for transglycoslation (favouring LGA formation) can be attributed to the bond dissociation energies and charge distribution.

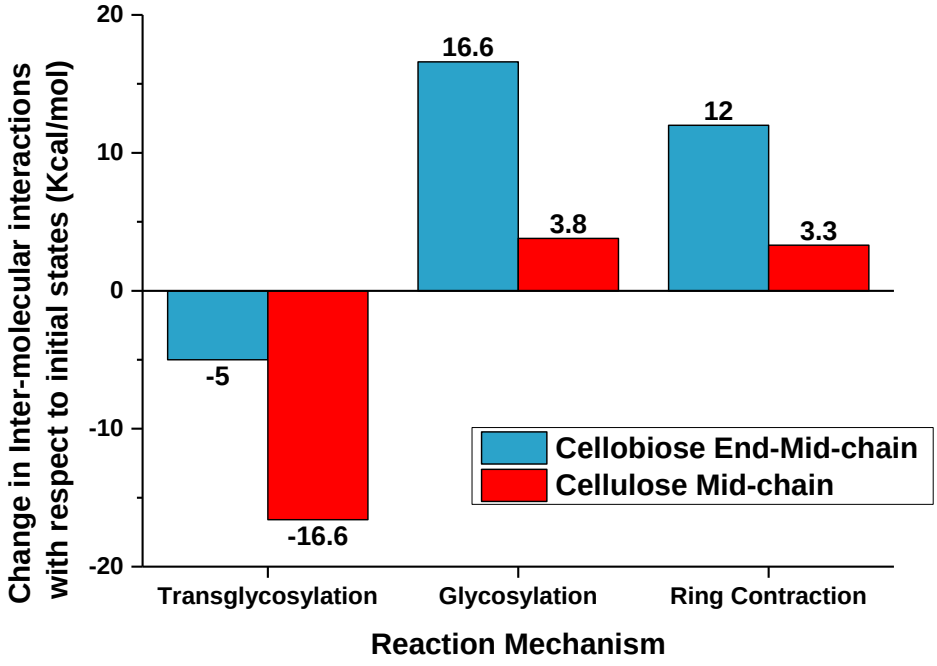

Figure 3.10 Change in inter-molecular interactions in cellulose and cellobiose. Changes in the interaction of the transition state is calculated with respect to the respective initial states

The change in intramolecular interactions is also evaluated using energy decomposition analysis and the results are plotted in Figure 3.11. The change in intramolecular interactions of the transition state with respect to its initial state is calculated by subtracting the single point electronic energy of the isolated transition state chains with isolated initial state chains. In comparison to the change in intermolecular interactions, intramolecular interactions are similar for both the end-mid-chain scission of cellobiose and mid-chain of cellulose. In summary, cellobiose end-mid-chain scission is more stabilised by intermolecular interactions, the intra-molecular interactions have similar stabilisation effect on

both the scissions. Hence, we can say it is the intermolecular interactions that play a key role in stabilising the end-chain scission transition state in condensed phase environment.

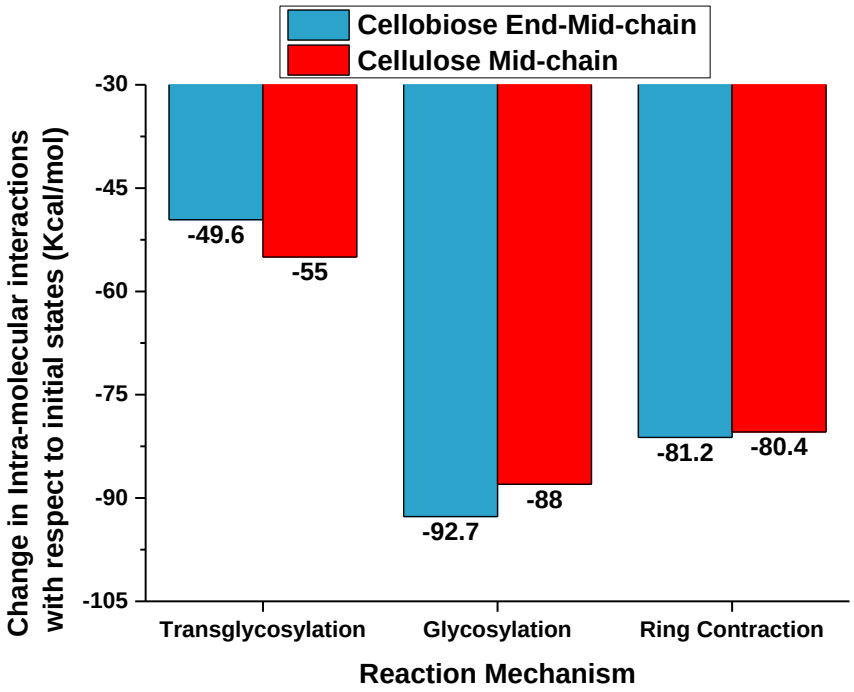

Figure 3.11 Change in intra-molecular interactions in cellulose and cellobiose. Changes in the interaction of the transition state are calculated with respect to the respective initial states

4. PERSPECTIVE AND FUTURE DIRECTIONS

This chapter discusses the future direction of the work presented in this thesis. Biomass consists of small amounts of inorganic salts and minerals. The product distribution of biomass pyrolysis is significantly influenced by the naturally occurring alkali and alkaline earth metals (AAEM). These metals found in inorganic salts acts as a homogenous catalyst influencing the reaction pathway. Therefore, it is important to understand the catalytic role of AAEM on cellulose decomposition. The present study in the periodic environment can be extended to investigate the role of AAEM in a condensed phase mid-chain and end-chain scission activation barriers. We can also investigate the role of multiple transition metals on glycosidic bond fragmentation.

To make the condensed phase environment more tractable, we can use multiscale molecular modelling methodology combining quantum mechanics and classical molecular dynamics known as Car-Parrinello Molecular Dynamics (CPMD). This will further enable to get a correct accounts of entropy effects on our systems and provides the flexibility of choosing multi-dimensional collective variables as reaction coordinates. This can provide conditions similar to the condensed phase environment as experimentally observed during cellulose melt phase also known as active cellulose. The free energy activation barrier thus obtained (having both enthalpic and entropic contribution) can be directly compared with the glycosidic bond cleavage activation barrier determined experimentally.

5. CONCLUSION

In this study, reactions involved in the initial stages of pyrolysis *viz.* glycosidic C-O bond fragmentation are investigated using first-principles DFT calculations. The activation barriers for LGA and precursors to furans and pyrans components for mid-chain scission and end-chain scission using cellotetraose as a model compound are evaluated. It is observed for all the three set of reactions that the activation barriers for end-chain scissions are lower than those of mid-chain scissions. The end-chain scission enthalpic activation barriers are calculated to be lower than mid-chain scission barriers by 18.7 kcal mol^{-1}, 6.5 kcal mol^{-1} and 5.1 kcal mol^{-1} for transglycosylation, glycosylation and ring contraction, respectively, with cellotetraose as a surrogate molecule. Energy decomposition analysis shows that the intermolecular interactions play a dominating role in stabilising the end-chain scission transition state while the mid-chain scission is more stabilized by intra-molecular interactions. The strength of intermolecular interactions for end-chain cleavage is observed to be higher than those of intramolecular interactions of mid-chain cleavage, leading to a more stable end-chain fragmentation transition state and lower end-chain C-O-C bond scission barriers.

This study is further extended to investigate the cellulosic system where the activation barriers of the three-discussed mechanisms were computed using cellobiose and cellulose. Cellulose fragmentation is a mid-chain cleavage, while the decomposition in cellobiose is both end and mid-chain cleavage due to only one glycosidic bond. The trend in activation barriers of cellulose and cellobiose are consistent with the cellotetraose results. The cellobiose mid-end chain

cleavage transition state is stabilised by a strong intermolecular interactive network and thus has a lower barrier compared to cellulose mid-chain scission.

Further, the periodic condensed phase environment considered in this study, a first of its kind, provides detailed insights into the end-chain and mid-chain scission activation barriers, using the crystal structure. This study focuses on the importance of intermolecular interactions in cellulose pyrolysis reactions and shows the need to incorporate periodic boundary conditions while simulating reaction mechanisms using DFT.

This computational analysis is also the first of kind study supporting the experimentally determined different kinetic regimes for glycosidic bond cleavage and further explaining that the change in product distribution has been attributed to different types of cleavage observed for cellulose decomposition.

REFERENCES

1. McKendry, P., Energy production from biomass (part 1): overview of biomass. *Bioresource Technology* **2002,** *83* (1), 37-46.

2. Mohan, D.; Pittman, C. U.; Steele, P. H., Pyrolysis of Wood/Biomass for Bio-oil: A Critical Review. *Energy & Fuels* **2006,** *20* (3), 848-889.

3. Balat, M., Production of bioethanol from lignocellulosic materials via the biochemical pathway: A review. *Energy Conversion and Management* **2011,** *52* (2), 858-875.

4. Nussbaumer, T., Combustion and Co-combustion of Biomass: Fundamentals, Technologies, and Primary Measures for Emission Reduction. *Energy & Fuels* **2003,** *17* (6), 1510-1521.

5. Molino, A.; Chianese, S.; Musmarra, D., Biomass gasification technology: The state of the art overview. *Journal of Energy Chemistry* **2016,** *25* (1), 10-25.

6. Patwardhan, P. R.; Satrio, J. A.; Brown, R. C.; Shanks, B. H., Product distribution from fast pyrolysis of glucose-based carbohydrates. *Journal of Analytical and Applied Pyrolysis* **2009,** *86* (2), 323-330.

7. Senneca, O., Kinetics of pyrolysis, combustion and gasification of three biomass fuels. *Fuel Processing Technology* **2007,** *88* (1), 87-97.

8. Lange, J.-P., Lignocellulose conversion: an introduction to chemistry, process and economics. *Biofuels, Bioproducts and Biorefining* **2007,** *1* (1), 39-48.

9. Chiaramonti, D.; Oasmaa, A.; Solantausta, Y., *Power generation using fast pyrolysis liquids from biomass*. 2007; Vol. 11, p 1056-1086.

10. Caputo, A. C.; Palumbo, M.; Pelagagge, P. M.; Scacchia, F., Economics of biomass energy utilization in combustion and gasification plants: effects of logistic variables. *Biomass and Bioenergy* **2005,** *28* (1), 35-51.

11. Brown, T. R.; Thilakaratne, R.; Brown, R. C.; Hu, G., Techno-economic analysis of biomass to transportation fuels and electricity via fast pyrolysis and hydroprocessing. *Fuel* **2013,** *106*, 463-469.

12. BRIDGWATER, A. V., BIOMASS FAST PYROLYSIS. *Thermal Science* **2016,** (2), 21-49%V 8.

13. Cordella, M.; Torri, C.; Adamiano, A.; Fabbri, D.; Barontini, F.; Cozzani, V., Bio-oils from biomass slow pyrolysis: a chemical and toxicological screening. *J Hazard Mater* **2012,** *231-232*, 26-35.

14. Kersten, S. R. A.; Wang, X.; Prins, W.; van Swaaij, W. P. M., Biomass Pyrolysis in a Fluidized Bed Reactor. Part 1: Literature Review and Model Simulations. *Industrial & Engineering Chemistry Research* **2005,** *44* (23), 8773-8785.

15. Lédé, J., Cellulose pyrolysis kinetics: An historical review on the existence and role of intermediate active cellulose. *Journal of Analytical and Applied Pyrolysis* **2012,** *94*, 17-32.

16. Debiagi, P. E. A.; Gentile, G.; Pelucchi, M.; Frassoldati, A.; Cuoci, A.; Faravelli, T.; Ranzi, E., Detailed kinetic mechanism of gas-phase reactions of volatiles released from biomass pyrolysis. *Biomass and Bioenergy* **2016,** *93*, 60-71.

17. Koo, J.-K.; Kim, S.-W., Reaction Kinetic Model for Optimal Pyrolysis of Plastic Waste Mixtures. *Waste Management & Research* **1993,** *11* (6), 515-529.

18. Mettler, M. S.; Mushrif, S. H.; Paulsen, A. D.; Javadekar, A. D.; Vlachos, D. G.; Dauenhauer, P. J., Revealing pyrolysis chemistry for biofuels production: Conversion of cellulose to furans and small oxygenates. *Energy Environ. Sci.* **2012,** *5* (1), 5414-5424.

19. Mayes, H. B.; Broadbelt, L. J., Unraveling the reactions that unravel cellulose. *J Phys Chem A* **2012,** *116* (26), 7098-106.

20. Krumm, C.; Pfaendtner, J.; Dauenhauer, P. J., Millisecond Pulsed Films Unify the Mechanisms of Cellulose Fragmentation. *Chemistry of Materials* **2016,** *28* (9), 3108-3114.

21. Zhu, C.; Krumm, C.; Facas, G. G.; Neurock, M.; Dauenhauer, P. J., Energetics of cellulose and cyclodextrin glycosidic bond cleavage. *Reaction Chemistry & Engineering* **2017,** *2* (2), 201-214.

22. Zhang, Y.; Liu, C.; Chen, X., Unveiling the initial pyrolytic mechanisms of cellulose by DFT study. *Journal of Analytical and Applied Pyrolysis* **2015,** *113*, 621-629.

23. Agarwal, V.; Dauenhauer, P. J.; Huber, G. W.; Auerbach, S. M., Ab initio dynamics of cellulose pyrolysis: nascent decomposition pathways at 327 and 600 degrees C. *J Am Chem Soc* **2012,** *134* (36), 14958-72.

24. Assary, R. S.; Curtiss, L. A., Thermochemistry and Reaction Barriers for the Formation of Levoglucosenone from Cellobiose. *ChemCatChem* **2012,** *4* (2), 200-205.

25. Zhang, M.; Geng, Z.; Yu, Y., Density Functional Theory (DFT) study on the pyrolysis of cellulose: The pyran ring breaking mechanism. *Computational and Theoretical Chemistry* **2015,** *1067*, 13-23.

26. Zhang, X.; Li, J.; Yang, W.; Blasiak, W., Formation Mechanism of Levoglucosan and Formaldehyde during Cellulose Pyrolysis. *Energy & Fuels* **2011,** *25* (8), 3739-3746.

27. Hosoya, T.; Sakaki, S., Levoglucosan formation from crystalline cellulose: importance of a hydrogen bonding network in the reaction. *ChemSusChem* **2013,** *6* (12), 2356-68.

28. Johnson, E. R.; Keinan, S.; Mori-Sánchez, P.; Contreras-García, J.; Cohen, A. J.; Yang, W., Revealing Noncovalent Interactions. *Journal of the American Chemical Society* **2010,** *132* (18), 6498-6506.

29. Contreras-García, J.; Boto, R. A.; Izquierdo-Ruiz, F.; Reva, I.; Woller, T.; Alonso, M., A benchmark for the non-covalent interaction (NCI) index or… is it really all in the geometry? *Theoretical Chemistry Accounts* **2016,** *135* (10).

30. Mushrif, S. H.; Vasudevan, V.; Krishnamurthy, C. B.; Venkatesh, B., Multiscale molecular modeling can be an effective tool to aid the development of biomass conversion technology: A perspective. *Chemical Engineering Science* **2015,** *121*, 217-235.

31. Kohn, W.; Sham, L. J., Self-Consistent Equations Including Exchange and Correlation Effects. *Physical Review* **1965,** *140* (4A), A1133-A1138.

32. Rajagopal, A. K.; Callaway, J., Inhomogeneous Electron Gas. *Physical Review B* **1973,** *7* (5), 1912-1919.

33. Steckel, D. S. S. a. J. A., *DFT Calculations for Simple Solids, Density Functional Theory*. 2009; p PP. 35–48.

34. Kresse, G.; Furthmüller, J., Efficient iterative schemes for ab initio total-energy calculations using a plane-wave basis set. *Physical Review B* **1996,** *54* (16), 11169-11186.

35. Perdew, J. P.; Burke, K.; Ernzerhof, M., Generalized Gradient Approximation Made Simple. *Physical Review Letters* **1996,** *77* (18), 3865-3868.

36. Blöchl, P. E., Projector augmented-wave method. *Physical Review B* **1994,** *50* (24), 17953-17979.

37. Kresse, G.; Joubert, D., From ultrasoft pseudopotentials to the projector augmented-wave method. *Physical Review B* **1999,** *59* (3), 1758-1775.

38. Grimme, S.; Antony, J.; Ehrlich, S.; Krieg, H., A consistent and accurate ab initio parametrization of density functional dispersion correction (DFT-D) for the 94 elements H-Pu. *J Chem Phys* **2010,** *132* (15), 154104.

39. Grimme, S.; Ehrlich, S.; Goerigk, L., Effect of the damping function in dispersion corrected density functional theory. *J Comput Chem* **2011,** *32* (7), 1456-65.

40. Henkelman, G.; Uberuaga, B. P.; Jónsson, H., A climbing image nudged elastic band method for finding saddle points and minimum energy paths. *The Journal of Chemical Physics* **2000,** *113* (22), 9901-9904.

41. Gessler, K.; Krauss, N.; Steiner, T.; Betzel, C.; Sarko, A.; Saenger, W., .beta.-D-Cellotetraose Hemihydrate as a Structural Model for Cellulose II. An X-ray Diffraction Study. *Journal of the American Chemical Society* **1995,** *117* (46), 11397-11406.

42. Nishiyama, Y.; Langan, P.; Chanzy, H., Crystal Structure and Hydrogen-Bonding System in Cellulose Iβ from Synchrotron X-ray and Neutron Fiber Diffraction. *Journal of the American Chemical Society* **2002,** *124* (31), 9074-9082.

43. Jacobson, R. A.; Wunderlich, J. A.; Lipscomb, W. N., The crystal and molecular structure of cellobiose. *Acta Crystallographica* **1961,** *14* (6), 598-607.

44. Irikura, K. K., Essential Statistical Thermodynamics, Appendix B. **1998,** *677*, 402-418.

45. Bader, R. F. W.; Essén, H., The characterization of atomic interactions. *The Journal of Chemical Physics* **1984,** *80* (5), 1943-1960.

46. Becke, A. D.; Edgecombe, K. E., A simple measure of electron localization in atomic and molecular systems. *The Journal of Chemical Physics* **1990,** *92* (9), 5397-5403.

47. Wu, S.; Shen, D.; Hu, J.; Zhang, H.; Xiao, R., Role of β -O-4 glycosidic bond on thermal degradation of cellulose. *Journal of Analytical and Applied Pyrolysis* **2016,** *119*, 147-156.

48. Mettler, M. S.; Paulsen, A. D.; Vlachos, D. G.; Dauenhauer, P. J., The chain length effect in pyrolysis: bridging the gap between glucose and cellulose. *Green Chemistry* **2012,** *14* (5), 1284.

49. Cho, J.; Davis, J. M.; Huber, G. W., The intrinsic kinetics and heats of reactions for cellulose pyrolysis and char formation. *ChemSusChem* **2010,** *3* (10), 1162-5.

50. Loerbroks, C.; Rinaldi, R.; Thiel, W., The electronic nature of the 1,4-beta-glycosidic bond and its chemical environment: DFT insights into cellulose chemistry. *Chemistry* **2013,** *19* (48), 16282-94.

Appendix A

The inset figure of the following transition states is provided

A	TS-transglycosylation-cellotetraose end chain scission
B	TS-transglycosylation-cellotetraose mid chain scission
C	TS-transglycosylation-cellobiose end-mid chain scission
D	TS-transglycosylation-cellulose mid chain scission
E	TS-glycosylation-cellotetraose end chain scission
F	TS-glycosylation-cellotetraose mid chain scission
G	TS-glycosylation-cellobiose end-mid chain scission
H	TS-glycosylation-cellulose mid chain scission
I	TS-ring contraction-cellotetraose end chain scission
J	TS- ring contraction -cellotetraose mid chain scission
K	TS- ring contraction -cellobiose end-mid chain scission
L	TS- ring contraction -cellulose mid chain scission


Oxygen


Hydrogen


Carbon

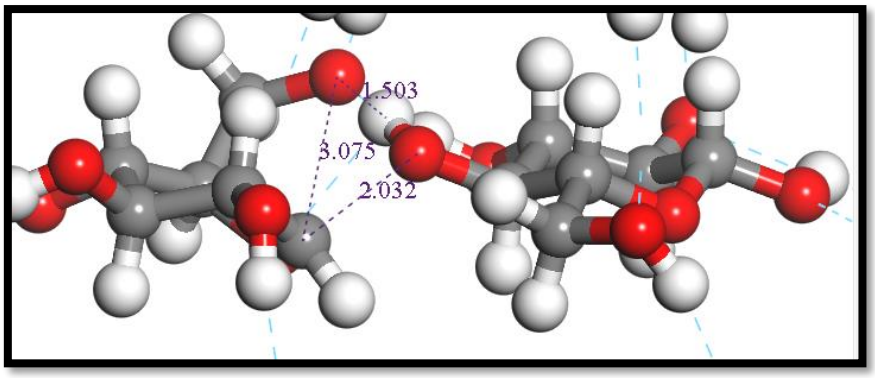

(A) TS-transglycosylation-cellotetraose end chain scission

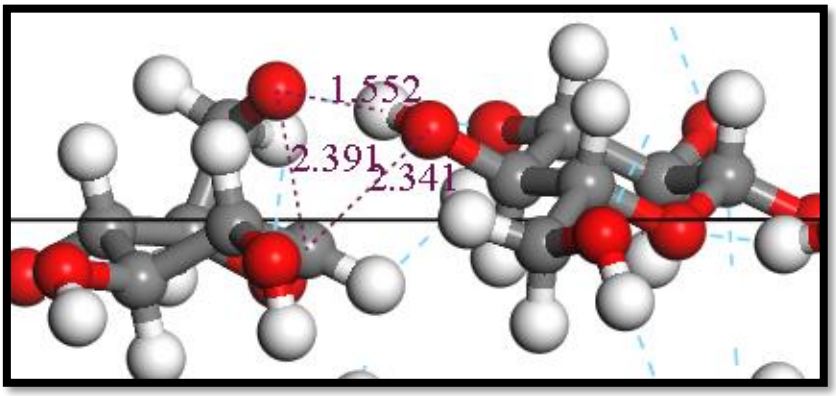

(B) TS-transglycosylation-cellotetraose mid chain scission

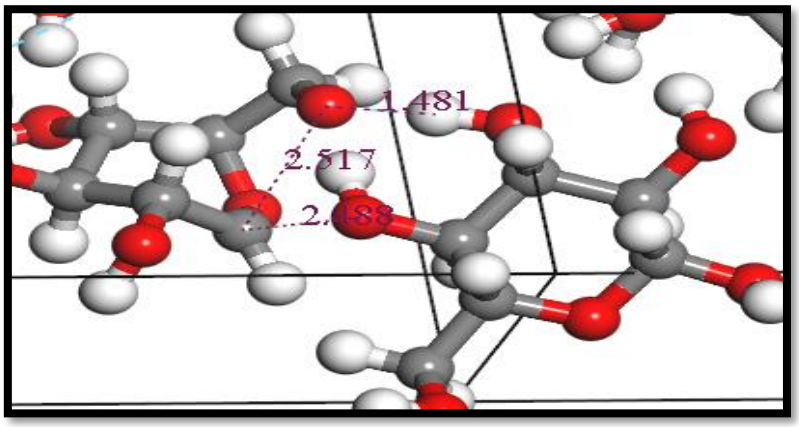

(C) TS-transglycosylation-cellobiose end-mid chain scission

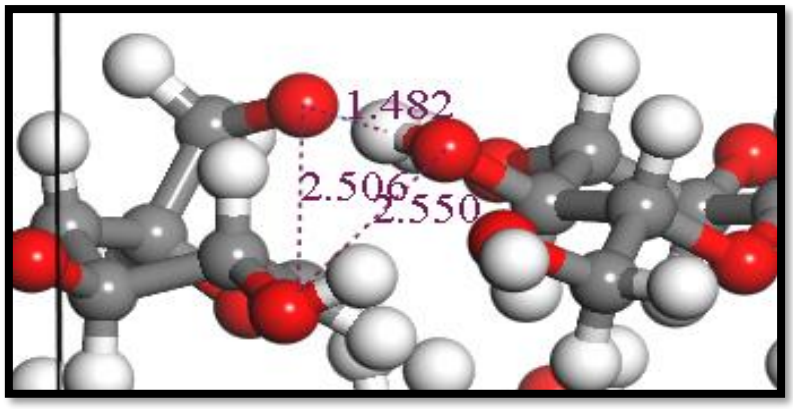

(D) TS-transglycosylation-cellulose mid chain scission

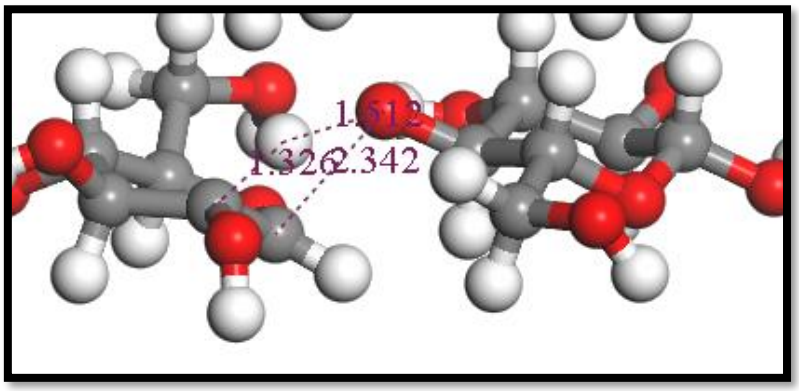

(E) TS-glycosylation-cellotetraose end chain scission

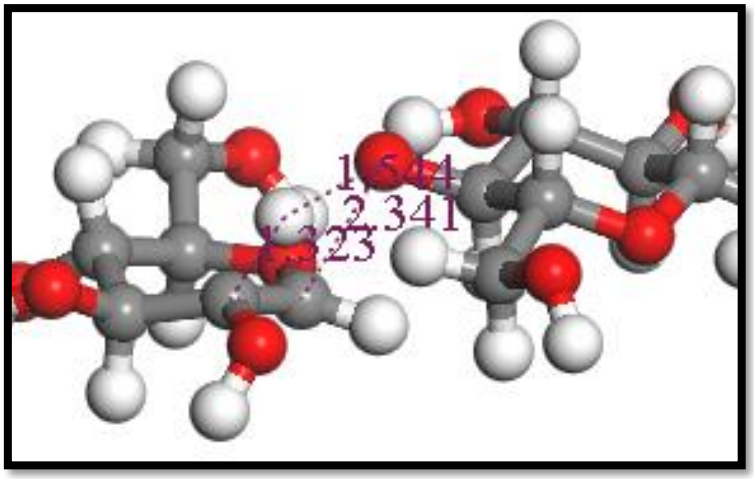

(F) TS-glycosylation-cellotetraose mid chain scission

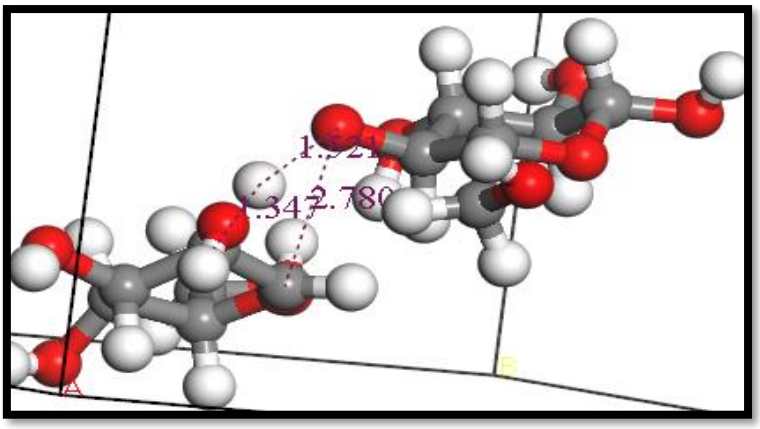

(G) TS-glycosylation-cellobiose end-mid chain scission

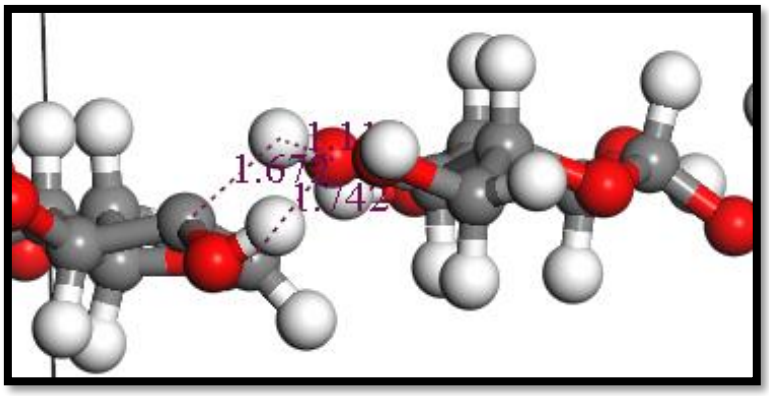

(H) TS-glycosylation-cellulose mid chain scission

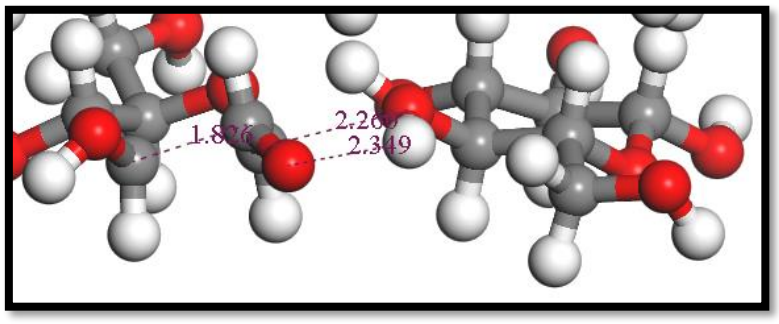

(I) TS-ring contraction-cellotetraose end chain scission

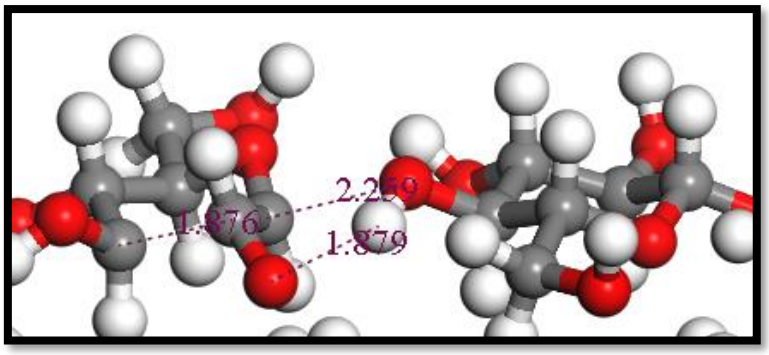

(J) TS- ring contraction -cellotetraose mid chain scission

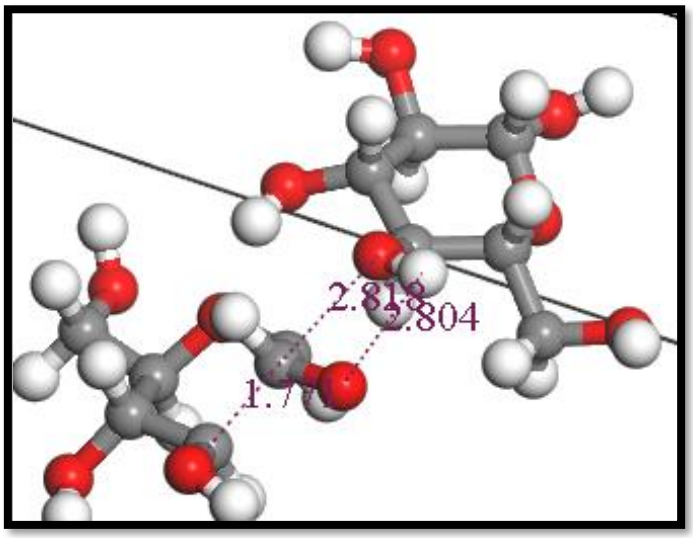

(K) TS- ring contraction -cellobiose end-mid chain scission

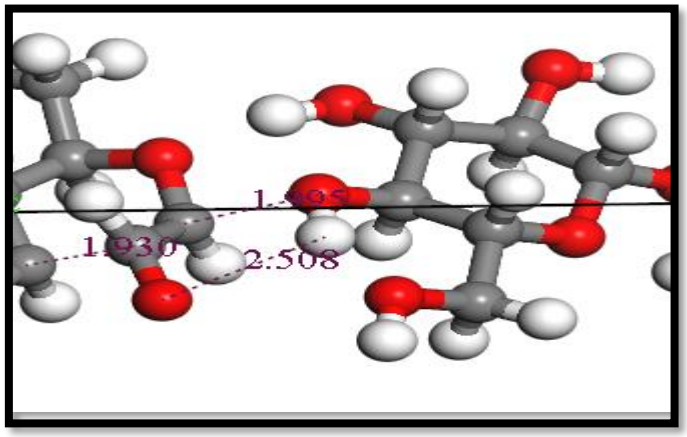

(L) TS- ring contraction -cellulose mid chain scission

Appendix B

Fractional coordinates of the optimised structures are given below.

IS – Initial state, TS- Transition state, FS – Final state

I. IS- cellotetraose

C2	C	0.81115	0.0144	0.88955
C3	C	0.98464	0.94346	0.84455
C4	C	0.93728	0.04291	0.78722
C5	C	0.76686	0.03174	0.76501
C6	C	0.60236	0.09682	0.81365
C7	C	0.43105	0.08721	0.79326
C8	C	0.76682	0.03797	0.65737
C9	C	0.6169	0.11029	0.61312
C10	C	0.69562	0.00826	0.55373
C11	C	0.87753	0.01598	0.53056
C12	C	0.01713	0.95177	0.57853
C13	C	0.19852	0.962	0.56037
C14	C	0.9438	0.00066	0.42316
C15	C	0.12182	0.92609	0.3802
C16	C	0.08198	0.03809	0.32512
C17	C	0.91845	0.0328	0.29575
C18	C	0.74857	0.09114	0.34261
C19	C	0.58576	0.0782	0.31731
C20	C	0.92147	0.05555	0.18823
C21	C	0.77075	0.13463	0.14446
C22	C	0.84384	0.03598	0.08485
C23	C	0.03489	0.02093	0.06048
C24	C	0.16673	0.96809	0.1107
C25	C	0.3489	0.97726	0.09279
C26	C	0.0443	0.51092	0.16263
C27	C	0.16515	0.52583	0.20907
C28	C	0.11679	0.46755	0.27002
C29	C	0.90404	0.55209	0.28599
C30	C	0.80114	0.53905	0.23336
C31	C	0.59077	0.632	0.24496
C32	C	0.84022	0.5435	0.39342
C33	C	0.69609	0.51662	0.43609
C34	C	0.69848	0.57264	0.50035
C35	C	0.89905	0.49436	0.51931
C36	C	0.04076	0.50897	0.47199
C37	C	0.23855	0.39803	0.48784
C38	C	0.88346	0.49698	0.628
C39	C	0.0052	0.51204	0.67429

C40	C	0.95441	0.46486	0.73703
C41	C	0.74211	0.5501	0.75308
C42	C	0.63916	0.52603	0.70257
C43	C	0.42836	0.62018	0.71431
C44	C	0.6851	0.5586	0.86117
C45	C	0.53665	0.54823	0.90649
C46	C	0.54158	0.62177	0.9676
C47	C	0.73857	0.54745	0.98855
C48	C	0.88472	0.53716	0.93742
C49	C	0.08399	0.4285	0.95218
H50	H	0.0157	0.81312	0.83401
H51	H	0.89776	0.17508	0.79828
H52	H	0.80491	0.89979	0.75459
H53	H	0.56601	0.22833	0.82499
H54	H	0.46299	0.9579	0.78142
H55	H	0.39309	0.16015	0.75262
H56	H	0.26172	0.24659	0.8593
H57	H	0.79988	0.90523	0.66404
H58	H	0.58539	0.24195	0.60602
H59	H	0.72988	0.87763	0.56398
H60	H	0.84698	0.14691	0.5214
H61	H	0.04797	0.82023	0.58666
H62	H	0.17355	0.09303	0.55759
H63	H	0.25193	0.90361	0.51568
H64	H	0.3509	0.21101	0.64642
H65	H	0.55836	0.14796	0.48819
H66	H	0.90728	0.13344	0.43257
H67	H	0.14858	0.79901	0.36642
H68	H	0.03878	0.16739	0.34087
H69	H	0.95817	0.90284	0.28168
H70	H	0.70754	0.22274	0.35533
H71	H	0.62849	0.94895	0.30231
H72	H	0.55084	0.1572	0.27803
H73	H	0.33093	0.99045	0.39051
H74	H	0.30807	0.04918	0.29536
H75	H	0.40151	0.22116	0.38383
H76	H	0.95525	0.9219	0.19268
H77	H	0.74686	0.2648	0.13816
H78	H	0.85627	0.90912	0.09206
H79	H	0.0172	0.14404	0.04432
H80	H	0.19852	0.83752	0.12132
H81	H	0.31897	0.10963	0.08861
H82	H	0.40857	0.91301	0.04919
H83	H	0.50158	0.24414	0.17664
H84	H	0.52691	0.97743	0.14957
H85	H	0.06886	0.37934	0.1574
H86	H	0.13294	0.65861	0.21385
H87	H	0.16251	0.33149	0.26639

H88	H	0.86078	0.68467	0.29705
H89	H	0.84092	0.4066	0.22344
H90	H	0.54753	0.76153	0.25962
H91	H	0.54128	0.57187	0.28047
H92	H	0.4184	0.51437	0.18861
H93	H	0.1804	0.47013	0.35221
H94	H	0.50253	0.72359	0.16632
H95	H	0.81126	0.67656	0.3919
H96	H	0.74048	0.38131	0.43618
H97	H	0.64216	0.70996	0.5026
H98	H	0.93888	0.36069	0.52594
H99	H	0.01634	0.63997	0.46838
H100	H	0.24783	0.27574	0.5005
H101	H	0.26885	0.45291	0.52654
H102	H	0.91361	0.36488	0.62056
H103	H	0.97912	0.64368	0.67686
H104	H	0.00288	0.32829	0.73714
H105	H	0.69741	0.68476	0.76023
H106	H	0.67957	0.39232	0.69556
H107	H	0.38581	0.74971	0.72877
H108	H	0.37738	0.56115	0.74977
H109	H	0.66357	0.68913	0.8556
H110	H	0.57238	0.41531	0.91179
H111	H	0.49703	0.7569	0.96256
H112	H	0.76959	0.42087	0.00445
H113	H	0.86653	0.66476	0.92851
H114	H	0.09825	0.30294	0.96279
H115	H	0.1155	0.48067	0.99149
H116	H	0.25085	0.50308	0.89899
H117	H	0.76655	0.99251	0.97607
H118	H	0.18097	0.02793	0.85609
H119	H	0.05654	0.01349	0.70435
H120	H	0.38333	0.95587	0.61581
H121	H	0.58885	0.14941	0.06122
H122	H	0.03979	0.91653	0.98052
H123	H	0.20869	0.5364	0.09796
H124	H	0.44922	0.7095	0.41703
H125	H	0.57068	0.56526	0.57832
H126	H	0.41154	0.46145	0.43351
H127	H	0.25947	0.48956	0.65576
H128	H	0.03127	0.47323	0.81729
H129	H	0.33157	0.71835	0.63777
H130	H	0.2972	0.74527	0.88308
H131	H	0.30143	0.70203	0.01502
H132	H	0.84889	0.60635	0.05583
H133	H	0.76895	0.14801	0.89939
O134	O	0.85075	0.92325	0.94172
O135	O	0.14016	0.94131	0.87142

O136	O	0.09568	0.97783	0.7446
O137	O	0.7087	0.12652	0.71162
O138	O	0.65982	0.9978	0.8655
O139	O	0.27754	0.14333	0.8377
O140	O	0.45315	0.09712	0.63659
O141	O	0.56224	0.05302	0.51123
O142	O	0.96381	0.91601	0.47674
O143	O	0.93378	0.04936	0.63302
O144	O	0.33162	0.87989	0.60244
O145	O	0.27978	0.91544	0.40864
O146	O	0.24066	0.98801	0.28325
O147	O	0.86556	0.13651	0.24454
O148	O	0.79627	0.98998	0.3943
O149	O	0.42376	0.1219	0.35865
O150	O	0.59905	0.12916	0.16388
O151	O	0.71305	0.11575	0.04078
O152	O	0.12109	0.89828	0.01354
O153	O	0.08143	0.07231	0.163
O154	O	0.47706	0.90118	0.13646
O155	O	0.07435	0.57334	0.1065
O156	O	0.35602	0.43621	0.18754
O157	O	0.21345	0.50614	0.31306
O158	O	0.84631	0.47891	0.33667
O159	O	0.85528	0.61079	0.18206
O160	O	0.5051	0.6303	0.19214
O161	O	0.5152	0.58525	0.41549
O162	O	0.58346	0.51888	0.53765
O163	O	0.91559	0.56627	0.57425
O164	O	0.02107	0.44827	0.41508
O165	O	0.37854	0.36596	0.4391
O166	O	0.19654	0.41383	0.65488
O167	O	0.05046	0.51328	0.77733
O168	O	0.68549	0.48603	0.80627
O169	O	0.69104	0.59105	0.64857
O170	O	0.34179	0.61899	0.66119
O171	O	0.35589	0.62066	0.88585
O172	O	0.41754	0.59663	0.01163
O173	O	0.73303	0.65399	0.0362
O174	O	0.86301	0.46283	0.88366
O175	O	0.21601	0.40811	0.9026

II. IS - cellobiose

C2	C	0.25564	0.2834	0.50209
C3	C	0.04766	0.59575	0.00021
C4	C	0.272	0.16791	0.46143
C5	C	0.17572	0.60914	0.11437
C6	C	0.3355	0.12251	0.7067

C7	C	0.23348	0.50333	0.16038
C8	C	0.45555	0.17983	0.76249
C9	C	0.14981	0.42825	0.30724
C10	C	0.43563	0.29676	0.76749
C11	C	0.01902	0.4289	0.19745
C12	C	0.55495	0.35633	0.78231
C13	C	0.92957	0.37134	0.37118
C14	C	0.75022	0.78351	0.46903
C15	C	0.95838	0.09584	0.97075
C16	C	0.73387	0.66803	0.50966
C17	C	0.83037	0.10929	0.85635
C18	C	0.67049	0.62258	0.26428
C19	C	0.77237	0.00363	0.8099
C20	C	0.55039	0.67982	0.20815
C21	C	0.85611	0.92833	0.6641
C22	C	0.57022	0.79677	0.20322
C23	C	0.98686	0.9288	0.77437
C24	C	0.45078	0.85616	0.18837
C25	C	0.07628	0.87126	0.60047
H26	H	0.20309	0.29982	0.6833
H27	H	0.05109	0.55429	0.80921
H28	H	0.92694	0.6793	0.83004
H29	H	0.33209	0.15783	0.29113
H30	H	0.11531	0.09775	0.55696
H31	H	0.16942	0.64906	0.3067
H32	H	0.33311	0.65726	0.95571
H33	H	0.27515	0.13056	0.87822
H34	H	0.29364	0.97043	0.70851
H35	H	0.25043	0.46966	0.96228
H36	H	0.37292	0.45509	0.37995
H37	H	0.51847	0.16118	0.60084
H38	H	0.49727	0.07489	0.03669
H39	H	0.1497	0.44948	0.51843
H40	H	0.37823	0.31729	0.9372
H41	H	0.01777	0.39392	0.9985
H42	H	0.61656	0.32842	0.62793
H43	H	0.5733	0.48504	0.58095
H44	H	0.96712	0.29545	0.42005
H45	H	0.80326	0.29522	0.15827
H46	H	0.59832	0.34145	0.97539
H47	H	0.91807	0.41456	0.55644
H48	H	0.80294	0.79991	0.28805
H49	H	0.95477	0.0546	0.16208
H50	H	0.07915	0.1794	0.14048
H51	H	0.67372	0.65789	0.67983
H52	H	0.89076	0.59797	0.41472
H53	H	0.83669	0.14931	0.66419
H54	H	0.67295	0.15744	0.01493

H55	H	0.73094	0.63061	0.09289
H56	H	0.71235	0.47045	0.26264
H57	H	0.75479	0.97009	0.0079
H58	H	0.63301	0.95564	0.58961
H59	H	0.48734	0.66114	0.36958
H60	H	0.50875	0.57484	0.93394
H61	H	0.85652	0.94946	0.45285
H62	H	0.62753	0.81736	0.03343
H63	H	0.98799	0.89378	0.97332
H64	H	0.38929	0.82821	0.34294
H65	H	0.43231	0.9849	0.38953
H66	H	0.03887	0.79529	0.55181
H67	H	0.20282	0.79536	0.81289
H68	H	0.40736	0.84118	-0.00459
H69	H	0.08751	0.91455	0.41522
O70	O	0.19738	0.32515	0.27947
O71	O	0.98882	0.68896	0.97378
O72	O	0.16041	0.11782	0.39627
O73	O	0.24383	0.66911	0.93145
O74	O	0.36361	0.01632	0.67022
O75	O	0.34423	0.51994	0.29938
O76	O	0.50894	0.15034	0.01039
O77	O	0.37427	0.32788	0.52668
O78	O	0.97754	0.53339	0.18013
O79	O	0.53499	0.4637	0.74992
O80	O	0.81222	0.36259	0.24942
O81	O	0.80828	0.82531	0.69185
O82	O	0.01733	0.18904	0.99669
O83	O	0.84554	0.61806	0.57519
O84	O	0.76223	0.16919	0.03945
O85	O	0.64239	0.51634	0.30065
O86	O	0.6621	0.02055	0.66938
O87	O	0.4972	0.65031	0.96009
O88	O	0.63157	0.82799	0.44399
O89	O	0.0286	0.03322	0.79174
O90	O	0.47051	0.96357	0.2204
O91	O	0.19382	0.86265	0.72146

III. IS-cellulose

C2	C	0.01328	0.96647	0.05764
C3	C	0.97534	0.81684	0.9698
C4	C	0.04562	0.85428	0.83563
C5	C	0.98759	0.01611	0.78837
C6	C	0.02755	0.15532	0.88629
C7	C	0.95393	0.31343	0.84867
C8	C	0.51458	0.45893	0.29814
C9	C	0.47541	0.31631	0.20364

C10	C	0.55928	0.36206	0.07415
C11	C	0.49956	0.52458	0.02955
C12	C	0.54194	0.66211	0.12851
C13	C	0.46577	0.82015	0.09489
C14	C	0.98672	0.03353	0.55764
C15	C	0.02466	0.18316	0.4698
C16	C	0.95438	0.14572	0.33563
C17	C	0.01241	0.98389	0.28837
C18	C	0.97245	0.84468	0.38629
C19	C	0.04607	0.68657	0.34867
C20	C	0.48542	0.54107	0.79814
C21	C	0.52459	0.68369	0.70364
C22	C	0.44072	0.63794	0.57415
C23	C	0.50044	0.47542	0.52955
C24	C	0.45806	0.33789	0.62851
C25	C	0.53423	0.17985	0.59489
H26	H	0.64202	0.49306	0.5151
H27	H	0.15472	0.99417	0.07375
H28	H	0.83291	0.79369	0.96365
H29	H	0.1876	0.86299	0.83346
H30	H	0.84584	0.99899	0.77301
H31	H	0.16971	0.18176	0.89757
H32	H	0.94148	0.38522	0.93694
H33	H	0.82427	0.28433	0.80594
H34	H	0.65474	0.47951	0.31843
H35	H	0.33367	0.29783	0.18626
H36	H	0.70134	0.37566	0.08565
H37	H	0.35798	0.50694	0.0151
H38	H	0.68261	0.68765	0.14314
H39	H	0.47314	0.89869	0.181
H40	H	0.329	0.78841	0.06783
H41	H	0.99666	0.64991	0.10532
H42	H	0.86449	0.69478	0.76209
H43	H	0.04528	0.52557	0.76821
H44	H	0.49147	0.15082	0.34224
H45	H	0.53372	0.27304	0.89654
H46	H	0.55607	0.02598	0.00491
H47	H	0.84528	0.00583	0.57375
H48	H	0.16709	0.20631	0.46365
H49	H	0.8124	0.13701	0.33346
H50	H	0.15416	0.00101	0.27301
H51	H	0.83029	0.81824	0.39757
H52	H	0.05852	0.61478	0.43694
H53	H	0.17573	0.71567	0.30594
H54	H	0.34526	0.52049	0.81843
H55	H	0.66633	0.70217	0.68626
H56	H	0.29866	0.62434	0.58565
H57	H	0.31739	0.31235	0.64314

H58	H	0.52686	0.10131	0.681
H59	H	0.671	0.21159	0.56783
H60	H	0.00334	0.35009	0.60532
H61	H	0.13551	0.30522	0.26209
H62	H	0.95472	0.47443	0.26821
H63	H	0.50853	0.84918	0.84224
H64	H	0.46628	0.72696	0.39654
H65	H	0.44393	0.97402	0.50491
O66	O	0.04781	0.67792	0.0187
O67	O	0.98935	0.71953	0.75025
O68	O	0.07276	0.07247	0.67288
O69	O	0.9473	0.10695	0.00556
O70	O	0.06595	0.40808	0.75969
O71	O	0.53504	0.17236	0.25178
O72	O	0.50699	0.2323	0.98498
O73	O	0.58126	0.57829	0.91011
O74	O	0.45886	0.60849	0.24828
O75	O	0.56079	0.90647	0.9928
O76	O	0.95219	0.32208	0.5187
O77	O	0.01065	0.28047	0.25025
O78	O	0.92724	0.92753	0.17288
O79	O	0.0527	0.89305	0.50556
O80	O	0.93405	0.59192	0.25969
O81	O	0.46496	0.82764	0.75178
O82	O	0.49301	0.7677	0.48498
O83	O	0.41874	0.42171	0.41011
O84	O	0.54114	0.39151	0.74828
O85	O	0.43921	0.09353	0.4928

A. TS-transglycosylation-cellotetraose end chain scission

C2	C	0.81375	0.01651	0.88951
C3	C	0.98692	0.94245	0.84427
C4	C	0.94023	0.04136	0.78682
C5	C	0.76846	0.03176	0.76518
C6	C	0.60374	0.09965	0.81357
C7	C	0.43402	0.08731	0.79299
C8	C	0.76692	0.0354	0.65782
C9	C	0.61493	0.10515	0.61421
C10	C	0.69162	0.00364	0.55491
C11	C	0.87122	0.01458	0.53068
C12	C	0.01361	0.95183	0.57804
C13	C	0.19315	0.96528	0.55982
C14	C	0.93709	0.99911	0.42328
C15	C	0.11583	0.91876	0.38109
C16	C	0.085	0.02671	0.32518
C17	C	0.91873	0.02777	0.29633
C18	C	0.74526	0.09046	0.34188

C19	C	0.58823	0.07104	0.31377
C20	C	0.92778	0.04868	0.18871
C21	C	0.77489	0.12472	0.14565
C22	C	0.84607	0.02973	0.08537
C23	C	0.0335	0.02214	0.06049
C24	C	0.16861	0.96885	0.10991
C25	C	0.34874	0.98149	0.09155
C26	C	0.05602	0.49782	0.15025
C27	C	0.17931	0.51704	0.19439
C28	C	0.13665	0.46407	0.25698
C29	C	0.9242	0.54937	0.27533
C30	C	0.81842	0.52516	0.22485
C31	C	0.60695	0.61715	0.23559
C32	C	0.77828	0.63149	0.40427
C33	C	0.68115	0.54154	0.43929
C34	C	0.68514	0.5729	0.50731
C35	C	0.8914	0.50018	0.52057
C36	C	0.01835	0.5369	0.47315
C37	C	0.18887	0.38364	0.4441
C38	C	0.88712	0.4915	0.62948
C39	C	0.00832	0.5074	0.67592
C40	C	0.95555	0.46345	0.73902
C41	C	0.74266	0.54724	0.75425
C42	C	0.64163	0.52284	0.70333
C43	C	0.43083	0.61765	0.71471
C44	C	0.68298	0.55437	0.86172
C45	C	0.53409	0.5454	0.90715
C46	C	0.54015	0.6215	0.96761
C47	C	0.73734	0.54857	0.98852
C48	C	0.88289	0.53622	0.9368
C49	C	0.083	0.42977	0.95105
H50	H	0.01509	0.81263	0.83401
H51	H	0.90311	0.17336	0.79741
H52	H	0.80494	0.89982	0.75523
H53	H	0.56781	0.23175	0.82375
H54	H	0.4695	0.9569	0.78147
H55	H	0.39585	0.15905	0.75208
H56	H	0.26211	0.24621	0.85864
H57	H	0.80211	0.90241	0.66517
H58	H	0.58222	0.23678	0.60642
H59	H	0.7277	0.87237	0.56475
H60	H	0.83737	0.1463	0.52168
H61	H	0.04727	0.81963	0.58629
H62	H	0.16589	0.09722	0.55917
H63	H	0.24553	0.91229	0.51438
H64	H	0.35061	0.20502	0.64818
H65	H	0.54775	0.1463	0.49188
H66	H	0.90602	0.13113	0.43254

H67	H	0.13879	0.79238	0.36781
H68	H	0.04965	0.15537	0.33994
H69	H	0.95488	0.89815	0.28268
H70	H	0.70193	0.22321	0.3536
H71	H	0.64819	0.95003	0.28932
H72	H	0.53492	0.16788	0.2804
H73	H	0.341	0.96194	0.38923
H74	H	0.33038	0.00313	0.29958
H75	H	0.3335	0.19308	0.36596
H76	H	0.96633	0.91414	0.19349
H77	H	0.74706	0.25605	0.1398
H78	H	0.86313	0.90103	0.09149
H79	H	0.00942	0.14825	0.04586
H80	H	0.20401	0.83714	0.11979
H81	H	0.31668	0.11494	0.09011
H82	H	0.40382	0.92498	0.04654
H83	H	0.50539	0.23307	0.17367
H84	H	0.53263	0.97259	0.14789
H85	H	0.08429	0.3652	0.14498
H86	H	0.14657	0.65028	0.19725
H87	H	0.1822	0.32747	0.25497
H88	H	0.88045	0.68401	0.28135
H89	H	0.86139	0.39122	0.217
H90	H	0.56324	0.74745	0.2495
H91	H	0.55512	0.55818	0.27093
H92	H	0.43455	0.50062	0.17498
H93	H	0.22856	0.45165	0.33508
H94	H	0.51828	0.70942	0.15715
H95	H	0.69556	0.74035	0.37884
H96	H	0.76599	0.40639	0.43089
H97	H	0.6141	0.70755	0.51859
H98	H	0.93989	0.3642	0.52332
H99	H	0.06805	0.61593	0.49543
H100	H	0.21569	0.27916	0.47479
H101	H	0.31038	0.41162	0.44242
H102	H	0.91652	0.35938	0.62221
H103	H	0.98257	0.63912	0.67775
H104	H	0.00585	0.32678	0.7404
H105	H	0.69743	0.682	0.76166
H106	H	0.68194	0.38895	0.69658
H107	H	0.38875	0.74713	0.72917
H108	H	0.37906	0.55913	0.75019
H109	H	0.66145	0.68507	0.85623
H110	H	0.56813	0.41294	0.91305
H111	H	0.49717	0.75606	0.96133
H112	H	0.76947	0.42258	0.00541
H113	H	0.86364	0.66364	0.92666
H114	H	0.09917	0.30423	0.96273

H115	H	0.11514	0.48452	0.9894
H116	H	0.24999	0.50277	0.89723
H117	H	0.7647	0.99227	0.97576
H118	H	0.18467	0.02544	0.8558
H119	H	0.05798	0.01259	0.70401
H120	H	0.38114	0.95339	0.61521
H121	H	0.5887	0.13716	0.06304
H122	H	0.03634	0.91973	0.98033
H123	H	0.21082	0.53117	0.0837
H124	H	0.42497	0.7024	0.42138
H125	H	0.55757	0.53618	0.58038
H126	H	0.0048	0.41746	0.35448
H127	H	0.26245	0.48426	0.65699
H128	H	0.03441	0.47466	0.81882
H129	H	0.32948	0.71838	0.63857
H130	H	0.29615	0.74348	0.88299
H131	H	0.29883	0.70656	0.01439
H132	H	0.84848	0.61203	0.05409
H133	H	0.77583	0.14951	0.89922
O134	O	0.85171	0.92468	0.94162
O135	O	0.14473	0.93765	0.87043
O136	O	0.09778	0.97358	0.7439
O137	O	0.71018	0.12557	0.71169
O138	O	0.65983	0.00324	0.86604
O139	O	0.27956	0.14229	0.83704
O140	O	0.45273	0.0909	0.63865
O141	O	0.55447	0.04879	0.51336
O142	O	0.95549	0.9152	0.47701
O143	O	0.93139	0.0489	0.6326
O144	O	0.32877	0.87875	0.60093
O145	O	0.27172	0.90624	0.41134
O146	O	0.24402	0.96622	0.28325
O147	O	0.87005	0.13051	0.24478
O148	O	0.78635	0.994	0.39473
O149	O	0.44137	0.07434	0.35483
O150	O	0.60645	0.1157	0.16691
O151	O	0.71122	0.11031	0.04245
O152	O	0.12108	0.90417	0.01217
O153	O	0.08454	0.07007	0.16301
O154	O	0.4821	0.89834	0.13304
O155	O	0.07777	0.56354	0.09396
O156	O	0.3684	0.4262	0.17139
O157	O	0.2375	0.50721	0.29684
O158	O	0.88013	0.48687	0.33222
O159	O	0.86786	0.59418	0.17164
O160	O	0.52352	0.61419	0.18225
O161	O	0.50529	0.57943	0.42061
O162	O	0.59267	0.4887	0.53931

O163	O	0.9219	0.56034	0.57605
O164	O	0.9165	0.64602	0.42592
O165	O	0.1651	0.33924	0.38631
O166	O	0.20024	0.40813	0.65762
O167	O	0.0488	0.51674	0.77885
O168	O	0.68355	0.48254	0.80677
O169	O	0.69495	0.58709	0.64956
O170	O	0.34517	0.61637	0.66119
O171	O	0.35351	0.61891	0.88642
O172	O	0.41469	0.6008	0.01239
O173	O	0.73154	0.65808	0.03498
O174	O	0.86059	0.45846	0.88409
O175	O	0.21215	0.40934	0.90052

FS-transglycosylation-cellotetraose end chain scission

C2	C	0.80505	0.00807	0.88716
C3	C	0.97415	0.92681	0.84098
C4	C	0.9263	0.02771	0.78396
C5	C	0.7474	0.02896	0.76329
C6	C	0.58827	0.0954	0.81377
C7	C	0.41311	0.08904	0.79515
C8	C	0.74814	0.05319	0.65589
C9	C	0.60021	0.13397	0.61125
C10	C	0.68065	0.05022	0.54937
C11	C	0.86645	0.05689	0.53115
C12	C	0.00042	0.98112	0.57991
C13	C	0.1865	0.98512	0.56583
C14	C	0.93734	0.02941	0.42259
C15	C	0.12113	0.94015	0.38339
C16	C	0.09883	0.0102	0.32041
C17	C	0.93524	0.00246	0.29318
C18	C	0.75752	0.06908	0.33683
C19	C	0.62467	0.01101	0.31205
C20	C	0.94099	0.03201	0.18469
C21	C	0.78519	0.1155	0.14306
C22	C	0.8504	0.03567	0.08029
C23	C	0.03208	0.0404	0.05644
C24	C	0.17151	0.9774	0.10444
C25	C	0.34898	0.99538	0.08853
C26	C	0.08684	0.51805	0.13805
C27	C	0.20337	0.50251	0.19064
C28	C	0.1537	0.41151	0.24182
C29	C	0.94299	0.49662	0.25818
C30	C	0.84126	0.51254	0.20222
C31	C	0.63205	0.6042	0.21562
C32	C	0.84826	0.60135	0.41609
C33	C	0.70881	0.5478	0.45118

C34	C	0.70968	0.57679	0.51859
C35	C	0.91346	0.51541	0.53482
C36	C	0.0296	0.56628	0.48831
C37	C	0.15038	0.42998	0.44183
C38	C	0.88877	0.50864	0.64201
C39	C	0.00659	0.51636	0.69068
C40	C	0.94902	0.46301	0.75102
C41	C	0.73559	0.54381	0.76433
C42	C	0.64065	0.52619	0.71072
C43	C	0.42968	0.61507	0.71942
C44	C	0.67129	0.54125	0.87025
C45	C	0.52022	0.53503	0.91532
C46	C	0.52139	0.62893	0.97215
C47	C	0.7141	0.56028	0.99626
C48	C	0.86829	0.52923	0.94544
C49	C	0.0628	0.42098	0.96387
H50	H	0.9936	0.79924	0.83141
H51	H	0.89549	0.15797	0.79513
H52	H	0.77634	0.90021	0.75087
H53	H	0.55668	0.22598	0.82478
H54	H	0.44607	0.96278	0.77889
H55	H	0.36468	0.17371	0.75773
H56	H	0.25076	0.22822	0.867
H57	H	0.78447	0.91874	0.65863
H58	H	0.56605	0.26716	0.60876
H59	H	0.71136	0.91719	0.55299
H60	H	0.83901	0.18761	0.52403
H61	H	0.02499	0.8499	0.58503
H62	H	0.16856	0.11443	0.56639
H63	H	0.24252	0.93207	0.52053
H64	H	0.33938	0.22224	0.64799
H65	H	0.60615	0.07742	0.4677
H66	H	0.89809	0.16448	0.4267
H67	H	0.15555	0.80654	0.38174
H68	H	0.06693	0.14289	0.32401
H69	H	0.97581	0.87125	0.28018
H70	H	0.69761	0.20655	0.33782
H71	H	0.66521	0.88188	0.32552
H72	H	0.6409	0.01371	0.26295
H73	H	0.31871	0.0197	0.38428
H74	H	0.34282	0.9782	0.28822
H75	H	0.37984	0.21738	0.31577
H76	H	0.98659	0.89582	0.18574
H77	H	0.75793	0.24736	0.14103
H78	H	0.87335	0.90471	0.08174
H79	H	0.00086	0.17122	0.04671
H80	H	0.2093	0.84389	0.11025
H81	H	0.31646	0.12893	0.08965

H82	H	0.4096	0.94281	0.04342
H83	H	0.51885	0.22644	0.17114
H84	H	0.54125	0.97439	0.14373
H85	H	0.12029	0.3908	0.12094
H86	H	0.17292	0.6291	0.20632
H87	H	0.19359	0.28173	0.22735
H88	H	0.90503	0.62344	0.27658
H89	H	0.88006	0.38532	0.18514
H90	H	0.59175	0.73157	0.23227
H91	H	0.58543	0.53959	0.25013
H92	H	0.45038	0.50014	0.16386
H93	H	0.16709	0.45322	0.32806
H94	H	0.51355	0.72252	0.14461
H95	H	0.78754	0.67216	0.3768
H96	H	0.75816	0.4133	0.44339
H97	H	0.6345	0.71158	0.52912
H98	H	0.97516	0.37849	0.53742
H99	H	0.11027	0.61742	0.51052
H100	H	0.19956	0.30305	0.45828
H101	H	0.26931	0.44995	0.42247
H102	H	0.91801	0.37784	0.63208
H103	H	0.98301	0.64688	0.69566
H104	H	0.99988	0.32616	0.74894
H105	H	0.68748	0.67771	0.77443
H106	H	0.68564	0.39323	0.69997
H107	H	0.37981	0.74435	0.73536
H108	H	0.3765	0.55128	0.75239
H109	H	0.65122	0.67158	0.86541
H110	H	0.55777	0.40385	0.92542
H111	H	0.48495	0.75905	0.95969
H112	H	0.73758	0.44356	0.01923
H113	H	0.85775	0.6523	0.93229
H114	H	0.07075	0.29985	0.97799
H115	H	0.0884	0.48284	0.00172
H116	H	0.23721	0.48049	0.90876
H117	H	0.75614	0.9941	0.97377
H118	H	0.17387	0.00588	0.85469
H119	H	0.04357	0.00685	0.70147
H120	H	0.37717	0.96004	0.62027
H121	H	0.58953	0.14859	0.06131
H122	H	0.02761	0.94168	0.97598
H123	H	0.24366	0.56602	0.07451
H124	H	0.4687	0.74273	0.43259
H125	H	0.57001	0.54351	0.58978
H126	H	0.93951	0.39676	0.33633
H127	H	0.25866	0.49315	0.66565
H128	H	0.0152	0.4625	0.83304
H129	H	0.32774	0.72147	0.6435

H130	H	0.28519	0.71969	0.88413
H131	H	0.27352	0.73772	0.01376
H132	H	0.76447	0.63316	0.07401
H133	H	0.76999	0.14137	0.8946
O134	O	0.84416	0.92268	0.94074
O135	O	0.14027	0.91152	0.86424
O136	O	0.08109	0.95677	0.74046
O137	O	0.68426	0.13187	0.71194
O138	O	0.64847	0.99576	0.86539
O139	O	0.2689	0.12908	0.8424
O140	O	0.43797	0.11368	0.63085
O141	O	0.54702	0.12788	0.50724
O142	O	0.95916	0.95728	0.47807
O143	O	0.91423	0.07131	0.63542
O144	O	0.31264	0.8929	0.60879
O145	O	0.26548	0.95951	0.41097
O146	O	0.26257	0.92426	0.28123
O147	O	0.88148	0.10481	0.24177
O148	O	0.79116	0.00676	0.39609
O149	O	0.43248	0.10313	0.33306
O150	O	0.61666	0.1071	0.16412
O151	O	0.70998	0.1248	0.03976
O152	O	0.11904	0.93793	0.00399
O153	O	0.09127	0.06519	0.16037
O154	O	0.475	0.90958	0.13176
O155	O	0.11394	0.61561	0.09284
O156	O	0.39402	0.41703	0.16923
O157	O	0.25665	0.40727	0.29229
O158	O	0.87976	0.40646	0.29913
O159	O	0.89372	0.60254	0.15693
O160	O	0.54407	0.61032	0.16243
O161	O	0.53027	0.62024	0.42933
O162	O	0.61815	0.49098	0.54981
O163	O	0.92799	0.5821	0.59088
O164	O	0.90668	0.69324	0.45124
O165	O	0.02259	0.45529	0.39568
O166	O	0.19876	0.41587	0.67337
O167	O	0.03744	0.50881	0.79473
O168	O	0.67546	0.47195	0.81466
O169	O	0.69576	0.60219	0.66093
O170	O	0.35602	0.61316	0.66331
O171	O	0.34183	0.59814	0.89344
O172	O	0.38574	0.63042	0.01791
O173	O	0.71353	0.68237	0.03671
O174	O	0.84676	0.44521	0.8944
O175	O	0.20308	0.38593	0.91555

B. TS-transglycosylation-cellotetraose mid chain scission

C2	C	0.80861	0.01518	0.89635
C3	C	0.97969	0.9466	0.85039
C4	C	0.93016	0.0485	0.79385
C5	C	0.75736	0.03874	0.77312
C6	C	0.59442	0.10211	0.82196
C7	C	0.42604	0.0874	0.80143
C8	C	0.74659	0.04398	0.66694
C9	C	0.59335	0.11375	0.62354
C10	C	0.6681	0.00691	0.56577
C11	C	0.8552	0.00099	0.54184
C12	C	0.99644	0.94823	0.58886
C13	C	0.17283	0.96459	0.56734
C14	C	0.94664	0.06961	0.41528
C15	C	0.11929	0.96315	0.37638
C16	C	0.09239	0.05206	0.31607
C17	C	0.91962	0.04936	0.29287
C18	C	0.7488	0.12585	0.33914
C19	C	0.67649	-0.00029	0.36274
C20	C	0.92732	0.05568	0.18589
C21	C	0.77437	0.12835	0.14329
C22	C	0.84655	0.03171	0.08375
C23	C	0.03611	0.02151	0.05886
C24	C	0.1698	0.96993	0.10864
C25	C	0.35346	0.9768	0.09095
C26	C	0.04438	0.5032	0.16177
C27	C	0.16714	0.51519	0.20825
C28	C	0.12027	0.45283	0.26859
C29	C	0.9075	0.54132	0.28565
C30	C	0.80112	0.53227	0.23316
C31	C	0.59135	0.63006	0.2453
C32	C	0.84464	0.53337	0.39287
C33	C	0.6914	0.52267	0.43616
C34	C	0.69507	0.58284	0.4995
C35	C	0.89446	0.49774	0.51889
C36	C	0.04025	0.50292	0.47103
C37	C	0.2353	0.40001	0.48982
C38	C	0.88167	0.5011	0.62729
C39	C	0.00344	0.51705	0.67335
C40	C	0.95531	0.46791	0.73604
C41	C	0.74354	0.55227	0.75242
C42	C	0.63951	0.52843	0.70222
C43	C	0.42908	0.62105	0.71563
C44	C	0.68627	0.56068	0.86022
C45	C	0.53737	0.54982	0.90512
C46	C	0.54098	0.62278	0.96646
C47	C	0.73777	0.54884	0.9875
C48	C	0.88239	0.54343	0.93669
C49	C	0.08173	0.44051	0.95241

H50	H	0.01016	0.8168	0.83905
H51	H	0.8935	0.18012	0.80493
H52	H	0.79577	0.90669	0.76253
H53	H	0.55587	0.23425	0.833
H54	H	0.46227	0.95578	0.79178
H55	H	0.38963	0.15449	0.75958
H56	H	0.25282	0.25386	0.8642
H57	H	0.77951	0.9116	0.67477
H58	H	0.5639	0.24429	0.6146
H59	H	0.68869	0.8797	0.57642
H60	H	0.82538	0.13165	0.53014
H61	H	0.03312	0.8172	0.59984
H62	H	0.1392	0.09752	0.56288
H63	H	0.22509	0.90247	0.52303
H64	H	0.32825	0.22182	0.65493
H65	H	0.53584	0.16186	0.5029
H66	H	0.96436	0.11573	0.45787
H67	H	0.1358	0.8359	0.36997
H68	H	0.06298	0.18305	0.32444
H69	H	0.95293	0.91812	0.28304
H70	H	0.64071	0.23934	0.32209
H71	H	0.65232	0.94387	0.32212
H72	H	0.54006	0.07146	0.38853
H73	H	0.27327	0.05744	0.41232
H74	H	0.34737	0.99591	0.28544
H75	H	0.84472	0.90158	0.46043
H76	H	0.9662	0.92157	0.19233
H77	H	0.74417	0.26006	0.13686
H78	H	0.86292	0.90334	0.09031
H79	H	0.01387	0.14645	0.04329
H80	H	0.20107	0.83985	0.12002
H81	H	0.32575	0.10903	0.08803
H82	H	0.41217	0.91496	0.04692
H83	H	0.50878	0.23029	0.17836
H84	H	0.53447	0.96892	0.14807
H85	H	0.06844	0.37194	0.15563
H86	H	0.13505	0.64774	0.21398
H87	H	0.16147	0.31794	0.2627
H88	H	0.86845	0.67285	0.29718
H89	H	0.83606	0.40097	0.22325
H90	H	0.55717	0.75901	0.25837
H91	H	0.53934	0.57612	0.28235
H92	H	0.41934	0.50395	0.18815
H93	H	0.19365	0.44584	0.35081
H94	H	0.50161	0.7176	0.16636
H95	H	0.8286	0.66262	0.39002
H96	H	0.72051	0.39179	0.43926
H97	H	0.64748	0.71935	0.50038

H98	H	0.92705	0.36547	0.52633
H99	H	0.01665	0.63215	0.46354
H100	H	0.24537	0.27898	0.50493
H101	H	0.25608	0.46311	0.52826
H102	H	0.91167	0.36874	0.62027
H103	H	0.97594	0.6491	0.67601
H104	H	0.00351	0.33124	0.73579
H105	H	0.69853	0.68712	0.75955
H106	H	0.68107	0.39455	0.69485
H107	H	0.38677	0.75016	0.73076
H108	H	0.38233	0.55964	0.75134
H109	H	0.66298	0.69174	0.85451
H110	H	0.57246	0.41684	0.90999
H111	H	0.49636	0.75802	0.96149
H112	H	0.77153	0.4205	0.00206
H113	H	0.85944	0.67214	0.92763
H114	H	0.09886	0.31531	0.96517
H115	H	0.10955	0.49923	0.9907
H116	H	0.25153	0.51089	0.89816
H117	H	0.76606	0.98483	0.98169
H118	H	0.17482	0.0322	0.86307
H119	H	0.04376	0.01816	0.7105
H120	H	0.35534	0.97168	0.62262
H121	H	0.58821	0.14235	0.0628
H122	H	0.03955	0.91352	0.9802
H123	H	0.20686	0.5301	0.09675
H124	H	0.45695	0.72241	0.41811
H125	H	0.5688	0.57919	0.57836
H126	H	0.4055	0.46201	0.43627
H127	H	0.25862	0.49469	0.65608
H128	H	0.03183	0.47719	0.81632
H129	H	0.32409	0.72324	0.64056
H130	H	0.29561	0.74876	0.88379
H131	H	0.30084	0.70237	0.01375
H132	H	0.84532	0.6029	0.05662
H133	H	0.76982	0.14741	0.90799
O134	O	0.85119	0.91769	0.9469
O135	O	0.13681	0.94231	0.87682
O136	O	0.08632	0.98197	0.75033
O137	O	0.69334	0.13464	0.72053
O138	O	0.65343	0.00316	0.8736
O139	O	0.27017	0.14678	0.84497
O140	O	0.42897	0.10453	0.64881
O141	O	0.54144	0.05889	0.52047
O142	O	0.93627	0.89165	0.49182
O143	O	0.91294	0.05375	0.64138
O144	O	0.31219	0.89042	0.60796
O145	O	0.28154	0.94788	0.40302

O146	O	0.24709	0.97201	0.27391
O147	O	0.86433	0.14367	0.24034
O148	O	0.79672	0.17742	0.39315
O149	O	0.8106	0.88582	0.39497
O150	O	0.60788	0.11657	0.16532
O151	O	0.7102	0.11276	0.04125
O152	O	0.12462	0.90038	0.0118
O153	O	0.08411	0.07625	0.16036
O154	O	0.48117	0.8958	0.13443
O155	O	0.07252	0.56911	0.10612
O156	O	0.35792	0.42613	0.18591
O157	O	0.22479	0.48159	0.31139
O158	O	0.84944	0.46741	0.33617
O159	O	0.85576	0.60311	0.18168
O160	O	0.49964	0.62914	0.1938
O161	O	0.51123	0.60043	0.41437
O162	O	0.57236	0.53881	0.5374
O163	O	0.91347	0.56943	0.57354
O164	O	0.02256	0.43021	0.41624
O165	O	0.37993	0.36397	0.4427
O166	O	0.19406	0.42027	0.65335
O167	O	0.05246	0.51557	0.77619
O168	O	0.68827	0.48713	0.80545
O169	O	0.68901	0.59518	0.64825
O170	O	0.33817	0.62191	0.66339
O171	O	0.35752	0.62339	0.88375
O172	O	0.41673	0.59674	0.01012
O173	O	0.73104	0.65277	0.03622
O174	O	0.86424	0.46659	0.88294
O175	O	0.21423	0.41717	0.9028

FS-transglycosylation-cellotetraose mid chain scission

C2	C	0.81528	0.98825	0.89338
C3	C	0.98249	0.91986	0.84632
C4	C	0.92859	0.03176	0.79241
C5	C	0.75089	0.02992	0.77217
C6	C	0.59258	0.08765	0.82248
C7	C	0.41967	0.07921	0.80294
C8	C	0.74278	0.04804	0.66669
C9	C	0.59441	0.11542	0.62175
C10	C	0.67802	0.99918	0.56657
C11	C	0.87209	0.98128	0.54464
C12	C	0.00225	0.94369	0.59401
C13	C	0.18209	0.95262	0.57255
C14	C	0.94395	0.03311	0.39827
C15	C	0.1245	0.9647	0.35687
C16	C	0.08041	0.04604	0.2962

C17	C	0.88739	0.06716	0.28073
C18	C	0.73589	0.14938	0.33276
C19	C	0.68198	0.02359	0.36406
C20	C	0.89371	0.08222	0.17498
C21	C	0.75657	0.15865	0.12807
C22	C	0.83825	0.05106	0.07131
C23	C	0.03438	0.03044	0.05033
C24	C	0.15581	0.9837	0.10313
C25	C	0.34135	0.98898	0.08901
C26	C	0.0761	0.52973	0.17017
C27	C	0.19516	0.5376	0.21873
C28	C	0.14276	0.47073	0.27721
C29	C	0.93007	0.55991	0.29305
C30	C	0.82798	0.55502	0.23885
C31	C	0.61746	0.64871	0.24775
C32	C	0.86361	0.53748	0.3995
C33	C	0.70166	0.52883	0.43898
C34	C	0.70144	0.58134	0.50376
C35	C	0.89475	0.48749	0.52682
C36	C	0.05293	0.48273	0.48171
C37	C	0.23892	0.36492	0.50259
C38	C	0.87632	0.49405	0.63593
C39	C	0.99796	0.51013	0.68215
C40	C	0.95417	0.45232	0.7438
C41	C	0.74351	0.53598	0.76158
C42	C	0.63543	0.5201	0.71105
C43	C	0.42588	0.61567	0.72523
C44	C	0.68854	0.53768	0.86928
C45	C	0.53966	0.52758	0.91444
C46	C	0.53859	0.61225	0.97392
C47	C	0.73291	0.54211	0.99648
C48	C	0.8829	0.52541	0.94568
C49	C	0.07944	0.42063	0.96353
H50	H	0.00754	0.79294	0.8329
H51	H	0.89486	0.16051	0.80675
H52	H	0.78508	0.90016	0.75927
H53	H	0.55682	0.21735	0.83633
H54	H	0.45462	0.95187	0.78744
H55	H	0.37161	0.16153	0.765
H56	H	0.25481	0.22455	0.87228
H57	H	0.77973	0.91424	0.67269
H58	H	0.56666	0.2446	0.61108
H59	H	0.69392	0.87528	0.58032
H60	H	0.85346	0.10202	0.52487
H61	H	0.03527	0.81668	0.60951
H62	H	0.15391	0.08303	0.56485
H63	H	0.23592	0.88233	0.52976
H64	H	0.32918	0.22441	0.65557

H65	H	0.54512	0.14906	0.50214
H66	H	0.97511	0.04155	0.44422
H67	H	0.18025	0.82892	0.35129
H68	H	0.07038	0.17258	0.30056
H69	H	0.9	0.94242	0.26994
H70	H	0.61943	0.2629	0.31937
H71	H	0.65973	0.93967	0.33398
H72	H	0.56117	0.08463	0.39682
H73	H	0.21816	0.11202	0.39142
H74	H	0.21363	0.00433	0.21536
H75	H	0.87797	0.8715	0.46912
H76	H	0.92732	0.94874	0.17984
H77	H	0.74057	0.28629	0.1204
H78	H	0.84695	0.92609	0.08048
H79	H	0.02114	0.15109	0.03297
H80	H	0.1818	0.85614	0.11614
H81	H	0.31624	0.11784	0.07897
H82	H	0.41783	0.90792	0.04988
H83	H	0.49797	0.26808	0.16789
H84	H	0.5124	0.00379	0.14467
H85	H	0.10079	0.39843	0.16296
H86	H	0.16667	0.66872	0.22614
H87	H	0.18259	0.33676	0.26916
H88	H	0.89138	0.69016	0.30632
H89	H	0.8647	0.42391	0.22725
H90	H	0.57056	0.78065	0.25988
H91	H	0.563	0.59369	0.2838
H92	H	0.44901	0.52308	0.1957
H93	H	0.21042	0.44927	0.36026
H94	H	0.51785	0.73577	0.1692
H95	H	0.8552	0.66425	0.39966
H96	H	0.72661	0.39822	0.43739
H97	H	0.66225	0.7165	0.50547
H98	H	0.916	0.35851	0.53522
H99	H	0.04492	0.60818	0.47837
H100	H	0.24637	0.23953	0.50581
H101	H	0.24787	0.40643	0.54763
H102	H	0.90504	0.36205	0.62914
H103	H	0.96466	0.64324	0.68665
H104	H	0.00233	0.31582	0.74084
H105	H	0.69997	0.66949	0.77108
H106	H	0.67265	0.38779	0.70233
H107	H	0.3867	0.74379	0.7408
H108	H	0.37827	0.55424	0.7607
H109	H	0.66568	0.66857	0.86382
H110	H	0.57892	0.39496	0.92229
H111	H	0.49499	0.74588	0.96555
H112	H	0.76274	0.41822	0.01467

H113	H	0.86541	0.65141	0.93455
H114	H	0.09038	0.29919	0.97858
H115	H	0.10662	0.48284	0.00102
H116	H	0.25556	0.4789	0.90832
H117	H	0.77136	0.96343	0.97739
H118	H	0.17958	0.00082	0.8618
H119	H	0.03545	0.0174	0.70876
H120	H	0.36149	0.9658	0.62696
H121	H	0.58781	0.17764	0.04651
H122	H	0.04733	0.90529	0.97482
H123	H	0.24089	0.55021	0.10387
H124	H	0.48168	0.7384	0.42019
H125	H	0.55526	0.59081	0.5799
H126	H	0.41391	0.44859	0.4644
H127	H	0.2506	0.49696	0.66579
H128	H	0.03113	0.45213	0.82468
H129	H	0.32233	0.72096	0.65041
H130	H	0.30001	0.7157	0.88639
H131	H	0.29353	0.70079	0.01775
H132	H	0.8318	0.60482	0.06592
H133	H	0.77843	0.11994	0.90501
O134	O	0.85885	0.89152	0.9441
O135	O	0.14542	0.90648	0.87137
O136	O	0.08058	0.97168	0.74762
O137	O	0.68359	0.13278	0.72138
O138	O	0.65718	0.97967	0.87164
O139	O	0.27484	0.12094	0.85002
O140	O	0.42805	0.10807	0.64573
O141	O	0.56426	0.0397	0.51806
O142	O	0.95909	0.84838	0.5022
O143	O	0.90876	0.06168	0.64283
O144	O	0.31652	0.8833	0.615
O145	O	0.26603	0.99257	0.38309
O146	O	0.22716	0.94675	0.25364
O147	O	0.82507	0.16794	0.22926
O148	O	0.81683	0.19115	0.38119
O149	O	0.84842	0.9273	0.39435
O150	O	0.57875	0.16241	0.1434
O151	O	0.71301	0.12636	0.02551
O152	O	0.12956	0.90186	0.00611
O153	O	0.06071	0.09634	0.15314
O154	O	0.44548	0.93462	0.14015
O155	O	0.10659	0.5973	0.11533
O156	O	0.38662	0.44486	0.19869
O157	O	0.24476	0.49109	0.32265
O158	O	0.86888	0.4824	0.34121
O159	O	0.88637	0.62828	0.18883
O160	O	0.54338	0.63519	0.19333

O161	O	0.52489	0.61803	0.41592
O162	O	0.56637	0.54667	0.53909
O163	O	0.90765	0.56173	0.58201
O164	O	0.03634	0.42497	0.42362
O165	O	0.39648	0.34685	0.46266
O166	O	0.18903	0.42045	0.66163
O167	O	0.05409	0.49264	0.7852
O168	O	0.69218	0.46528	0.81412
O169	O	0.68459	0.58899	0.65764
O170	O	0.33275	0.62066	0.67323
O171	O	0.36098	0.5923	0.89262
O172	O	0.40976	0.59603	0.01858
O173	O	0.72439	0.65528	0.04255
O174	O	0.86555	0.44412	0.89293
O175	O	0.21768	0.38615	0.91488

C. TS-transglycosylation-cellobiose end-mid chain scission

C2	C	0.259	0.28728	0.52055
C3	C	0.04632	0.59689	0.00432
C4	C	0.27605	0.17206	0.47326
C5	C	0.17338	0.61265	0.12355
C6	C	0.34046	0.12441	0.71618
C7	C	0.23213	0.50771	0.17989
C8	C	0.45955	0.18333	0.7656
C9	C	0.14921	0.43236	0.32607
C10	C	0.44002	0.29922	0.78362
C11	C	0.01885	0.43102	0.21444
C12	C	0.56137	0.35525	0.79752
C13	C	0.92996	0.37692	0.39613
C14	C	0.75452	0.76971	0.30029
C15	C	0.96925	0.11598	0.99251
C16	C	0.72954	0.66955	0.43524
C17	C	0.83968	0.12427	0.88301
C18	C	0.65881	0.60721	0.22055
C19	C	0.78668	0.01616	0.86112
C20	C	0.53743	0.66435	0.17916
C21	C	0.8707	0.94421	0.70573
C22	C	0.5522	0.78183	0.16512
C23	C	0.00128	0.94738	0.81304
C24	C	0.51369	0.84849	0.40342
C25	C	0.08988	0.8856	0.64655
H26	H	0.20606	0.30202	0.70206
H27	H	0.05202	0.55521	0.81402
H28	H	0.92667	0.68439	0.82801
H29	H	0.33633	0.16272	0.30284
H30	H	0.11872	0.10598	0.56783
H31	H	0.16415	0.65443	0.31285

H32	H	0.3307	0.65345	0.94713
H33	H	0.28105	0.13232	0.88985
H34	H	0.30755	0.97274	0.7278
H35	H	0.25228	0.47227	0.98527
H36	H	0.36903	0.45879	0.40419
H37	H	0.51834	0.16775	0.59453
H38	H	0.55565	0.08129	0.94747
H39	H	0.14862	0.45401	0.5371
H40	H	0.38473	0.31871	0.95754
H41	H	0.01771	0.39251	0.02026
H42	H	0.62315	0.32346	0.64817
H43	H	0.57925	0.48109	0.57855
H44	H	0.96665	0.30118	0.4506
H45	H	0.80449	0.30051	0.18184
H46	H	0.60183	0.34187	0.99396
H47	H	0.92024	0.4223	0.57844
H48	H	0.84764	0.79698	0.27981
H49	H	0.96785	0.07806	0.1884
H50	H	0.0885	0.20402	0.14746
H51	H	0.66657	0.6807	0.60013
H52	H	0.88832	0.59703	0.39579
H53	H	0.84105	0.16093	0.6859
H54	H	0.6819	0.17585	0.03022
H55	H	0.7104	0.60633	0.03487
H56	H	0.71043	0.46015	0.2775
H57	H	0.78186	0.98524	0.06516
H58	H	0.63489	0.95105	0.69006
H59	H	0.47912	0.64479	0.34755
H60	H	0.4962	0.56039	0.89984
H61	H	0.86979	0.96971	0.49618
H62	H	0.50818	0.80887	0.98249
H63	H	0.00325	0.91603	0.01625
H64	H	0.42454	0.81738	0.46575
H65	H	0.74116	0.8394	0.69079
H66	H	0.04817	0.81094	0.60077
H67	H	0.21209	0.8013	0.84768
H68	H	0.4968	0.92712	0.32928
H69	H	0.10567	0.92665	0.45942
O70	O	0.20018	0.33033	0.29912
O71	O	0.98654	0.68982	0.9752
O72	O	0.16333	0.12473	0.4052
O73	O	0.24144	0.67164	0.94013
O74	O	0.37299	0.02066	0.67573
O75	O	0.34033	0.52455	0.32783
O76	O	0.52012	0.14845	0.0021
O77	O	0.37697	0.33356	0.54744
O78	O	0.97581	0.5348	0.18363
O79	O	0.54753	0.46229	0.75711

O80	O	0.81205	0.3675	0.27863
O81	O	0.83116	0.84085	0.72711
O82	O	0.02497	0.21083	0.00697
O83	O	0.83598	0.62364	0.54008
O84	O	0.77084	0.18498	0.06423
O85	O	0.63681	0.50503	0.30046
O86	O	0.66854	0.02323	0.7474
O87	O	0.47868	0.63494	0.93764
O88	O	0.67959	0.80874	0.13037
O89	O	0.0411	0.05239	0.81999
O90	O	0.59916	0.84646	0.60638
O91	O	0.20441	0.8724	0.77758

FS-transglycosylation-cellobiose end-mid chain scission

C2	C	0.26248	0.28301	0.51313
C3	C	0.04343	0.59439	0.01186
C4	C	0.28202	0.16797	0.46438
C5	C	0.17337	0.60781	0.11528
C6	C	0.34905	0.12203	0.70623
C7	C	0.23077	0.50245	0.17001
C8	C	0.4667	0.18259	0.75522
C9	C	0.14942	0.42926	0.32675
C10	C	0.44592	0.29862	0.76642
C11	C	0.01685	0.43068	0.22703
C12	C	0.56724	0.35528	0.7712
C13	C	0.92936	0.37803	0.41401
C14	C	0.70665	0.79117	0.35106
C15	C	0.9779	0.12015	0.9967
C16	C	0.70493	0.67553	0.42919
C17	C	0.84651	0.12347	0.8966
C18	C	0.64931	0.61501	0.19713
C19	C	0.79657	0.01441	0.89006
C20	C	0.52421	0.66319	0.13491
C21	C	0.87986	0.94012	0.74463
C22	C	0.53409	0.78088	0.12266
C23	C	0.01264	0.94942	0.83625
C24	C	0.50421	0.83709	0.37965
C25	C	0.09694	0.88626	0.66233
H26	H	0.21256	0.297	0.69856
H27	H	0.0421	0.55269	0.82103
H28	H	0.92699	0.69044	0.84728
H29	H	0.34159	0.16004	0.29217
H30	H	0.12622	0.10317	0.56527
H31	H	0.16949	0.65091	0.30329
H32	H	0.32657	0.64429	0.91226
H33	H	0.29006	0.12876	0.88059
H34	H	0.31783	0.97009	0.71869

H35	H	0.24594	0.46548	0.97501
H36	H	0.37108	0.45299	0.38482
H37	H	0.52698	0.16599	0.58748
H38	H	0.55969	0.08183	0.95204
H39	H	0.15384	0.45124	0.53723
H40	H	0.39205	0.3192	0.94174
H41	H	0.01114	0.39278	0.03226
H42	H	0.62859	0.321	0.62486
H43	H	0.58261	0.47873	0.53612
H44	H	0.96571	0.30245	0.47232
H45	H	0.80608	0.30366	0.19566
H46	H	0.60836	0.34573	0.96868
H47	H	0.92089	0.42507	0.59363
H48	H	0.79806	0.8233	0.36739
H49	H	0.982	0.08646	0.19713
H50	H	0.09475	0.21821	0.12713
H51	H	0.64298	0.66836	0.59716
H52	H	0.8697	0.61326	0.37491
H53	H	0.84367	0.15673	0.69582
H54	H	0.68883	0.17797	0.03612
H55	H	0.70764	0.62153	0.02236
H56	H	0.71209	0.46998	0.2503
H57	H	0.7911	0.98797	0.09785
H58	H	0.65596	0.95424	0.6801
H59	H	0.46269	0.641	0.2948
H60	H	0.49667	0.55668	0.85141
H61	H	0.87408	0.95934	0.53044
H62	H	0.48225	0.81051	0.95302
H63	H	0.02035	0.92127	0.0416
H64	H	0.44274	0.79261	0.50505
H65	H	0.76623	0.8317	0.87263
H66	H	0.05262	0.81259	0.6172
H67	H	0.21833	0.7977	0.84832
H68	H	0.46727	0.91422	0.34761
H69	H	0.1105	0.92801	0.47552
O70	O	0.19861	0.32591	0.29762
O71	O	0.98786	0.68924	-0.0081
O72	O	0.17104	0.11791	0.40049
O73	O	0.23814	0.66514	0.92221
O74	O	0.38326	0.01814	0.66655
O75	O	0.34203	0.51825	0.30622
O76	O	0.52602	0.15048	0.99627
O77	O	0.38001	0.33042	0.53167
O78	O	0.97658	0.53512	0.20234
O79	O	0.55282	0.46113	0.71819
O80	O	0.81061	0.36859	0.30013
O81	O	0.84608	0.83688	0.78576
O82	O	0.02905	0.21688	0.99178

O83	O	0.819	0.63754	0.52165
O84	O	0.77752	0.18514	0.07526
O85	O	0.63389	0.50879	0.25847
O86	O	0.67723	0.01868	0.77637
O87	O	0.47312	0.63046	0.88826
O88	O	0.66079	0.80791	0.09102
O89	O	0.04882	0.05534	0.82614
O90	O	0.62231	0.84751	0.51161
O91	O	0.21363	0.86973	0.78253

D. TS-transglycosylation-cellulose mid chain scission

C2	C	0.01662	0.95988	0.07485
C3	C	0.96893	0.81319	0.98589
C4	C	0.02554	0.84432	0.84826
C5	C	0.97232	0.01088	0.8057
C6	C	0.02674	0.14853	0.90276
C7	C	0.95959	0.31178	0.86905
C8	C	0.60644	0.48659	0.25615
C9	C	0.51834	0.33821	0.18625
C10	C	0.57346	0.36405	0.0464
C11	C	0.50932	0.52804	0.00773
C12	C	0.55238	0.67234	0.0997
C13	C	0.39573	0.73872	0.16352
C14	C	0.95928	0.02669	0.57497
C15	C	0.01447	0.17054	0.48637
C16	C	0.9721	0.13731	0.34604
C17	C	0.0115	0.9643	0.30721
C18	C	0.94183	0.8325	0.40502
C19	C	0.00591	0.66361	0.3922
C20	C	0.4838	0.53932	0.78056
C21	C	0.51568	0.67969	0.68528
C22	C	0.41373	0.63378	0.56516
C23	C	0.45851	0.46327	0.52233
C24	C	0.4384	0.32789	0.62385
C25	C	0.52265	0.17519	0.58473
H26	H	0.59897	0.48071	0.50041
H27	H	0.15818	0.98524	0.09019
H28	H	0.82587	0.80199	0.98327
H29	H	0.16622	0.84587	0.83608
H30	H	0.8296	0.00025	0.79612
H31	H	0.16979	0.16799	0.90959
H32	H	0.96403	0.38494	0.95803
H33	H	0.82414	0.28832	0.83613
H34	H	0.67637	0.46656	0.34455
H35	H	0.37653	0.3358	0.18758
H36	H	0.71583	0.37449	0.03984
H37	H	0.36779	0.5047	0.99569

H38	H	0.63079	0.77306	0.05113
H39	H	0.2991	0.74422	0.08571
H40	H	0.43778	0.86543	0.19716
H41	H	0.9979	0.64947	0.12445
H42	H	0.83742	0.66856	0.81216
H43	H	0.03317	0.51836	0.7763
H44	H	0.51214	0.16809	0.32374
H45	H	0.51743	0.26279	0.87952
H46	H	0.35051	0.49691	0.35113
H47	H	0.81776	0.01161	0.59278
H48	H	0.15683	0.18664	0.49371
H49	H	0.83548	0.14806	0.3244
H50	H	0.15304	0.96386	0.2987
H51	H	0.79868	0.82333	0.4064
H52	H	0.95551	0.59121	0.47591
H53	H	0.14684	0.68495	0.40017
H54	H	0.34511	0.51861	0.8062
H55	H	0.65466	0.69954	0.66036
H56	H	0.27385	0.62778	0.58621
H57	H	0.30222	0.29637	0.65183
H58	H	0.51508	0.0916	0.66794
H59	H	0.65987	0.21603	0.56401
H60	H	0.99114	0.34377	0.61452
H61	H	0.17848	0.29174	0.32163
H62	H	0.00696	0.46718	0.28086
H63	H	0.52321	0.84471	0.82155
H64	H	0.40862	0.71719	0.3841
H65	H	0.44339	0.97052	0.48765
O66	O	0.0274	0.66662	0.0308
O67	O	0.94725	0.70877	0.77039
O68	O	0.05089	0.06593	0.68844
O69	O	0.95155	0.10282	0.02492
O70	O	0.06229	0.40309	0.77218
O71	O	0.57374	0.19607	0.24047
O72	O	0.49556	0.2319	0.97065
O73	O	0.58469	0.58619	0.88781
O74	O	0.65576	0.6266	0.20486
O75	O	0.33373	0.63496	0.26051
O76	O	0.94315	0.31411	0.52758
O77	O	0.07266	0.26316	0.27062
O78	O	0.92942	0.91585	0.18844
O79	O	0.01261	0.87908	0.52843
O80	O	0.95982	0.57484	0.27659
O81	O	0.46002	0.82465	0.74081
O82	O	0.46383	0.75655	0.47062
O83	O	0.36001	0.40431	0.41419
O84	O	0.53842	0.38889	0.73475
O85	O	0.44086	0.09088	0.47598

FS-transglycosylation-cellulose mid chain scission

C2	C	0.03756	0.94375	0.08288
C3	C	0.00798	0.79244	0.99503
C4	C	0.04425	0.82581	0.85383
C5	C	0.97727	0.98775	0.81386
C6	C	0.02895	0.12684	0.90953
C7	C	0.9539	0.28662	0.87906
C8	C	0.58841	0.53651	0.24583
C9	C	0.51667	0.36963	0.18408
C10	C	0.56207	0.38605	0.04265
C11	C	0.51534	0.55343	0.99539
C12	C	0.58314	0.69877	0.07991
C13	C	0.45106	0.76046	0.16747
C14	C	0.9438	0.00255	0.58313
C15	C	-0.01021	0.14858	0.49391
C16	C	0.9561	0.11358	0.35248
C17	C	0.01305	0.94678	0.31654
C18	C	0.94135	0.81017	0.40891
C19	C	0.01994	0.64844	0.39368
C20	C	0.48527	0.55054	0.7703
C21	C	0.51918	0.68994	0.67597
C22	C	0.39391	0.65489	0.56759
C23	C	0.41602	0.48114	0.51463
C24	C	0.40969	0.34419	0.61548
C25	C	0.48753	0.19043	0.57034
H26	H	0.54714	0.48845	0.47334
H27	H	0.1764	0.98427	0.10071
H28	H	0.86806	0.75666	0.00186
H29	H	0.18319	0.83379	0.83123
H30	H	0.834	0.96932	0.81027
H31	H	0.17147	0.1519	0.916
H32	H	0.96679	0.36099	0.96746
H33	H	0.8151	0.25817	0.85611
H34	H	0.65558	0.51798	0.3363
H35	H	0.37452	0.35426	0.19261
H36	H	0.70315	0.38581	0.03334
H37	H	0.37409	0.54683	0.98388
H38	H	0.65141	0.79818	0.0229
H39	H	0.32299	0.76007	0.12371
H40	H	0.49921	0.8802	0.20947
H41	H	0.04743	0.6264	0.12634
H42	H	0.84532	0.66124	0.81438
H43	H	0.02468	0.49369	0.7851
H44	H	0.51608	0.19639	0.31687
H45	H	0.49962	0.27486	0.87949
H46	H	0.29575	0.50733	0.352
H47	H	0.80376	0.9854	0.60648
H48	H	0.13105	0.17508	0.50369

H49	H	0.81957	0.11585	0.32637
H50	H	0.15588	0.95646	0.31847
H51	H	0.79842	0.79351	0.40249
H52	H	0.97513	0.5693	0.47509
H53	H	0.15899	0.68463	0.40602
H54	H	0.34862	0.53945	0.80168
H55	H	0.65348	0.6963	0.63986
H56	H	0.26081	0.65685	0.60354
H57	H	0.27693	0.31615	0.6523
H58	H	0.47241	0.1012	0.64966
H59	H	0.62639	0.2268	0.55391
H60	H	0.95483	0.31894	0.62098
H61	H	0.15973	0.27127	0.32707
H62	H	0.99185	0.44098	0.28995
H63	H	0.55948	0.85108	0.81404
H64	H	0.44522	0.73419	0.39036
H65	H	0.40616	0.99489	0.46828
O66	O	0.09566	0.66074	0.03935
O67	O	0.96316	0.68774	0.78049
O68	O	0.04287	0.04419	0.69301
O69	O	0.95658	0.07634	0.03119
O70	O	0.04241	0.37579	0.77533
O71	O	0.58741	0.23565	0.24081
O72	O	0.47228	0.25464	0.97113
O73	O	0.59586	0.5891	0.87304
O74	O	0.70071	0.63935	0.16976
O75	O	0.44033	0.6333	0.2656
O76	O	0.90654	0.28526	0.5349
O77	O	0.05172	0.24263	0.27822
O78	O	0.9496	0.89307	0.19424
O79	O	-0.00257	0.85428	0.53625
O80	O	0.98676	0.56084	0.27615
O81	O	0.4881	0.84044	0.73656
O82	O	0.43024	0.78535	0.47614
O83	O	0.28696	0.42713	0.42297
O84	O	0.52392	0.39793	0.72025
O85	O	0.40916	0.11535	0.45615

E. TS-glycosylation-cellotetraose end chain scission

C2	C	0.81258	0.01153	0.88824
C3	C	0.98477	0.93548	0.84282
C4	C	0.93809	0.03403	0.7853
C5	C	0.76492	0.02604	0.76389
C6	C	0.60153	0.09418	0.81288
C7	C	0.42958	0.08426	0.79299
C8	C	0.76704	0.03442	0.65612
C9	C	0.61675	0.1068	0.61178

C10	C	0.69599	0.01548	0.55086
C11	C	0.87644	0.02889	0.53008
C12	C	0.01595	0.95932	0.57765
C13	C	0.19672	0.97084	0.56025
C14	C	0.94275	0.01571	0.42196
C15	C	0.1216	0.93458	0.37934
C16	C	0.08785	0.0212	0.31919
C17	C	0.91704	0.01562	0.29509
C18	C	0.7469	0.09023	0.34112
C19	C	0.57837	0.07673	0.32022
C20	C	0.92516	0.03158	0.18713
C21	C	0.7786	0.11628	0.143
C22	C	0.85189	0.02823	0.08177
C23	C	0.03989	0.02321	0.05969
C24	C	0.17387	0.95629	0.10929
C25	C	0.35485	0.96991	0.09478
C26	C	0.05025	0.49431	0.14991
C27	C	0.18013	0.5	0.19439
C28	C	0.14542	0.42834	0.25366
C29	C	0.93515	0.5029	0.27625
C30	C	0.82308	0.49779	0.22421
C31	C	0.61324	0.58803	0.2378
C32	C	0.82209	0.64253	0.40191
C33	C	0.69879	0.58534	0.43266
C34	C	0.70984	0.57336	0.5004
C35	C	0.91123	0.50749	0.51804
C36	C	0.04337	0.55566	0.47779
C37	C	0.23808	0.40853	0.47101
C38	C	0.8903	0.48934	0.62711
C39	C	0.00978	0.50256	0.67449
C40	C	0.956	0.45701	0.73695
C41	C	0.74287	0.54102	0.75145
C42	C	0.64419	0.51484	0.70002
C43	C	0.43306	0.60893	0.71
C44	C	0.68118	0.55089	0.85902
C45	C	0.53253	0.54132	0.9044
C46	C	0.53512	0.6214	0.9645
C47	C	0.731	0.54933	0.98636
C48	C	0.87832	0.53603	0.93508
C49	C	0.077	0.42931	0.95071
H50	H	0.01093	0.80598	0.83293
H51	H	0.90185	0.16593	0.79585
H52	H	0.79994	0.89453	0.7537
H53	H	0.5673	0.22578	0.82332
H54	H	0.46387	0.95512	0.77991
H55	H	0.3879	0.16059	0.75319
H56	H	0.25898	0.24003	0.85964
H57	H	0.80418	0.90051	0.66188

H58	H	0.58042	0.24005	0.60672
H59	H	0.73229	0.88205	0.55764
H60	H	0.84217	0.16102	0.52251
H61	H	0.04699	0.82693	0.58421
H62	H	0.17319	0.10158	0.56325
H63	H	0.24267	0.92765	0.51345
H64	H	0.35247	0.19977	0.64545
H65	H	0.61764	0.05097	0.46872
H66	H	0.90611	0.14905	0.43019
H67	H	0.15486	0.80213	0.37262
H68	H	0.05512	0.15424	0.326
H69	H	0.94982	0.88485	0.28416
H70	H	0.71263	0.22282	0.34923
H71	H	0.61211	0.94694	0.30847
H72	H	0.53736	0.15052	0.2799
H73	H	0.31748	0.0208	0.38682
H74	H	0.23058	0.98459	0.23994
H75	H	0.41016	0.24056	0.38256
H76	H	0.95725	0.89807	0.19069
H77	H	0.75526	0.2472	0.13985
H78	H	0.86921	0.89883	0.08532
H79	H	0.01781	0.15169	0.04929
H80	H	0.20619	0.82367	0.11534
H81	H	0.32274	0.10331	0.09253
H82	H	0.42126	0.90855	0.05114
H83	H	0.50581	0.2276	0.16898
H84	H	0.54265	0.95831	0.14913
H85	H	0.07968	0.36305	0.13997
H86	H	0.14829	0.63158	0.20259
H87	H	0.19573	0.29197	0.24749
H88	H	0.89205	0.63961	0.28355
H89	H	0.86437	0.36777	0.21027
H90	H	0.57051	0.71449	0.25605
H91	H	0.56465	0.52087	0.27071
H92	H	0.43321	0.48947	0.17323
H93	H	0.20068	0.44424	0.33541
H94	H	0.52289	0.6943	0.16083
H95	H	0.78979	0.71047	0.36043
H96	H	0.79968	0.47483	0.38928
H97	H	0.62995	0.70219	0.51865
H98	H	0.9668	0.37043	0.51855
H99	H	0.04896	0.66384	0.49806
H100	H	0.22579	0.29256	0.46354
H101	H	0.29888	0.39663	0.51404
H102	H	0.92469	0.3573	0.61713
H103	H	0.98467	0.63409	0.67699
H104	H	0.00524	0.32037	0.73772
H105	H	0.69677	0.67607	0.75845

H106	H	0.68582	0.3807	0.69347
H107	H	0.38946	0.73916	0.72384
H108	H	0.37882	0.5517	0.74528
H109	H	0.65808	0.68185	0.85307
H110	H	0.56919	0.40863	0.91113
H111	H	0.49232	0.75556	0.95733
H112	H	0.76226	0.42384	0.00355
H113	H	0.85972	0.6632	0.92487
H114	H	0.09046	0.30526	0.96349
H115	H	0.10737	0.48642	0.98885
H116	H	0.2485	0.49655	0.89647
H117	H	0.76604	0.99343	0.97485
H118	H	0.18301	0.01806	0.85485
H119	H	0.05605	0.00709	0.70271
H120	H	0.39295	0.94224	0.61369
H121	H	0.59488	0.14682	0.06055
H122	H	0.03993	0.92904	0.9781
H123	H	0.19843	0.53772	0.08425
H124	H	0.43929	0.75919	0.41357
H125	H	0.57777	0.51492	0.56677
H126	H	0.41232	0.49569	0.42903
H127	H	0.26376	0.47906	0.65375
H128	H	0.02845	0.46957	0.81759
H129	H	0.33897	0.70595	0.63279
H130	H	0.2935	0.7358	0.8798
H131	H	0.29444	0.71087	0.01132
H132	H	0.83999	0.61287	0.05282
H133	H	0.77426	0.14514	0.89687
O134	O	0.85146	0.92284	0.94093
O135	O	0.14414	0.92877	0.86839
O136	O	0.09552	0.96527	0.74241
O137	O	0.70501	0.12116	0.71063
O138	O	0.6587	0.99695	0.86514
O139	O	0.27889	0.13488	0.83828
O140	O	0.45615	0.08729	0.63458
O141	O	0.55792	0.08337	0.50975
O142	O	0.96567	0.93178	0.47584
O143	O	0.93185	0.05163	0.63302
O144	O	0.33715	0.87183	0.59818
O145	O	0.27277	0.94217	0.4069
O146	O	0.25278	0.93795	0.28
O147	O	0.86396	0.11363	0.24254
O148	O	0.79146	0.00255	0.39631
O149	O	0.42796	0.13133	0.36614
O150	O	0.60786	0.10963	0.16145
O151	O	0.71782	0.11503	0.03928
O152	O	0.12813	0.91568	0.00853
O153	O	0.09032	0.04708	0.1649

O154	O	0.47326	0.8934	0.14097
O155	O	0.06529	0.57425	0.09594
O156	O	0.36725	0.41576	0.16735
O157	O	0.24796	0.46286	0.29579
O158	O	0.9128	0.42777	0.32935
O159	O	0.86485	0.58362	0.17404
O160	O	0.52303	0.59895	0.18441
O161	O	0.52066	0.63443	0.41433
O162	O	0.62381	0.47403	0.52535
O163	O	0.92381	0.56706	0.57586
O164	O	0.98361	0.61701	0.41865
O165	O	0.35605	0.41899	0.42208
O166	O	0.20142	0.40273	0.65581
O167	O	0.04854	0.50868	0.77752
O168	O	0.68386	0.47697	0.80417
O169	O	0.6975	0.5794	0.64634
O170	O	0.35191	0.60508	0.65564
O171	O	0.35301	0.611	0.88297
O172	O	0.4073	0.60282	0.00889
O173	O	0.72452	0.65948	0.03282
O174	O	0.85852	0.4573	0.88206
O175	O	0.20984	0.40372	0.90088

FS-glycosylation-cellotetraose end chain scission

C2	C	0.81702	0.00492	0.88275
C3	C	0.98546	0.92189	0.83651
C4	C	0.93745	0.0191	0.77867
C5	C	0.75719	0.02004	0.75927
C6	C	0.59871	0.09172	0.80984
C7	C	0.42073	0.08818	0.79239
C8	C	0.75818	0.0314	0.65152
C9	C	0.61083	0.10791	0.60674
C10	C	0.68928	0.01956	0.54525
C11	C	0.87298	0.02904	0.52554
C12	C	0.00931	0.95718	0.57389
C13	C	0.19009	0.97048	0.56005
C14	C	0.93756	0.01447	0.41719
C15	C	0.1119	0.92679	0.37311
C16	C	0.07848	0.00917	0.31226
C17	C	0.89852	0.01625	0.29051
C18	C	0.73367	0.09376	0.33863
C19	C	0.5609	0.08337	0.32015
C20	C	0.91292	0.03402	0.18261
C21	C	0.77393	0.12028	0.13665
C22	C	0.84891	0.03246	0.07557
C23	C	0.03656	0.03017	0.05581
C24	C	0.16667	0.96137	0.10636

C25	C	0.34601	0.97831	0.09389
C26	C	0.10877	0.51432	0.14038
C27	C	0.23105	0.52339	0.18718
C28	C	0.19685	0.45081	0.24616
C29	C	0.98843	0.5107	0.26452
C30	C	0.8805	0.51051	0.21148
C31	C	0.67084	0.59605	0.22609
C32	C	0.73528	0.58213	0.4159
C33	C	0.61603	0.60306	0.46386
C34	C	0.67326	0.57237	0.52629
C35	C	0.88733	0.49948	0.5275
C36	C	0.98959	0.54345	0.47439
C37	C	0.19662	0.42542	0.47097
C38	C	0.90422	0.49025	0.63388
C39	C	0.02448	0.50276	0.68105
C40	C	0.96779	0.45295	0.74268
C41	C	0.75468	0.53608	0.75755
C42	C	0.65674	0.51828	0.7047
C43	C	0.44604	0.60984	0.71363
C44	C	0.68736	0.54122	0.86419
C45	C	0.53601	0.53247	0.90859
C46	C	0.53258	0.62365	0.96674
C47	C	0.72414	0.55331	0.99155
C48	C	0.87955	0.52999	0.94178
C49	C	0.07328	0.41976	0.9606
H50	H	0.00499	0.79386	0.82787
H51	H	0.90869	0.14965	0.78839
H52	H	0.78473	0.89035	0.74909
H53	H	0.57024	0.22199	0.82002
H54	H	0.4508	0.96314	0.77554
H55	H	0.37025	0.17497	0.75566
H56	H	0.2622	0.22632	0.86504
H57	H	0.79308	0.89778	0.65665
H58	H	0.57931	0.23989	0.60208
H59	H	0.72185	0.88637	0.55024
H60	H	0.84143	0.16057	0.51831
H61	H	0.04044	0.82451	0.57924
H62	H	0.16348	0.10218	0.56067
H63	H	0.25069	0.91709	0.51519
H64	H	0.35032	0.20529	0.64342
H65	H	0.60878	0.05066	0.46378
H66	H	0.90501	0.14735	0.42436
H67	H	0.13648	0.79615	0.36773
H68	H	0.05863	0.13877	0.31713
H69	H	0.92168	0.88815	0.27953
H70	H	0.70308	0.22562	0.34665
H71	H	0.59326	0.95316	0.30988
H72	H	0.51969	0.15493	0.27935

H73	H	0.30755	0.01273	0.38315
H74	H	0.21991	0.97092	0.23299
H75	H	0.3892	0.24945	0.38334
H76	H	0.9443	0.90071	0.18553
H77	H	0.75911	0.2487	0.1336
H78	H	0.8656	0.90321	0.0778
H79	H	0.01278	0.16008	0.04767
H80	H	0.19877	0.82877	0.11121
H81	H	0.3124	0.11106	0.0884
H82	H	0.42377	0.90783	0.05279
H83	H	0.5098	0.24957	0.16186
H84	H	0.52435	0.98355	0.14898
H85	H	0.14348	0.38133	0.13086
H86	H	0.19878	0.65492	0.1955
H87	H	0.25666	0.31362	0.24015
H88	H	0.9314	0.63928	0.28329
H89	H	0.9236	0.38002	0.19703
H90	H	0.62528	0.72158	0.24567
H91	H	0.62672	0.52406	0.25825
H92	H	0.48783	0.50826	0.16684
H93	H	0.25903	0.46605	0.32999
H94	H	0.53701	0.72591	0.15742
H95	H	0.69382	0.6026	0.37047
H96	H	0.98935	0.43066	0.34701
H97	H	0.60758	0.69146	0.5519
H98	H	0.93973	0.36275	0.52829
H99	H	0.96614	0.67379	0.47872
H100	H	0.21506	0.29611	0.4702
H101	H	0.25574	0.44311	0.5111
H102	H	0.92694	0.3597	0.62738
H103	H	0.99991	0.63386	0.68454
H104	H	0.01664	0.31624	0.74124
H105	H	0.70885	0.66999	0.76684
H106	H	0.69903	0.38524	0.69466
H107	H	0.39842	0.74016	0.72785
H108	H	0.3911	0.55027	0.7478
H109	H	0.66359	0.67232	0.85845
H110	H	0.57581	0.40048	0.91789
H111	H	0.49432	0.75526	0.95608
H112	H	0.74941	0.4324	0.01146
H113	H	0.86769	0.6547	0.93067
H114	H	0.07898	0.29855	0.97366
H115	H	0.09854	0.47861	0.99934
H116	H	0.25009	0.47886	0.90597
H117	H	0.76762	0.99418	0.96934
H118	H	0.18241	0.00411	0.85096
H119	H	0.05289	0.99089	0.69562
H120	H	0.37769	0.95397	0.61514

H121	H	0.59374	0.15583	0.05363
H122	H	0.03927	0.93539	0.97404
H123	H	0.25757	0.55414	0.07291
H124	H	0.37885	0.75892	0.43325
H125	H	0.53962	0.50983	0.59235
H126	H	0.35934	0.51671	0.42999
H127	H	0.27772	0.47939	0.65924
H128	H	0.03499	0.45733	0.82445
H129	H	0.33622	0.71554	0.63829
H130	H	0.30006	0.71589	0.87781
H131	H	0.2852	0.7271	0.00944
H132	H	0.77626	0.61289	0.07131
H133	H	0.78319	0.13821	0.88957
O134	O	0.85588	0.92092	0.93655
O135	O	0.15185	0.90757	0.85927
O136	O	0.09107	0.94411	0.73499
O137	O	0.6953	0.11686	0.70654
O138	O	0.65888	0.99357	0.86178
O139	O	0.27942	0.12716	0.84055
O140	O	0.4467	0.09318	0.62833
O141	O	0.55216	0.09433	0.50433
O142	O	0.96405	0.93178	0.47118
O143	O	0.92367	0.04747	0.62948
O144	O	0.31505	0.88421	0.60398
O145	O	0.27143	0.92403	0.39757
O146	O	0.23786	0.91656	0.27191
O147	O	0.84573	0.1157	0.23804
O148	O	0.78235	0.00432	0.39296
O149	O	0.41131	0.13935	0.36641
O150	O	0.59614	0.12621	0.15266
O151	O	0.71753	0.12204	0.03268
O152	O	0.12828	0.92926	0.00339
O153	O	0.07969	0.0497	0.16226
O154	O	0.45389	0.91685	0.14389
O155	O	0.12531	0.59428	0.08778
O156	O	0.41786	0.43631	0.16203
O157	O	0.289	0.4949	0.28943
O158	O	0.96208	0.40326	0.30771
O159	O	0.91923	0.59864	0.16233
O160	O	0.58428	0.60819	0.17207
O161	O	0.42801	0.65531	0.45791
O162	O	0.60793	0.4598	0.55342
O163	O	0.94286	0.55288	0.57962
O164	O	0.92482	0.52591	0.41775
O165	O	0.29845	0.44629	0.41816
O166	O	0.21685	0.40257	0.66412
O167	O	0.06014	0.49814	0.78528
O168	O	0.69644	0.46676	0.809

O169	O	0.71369	0.59085	0.65436
O170	O	0.3708	0.60522	0.65787
O171	O	0.35893	0.5936	0.88588
O172	O	0.39696	0.61847	0.01116
O173	O	0.71804	0.66967	0.03594
O174	O	0.86237	0.4494	0.88895
O175	O	0.21598	0.38452	0.91298

F. TS-glycosylation-cellotetraose mid chain scission

C2	C	0.81565	0.00071	0.89867
C3	C	0.98785	0.92442	0.85351
C4	C	0.9414	0.02017	0.79547
C5	C	0.76875	0.00954	0.77471
C6	C	0.60464	0.07968	0.82346
C7	C	0.43344	0.06704	0.80449
C8	C	0.76611	0.00608	0.66752
C9	C	0.61572	0.07817	0.62331
C10	C	0.69495	0.97239	0.56597
C11	C	0.87919	0.97501	0.54103
C12	C	0.02089	0.9096	0.5883
C13	C	0.19646	0.92889	0.56972
C14	C	0.8999	0.12356	0.4251
C15	C	0.07606	0.02942	0.39283
C16	C	0.07322	0.04915	0.32527
C17	C	0.89644	0.05129	0.30302
C18	C	0.7158	0.15053	0.34229
C19	C	0.57615	0.08182	0.33474
C20	C	0.91836	0.04314	0.19379
C21	C	0.77492	0.12668	0.14871
C22	C	0.84789	0.03392	0.08852
C23	C	0.03897	0.0235	0.06682
C24	C	0.17148	0.95851	0.11689
C25	C	0.35033	0.97567	0.10188
C26	C	0.05092	0.50662	0.16648
C27	C	0.17054	0.5245	0.2127
C28	C	0.12021	0.47663	0.27545
C29	C	0.90655	0.55736	0.2902
C30	C	0.80699	0.53682	0.23798
C31	C	0.59677	0.63145	0.24914
C32	C	0.84299	0.55483	0.3983
C33	C	0.68889	0.54146	0.44029
C34	C	0.70132	0.57626	0.50624
C35	C	0.90347	0.48593	0.52402
C36	C	0.03906	0.51192	0.4778
C37	C	0.24275	0.41246	0.48933
C38	C	0.89232	0.47239	0.63292
C39	C	0.01439	0.48567	0.67954

C40	C	0.96445	0.4376	0.74222
C41	C	0.75266	0.52318	0.75817
C42	C	0.64944	0.49835	0.70787
C43	C	0.43887	0.59211	0.72112
C44	C	0.68969	0.53976	0.86597
C45	C	0.53846	0.5334	0.91121
C46	C	0.53907	0.61514	0.97123
C47	C	0.73412	0.54266	0.99354
C48	C	0.88185	0.53143	0.94272
C49	C	0.08039	0.42954	0.95969
H50	H	0.01596	0.79413	0.84422
H51	H	0.9037	0.15283	0.80517
H52	H	0.80494	0.87706	0.76593
H53	H	0.56936	0.21202	0.83287
H54	H	0.46723	0.93621	0.7944
H55	H	0.39365	0.13618	0.76314
H56	H	0.26276	0.2309	0.86949
H57	H	0.79244	0.87564	0.67629
H58	H	0.58656	0.20867	0.61475
H59	H	0.72469	0.84277	0.57708
H60	H	0.845	0.111	0.53895
H61	H	0.05561	0.77781	0.59713
H62	H	0.16203	0.06217	0.56636
H63	H	0.25157	0.87048	0.52501
H64	H	0.34915	0.18581	0.65536
H65	H	0.64828	0.99793	0.48397
H66	H	0.88976	0.16851	0.47089
H67	H	0.03425	0.92709	0.42708
H68	H	0.06626	0.17425	0.31775
H69	H	0.92218	0.9203	0.29706
H70	H	0.65892	0.28146	0.32922
H71	H	0.632	0.95253	0.35038
H72	H	0.56332	0.07789	0.28629
H73	H	0.29182	0.08127	0.39692
H74	H	0.23694	0.95857	0.2519
H75	H	0.3972	0.26768	0.39182
H76	H	0.94197	0.91234	0.20006
H77	H	0.75501	0.25644	0.14434
H78	H	0.86104	0.90598	0.09319
H79	H	0.01949	0.1508	0.05545
H80	H	0.20512	0.82569	0.12305
H81	H	0.31451	0.1095	0.09824
H82	H	0.41927	0.91122	0.05892
H83	H	0.50478	0.23921	0.18109
H84	H	0.53583	0.97342	0.15582
H85	H	0.07855	0.37397	0.16123
H86	H	0.14151	0.65696	0.2152
H87	H	0.17294	0.33957	0.27619

H88	H	0.85993	0.69181	0.2989
H89	H	0.84684	0.40344	0.22978
H90	H	0.55732	0.76189	0.26176
H91	H	0.54359	0.57849	0.28614
H92	H	0.42636	0.50623	0.1932
H93	H	0.19723	0.48726	0.35549
H94	H	0.51161	0.71426	0.16991
H95	H	0.82302	0.68561	0.39533
H96	H	0.71003	0.41232	0.43644
H97	H	0.6534	0.71181	0.51311
H98	H	0.94151	0.35142	0.52696
H99	H	0.00402	0.64613	0.47611
H100	H	0.27633	0.2809	0.49682
H101	H	0.27405	0.46195	0.52915
H102	H	0.92293	0.34064	0.624
H103	H	0.98793	0.61746	0.68229
H104	H	0.01248	0.30105	0.74222
H105	H	0.70826	0.65812	0.76459
H106	H	0.69052	0.36449	0.70057
H107	H	0.39808	0.72114	0.73605
H108	H	0.39149	0.53182	0.75711
H109	H	0.66711	0.67012	0.85878
H110	H	0.57393	0.4011	0.91841
H111	H	0.49646	0.74912	0.96379
H112	H	0.76599	0.41596	0.00953
H113	H	0.86014	0.65893	0.93174
H114	H	0.0947	0.3071	0.97506
H115	H	0.10755	0.4935	0.99659
H116	H	0.25398	0.49056	0.90402
H117	H	0.76707	0.98445	0.98465
H118	H	0.18329	0.01055	0.86596
H119	H	0.05864	0.97968	0.71228
H120	H	0.37959	0.93352	0.62487
H121	H	0.59259	0.15919	0.06615
H122	H	0.04163	0.92376	0.98608
H123	H	0.21203	0.5308	0.09983
H124	H	0.45367	0.75451	0.43119
H125	H	0.57135	0.55903	0.58215
H126	H	0.38972	0.51175	0.43784
H127	H	0.26915	0.46277	0.66196
H128	H	0.03886	0.44903	0.82267
H129	H	0.33454	0.69418	0.64604
H130	H	0.29872	0.72839	0.88704
H131	H	0.29777	0.70541	0.01828
H132	H	0.84164	0.60294	0.06112
H133	H	0.77779	0.1343	0.90724
O134	O	0.85532	0.91254	0.9517
O135	O	0.14567	0.92031	0.87951

O136	O	0.09907	0.95077	0.75291
O137	O	0.71033	0.10022	0.72084
O138	O	0.66154	0.9857	0.87655
O139	O	0.28091	0.12487	0.84947
O140	O	0.44966	0.06962	0.64807
O141	O	0.56555	0.0295	0.52131
O142	O	0.93426	0.89666	0.4845
O143	O	0.93685	0.00924	0.64305
O144	O	0.33285	0.85357	0.61137
O145	O	0.23403	0.0132	0.41879
O146	O	0.23573	0.92614	0.29388
O147	O	0.8542	0.13529	0.24723
O148	O	0.73783	0.15669	0.40605
O149	O	0.3972	0.17861	0.36447
O150	O	0.60148	0.12435	0.16721
O151	O	0.71703	0.1204	0.04527
O152	O	0.12842	0.9123	0.01695
O153	O	0.08843	0.04949	0.17254
O154	O	0.46853	0.90599	0.14877
O155	O	0.07801	0.57068	0.11031
O156	O	0.36196	0.4301	0.19204
O157	O	0.20938	0.5318	0.3159
O158	O	0.84544	0.48941	0.34151
O159	O	0.86118	0.60432	0.18543
O160	O	0.51095	0.6246	0.19682
O161	O	0.50714	0.63544	0.42051
O162	O	0.58131	0.52184	0.54031
O163	O	0.92467	0.54637	0.58062
O164	O	0.0189	0.45344	0.42012
O165	O	0.36025	0.41501	0.4378
O166	O	0.2052	0.38791	0.66001
O167	O	0.06098	0.486	0.78251
O168	O	0.69558	0.46117	0.812
O169	O	0.69959	0.5651	0.65403
O170	O	0.34699	0.59338	0.66918
O171	O	0.36018	0.60302	0.88899
O172	O	0.41017	0.59729	0.01562
O173	O	0.72566	0.6501	0.04161
O174	O	0.86572	0.44846	0.89041
O175	O	0.21565	0.39786	0.91028

FS-glycosylation-cellotetraose mid chain scission

C2	C	0.81125	0.98849	0.89503
C3	C	0.98083	0.91077	0.84889
C4	C	0.93219	0.01192	0.7921
C5	C	0.75442	0.0093	0.77226
C6	C	0.59413	0.0774	0.82204

C7	C	0.41919	0.0707	0.80338
C8	C	0.75145	0.01598	0.66558
C9	C	0.60249	0.08624	0.62101
C10	C	0.68112	0.98067	0.56294
C11	C	0.87166	0.97114	0.5406
C12	C	0.00625	0.91823	0.58979
C13	C	0.1879	0.92687	0.57064
C14	C	0.96421	0.09867	0.41095
C15	C	0.1137	0.04583	0.37086
C16	C	0.08813	0.07533	0.30543
C17	C	0.90533	0.07154	0.29225
C18	C	0.73904	0.16197	0.3385
C19	C	0.60345	0.08736	0.33449
C20	C	0.89996	0.06498	0.18486
C21	C	0.75998	0.14447	0.13852
C22	C	0.83686	0.04179	0.08036
C23	C	0.03126	0.02378	0.05855
C24	C	0.1576	0.97025	0.11021
C25	C	0.33989	0.98169	0.09589
C26	C	0.07038	0.51978	0.17351
C27	C	0.18432	0.54229	0.22072
C28	C	0.12663	0.49822	0.28317
C29	C	0.91271	0.57403	0.29619
C30	C	0.81967	0.55354	0.24207
C31	C	0.60923	0.64634	0.24966
C32	C	0.84918	0.55082	0.40382
C33	C	0.69824	0.52473	0.4436
C34	C	0.70174	0.56524	0.50966
C35	C	0.89992	0.47804	0.5298
C36	C	0.04586	0.49307	0.48457
C37	C	0.23931	0.37783	0.5013
C38	C	0.88485	0.47379	0.6389
C39	C	0.00757	0.4861	0.68549
C40	C	0.95972	0.43291	0.7475
C41	C	0.74852	0.51814	0.76443
C42	C	0.64408	0.49728	0.71376
C43	C	0.43377	0.58983	0.72644
C44	C	0.68949	0.5286	0.87215
C45	C	0.53947	0.52181	0.91772
C46	C	0.5387	0.60944	0.97654
C47	C	0.7332	0.53999	0.99916
C48	C	0.8845	0.51944	0.94827
C49	C	0.08031	0.41213	0.96639
H50	H	0.00379	0.7825	0.83862
H51	H	0.90016	0.14249	0.80318
H52	H	0.78598	0.87869	0.76187
H53	H	0.56211	0.2081	0.83307
H54	H	0.45158	0.94412	0.78766

H55	H	0.37058	0.15427	0.76573
H56	H	0.25828	0.21423	0.87392
H57	H	0.78497	0.88322	0.67258
H58	H	0.57249	0.21715	0.61281
H59	H	0.70017	0.8539	0.57358
H60	H	0.8477	0.09799	0.52711
H61	H	0.03692	0.78875	0.60153
H62	H	0.16185	0.05735	0.56412
H63	H	0.24593	0.85836	0.52762
H64	H	0.33885	0.19001	0.65594
H65	H	0.55879	0.13285	0.499
H66	H	0.97995	0.11341	0.45788
H67	H	0.98692	0.9071	0.45724
H68	H	0.07179	0.20287	0.29694
H69	H	0.9361	0.93902	0.28715
H70	H	0.67315	0.29453	0.32738
H71	H	0.66562	0.96209	0.35372
H72	H	0.58495	0.07398	0.28721
H73	H	0.34378	0.06076	0.38081
H74	H	0.23356	0.99357	0.22803
H75	H	0.42645	0.24979	0.39947
H76	H	0.92919	0.93283	0.19119
H77	H	0.74548	0.27197	0.13188
H78	H	0.84618	0.91595	0.08778
H79	H	0.01603	0.14679	0.0431
H80	H	0.18728	0.84018	0.12054
H81	H	0.30878	0.1125	0.08683
H82	H	0.41803	0.90331	0.05634
H83	H	0.49786	0.25931	0.17677
H84	H	0.51197	0.99702	0.15163
H85	H	0.0977	0.38685	0.17013
H86	H	0.15725	0.67437	0.22199
H87	H	0.18369	0.36118	0.2844
H88	H	0.86128	0.70789	0.30714
H89	H	0.86087	0.41992	0.23373
H90	H	0.56308	0.77862	0.26071
H91	H	0.55208	0.59485	0.28615
H92	H	0.44164	0.51968	0.1992
H93	H	0.20588	0.49756	0.36275
H94	H	0.51584	0.72864	0.17059
H95	H	0.82686	0.68232	0.40529
H96	H	0.73308	0.39219	0.43903
H97	H	0.6501	0.70137	0.51525
H98	H	0.93331	0.34519	0.53556
H99	H	0.02557	0.6226	0.48499
H100	H	0.25406	0.25	0.50421
H101	H	0.25774	0.41675	0.54553
H102	H	0.91481	0.34211	0.63048

H103	H	0.9804	0.61782	0.68949
H104	H	0.00698	0.29644	0.74555
H105	H	0.70451	0.65236	0.77242
H106	H	0.68508	0.364	0.70536
H107	H	0.39043	0.71936	0.74111
H108	H	0.38512	0.52936	0.76202
H109	H	0.66693	0.65899	0.86538
H110	H	0.57769	0.38986	0.92661
H111	H	0.49531	0.74266	0.96739
H112	H	0.76194	0.41725	0.01825
H113	H	0.86959	0.64448	0.9365
H114	H	0.08816	0.29147	0.98122
H115	H	0.10852	0.47296	0.00405
H116	H	0.2569	0.46882	0.91113
H117	H	0.76327	0.97497	0.98063
H118	H	0.17778	0.99311	0.86295
H119	H	0.04507	0.98256	0.7086
H120	H	0.36729	0.93462	0.62603
H121	H	0.58451	0.16755	0.0564
H122	H	0.03767	0.90767	0.98122
H123	H	0.23775	0.53442	0.10665
H124	H	0.46868	0.72785	0.42189
H125	H	0.56753	0.55086	0.58539
H126	H	0.40402	0.47161	0.45749
H127	H	0.26252	0.46453	0.66808
H128	H	0.03385	0.43726	0.82842
H129	H	0.3296	0.69033	0.65071
H130	H	0.29971	0.70875	0.88914
H131	H	0.29348	0.69885	0.02081
H132	H	0.83446	0.60452	0.06738
H133	H	0.77607	0.1214	0.90368
O134	O	0.85011	0.90011	0.94778
O135	O	0.14406	0.89905	0.8732
O136	O	0.08646	0.94225	0.74835
O137	O	0.69208	0.10529	0.71961
O138	O	0.65389	0.97759	0.8735
O139	O	0.27531	0.11289	0.85083
O140	O	0.43777	0.07516	0.64473
O141	O	0.55667	0.03355	0.51733
O142	O	0.94866	0.85599	0.49149
O143	O	0.91878	0.02667	0.64159
O144	O	0.31742	0.85537	0.61448
O145	O	0.28713	0.98058	0.39128
O146	O	0.24384	0.95765	0.26974
O147	O	0.83435	0.15626	0.23813
O148	O	0.78127	0.15381	0.39999
O149	O	0.42315	0.1852	0.3636
O150	O	0.5816	0.15019	0.15483

O151	O	0.70958	0.12206	0.03544
O152	O	0.12267	0.901	0.01207
O153	O	0.06801	0.07486	0.16239
O154	O	0.44506	0.92786	0.1468
O155	O	0.10323	0.57609	0.11643
O156	O	0.37706	0.44324	0.20343
O157	O	0.20779	0.55638	0.32571
O158	O	0.85289	0.49732	0.34521
O159	O	0.87963	0.61913	0.19015
O160	O	0.53678	0.62977	0.19532
O161	O	0.51519	0.60657	0.42393
O162	O	0.58083	0.51087	0.54383
O163	O	0.91538	0.54629	0.586
O164	O	0.02684	0.44569	0.42534
O165	O	0.38718	0.36842	0.45845
O166	O	0.19823	0.38989	0.66546
O167	O	0.05871	0.47517	0.78864
O168	O	0.69441	0.45198	0.81772
O169	O	0.69299	0.56662	0.66046
O170	O	0.34637	0.58865	0.6736
O171	O	0.36099	0.58555	0.89573
O172	O	0.4103	0.59481	0.02176
O173	O	0.72591	0.65466	0.0444
O174	O	0.86601	0.4366	0.8962
O175	O	0.2201	0.37567	0.91801

G. TS-glycosylation-cellobiose end-mid chain scission

C2	C	0.25216	0.28343	0.52684
C3	C	0.05107	0.60386	0.00856
C4	C	0.26383	0.16693	0.49517
C5	C	0.18157	0.60547	0.11622
C6	C	0.33053	0.12165	0.73672
C7	C	0.23469	0.49782	0.15529
C8	C	0.45196	0.17743	0.78689
C9	C	0.14962	0.42756	0.31095
C10	C	0.43423	0.29456	0.78832
C11	C	0.01977	0.42751	0.19471
C12	C	0.55426	0.35287	0.80218
C13	C	0.92893	0.37611	0.37945
C14	C	0.77116	0.78833	0.31986
C15	C	0.95386	0.0973	0.02507
C16	C	0.76483	0.68669	0.42235
C17	C	0.82413	0.10157	0.91665
C18	C	0.6729	0.62233	0.25923
C19	C	0.77221	0.99192	0.92534
C20	C	0.55229	0.6792	0.20776
C21	C	0.85469	0.90851	0.80368

C22	C	0.56609	0.7957	0.16043
C23	C	0.99135	0.92464	0.8711
C24	C	0.45267	0.85469	0.24323
C25	C	0.07364	0.86959	0.67613
H26	H	0.20022	0.304	0.70596
H27	H	0.04702	0.58046	0.79872
H28	H	0.93106	0.72006	0.93561
H29	H	0.32039	0.15419	0.32014
H30	H	0.1082	0.09957	0.60898
H31	H	0.17999	0.64363	0.31165
H32	H	0.34008	0.65396	0.96196
H33	H	0.27263	0.13069	0.91199
H34	H	0.28939	0.96823	0.74078
H35	H	0.24672	0.46266	0.95718
H36	H	0.37202	0.44645	0.37761
H37	H	0.51372	0.15701	0.62388
H38	H	0.49782	0.07222	0.05737
H39	H	0.14854	0.45341	0.51892
H40	H	0.378	0.3163	0.95879
H41	H	0.01905	0.38686	0.00326
H42	H	0.61394	0.3269	0.6417
H43	H	0.57565	0.4875	0.62294
H44	H	0.96405	0.30057	0.44005
H45	H	0.79938	0.29762	0.18414
H46	H	0.59935	0.33453	0.99161
H47	H	0.92028	0.42389	0.55815
H48	H	0.85412	0.83286	0.3447
H49	H	0.95483	0.06315	0.22589
H50	H	0.0717	0.19008	0.16878
H51	H	0.75503	0.74395	0.64253
H52	H	0.90651	0.59436	0.37026
H53	H	0.82591	0.13092	0.71152
H54	H	0.66638	0.15808	0.05169
H55	H	0.71778	0.61239	0.06636
H56	H	0.71001	0.47176	0.30375
H57	H	0.75945	0.9757	0.13614
H58	H	0.65732	0.96756	0.62431
H59	H	0.49395	0.66457	0.38006
H60	H	0.50245	0.56696	0.9553
H61	H	0.8479	0.92535	0.58793
H62	H	0.58491	0.80827	0.95034
H63	H	0.01173	0.8969	0.07307
H64	H	0.41905	0.824	0.4318
H65	H	0.43047	0.98518	0.42794
H66	H	0.03721	0.7931	0.63004
H67	H	0.21155	0.79277	0.84379
H68	H	0.38183	0.83996	0.09146
H69	H	0.07412	0.91471	0.49175

O70	O	0.19572	0.3232	0.29888
O71	O	0.00255	0.69975	0.05049
O72	O	0.14932	0.11965	0.44356
O73	O	0.25029	0.6647	0.93292
O74	O	0.35815	0.01557	0.70049
O75	O	0.3485	0.51044	0.28574
O76	O	0.50477	0.14823	0.03542
O77	O	0.37253	0.32517	0.54723
O78	O	0.97762	0.5312	0.15862
O79	O	0.53451	0.46054	0.78344
O80	O	0.81036	0.36705	0.26308
O81	O	0.81621	0.80709	0.85925
O82	O	0.00888	0.19315	0.02679
O83	O	0.8678	0.63638	0.51241
O84	O	0.75548	0.16904	0.08206
O85	O	0.64818	0.52276	0.36044
O86	O	0.65296	0.98777	0.80998
O87	O	0.49285	0.64326	0.97181
O88	O	0.67073	0.8431	0.29352
O89	O	0.0236	0.03195	0.85431
O90	O	0.47598	0.96173	0.26922
O91	O	0.19672	0.86253	0.76889

FS-glycosylation-cellobiose end-mid chain scission

C2	C	0.25564	0.2834	0.50209
C3	C	0.04766	0.59575	0.00021
C4	C	0.272	0.16791	0.46143
C5	C	0.17572	0.60914	0.11437
C6	C	0.3355	0.12251	0.7067
C7	C	0.23348	0.50333	0.16038
C8	C	0.45555	0.17983	0.76249
C9	C	0.14981	0.42825	0.30724
C10	C	0.43563	0.29676	0.76749
C11	C	0.01902	0.4289	0.19745
C12	C	0.55495	0.35633	0.78231
C13	C	0.92957	0.37134	0.37118
C14	C	0.75022	0.78351	0.46903
C15	C	0.95838	0.09584	0.97075
C16	C	0.73387	0.66803	0.50966
C17	C	0.83037	0.10929	0.85635
C18	C	0.67049	0.62258	0.26428
C19	C	0.77237	0.00363	0.8099
C20	C	0.55039	0.67982	0.20815
C21	C	0.85611	0.92833	0.6641
C22	C	0.57022	0.79677	0.20322
C23	C	0.98686	0.9288	0.77437
C24	C	0.45078	0.85616	0.18837

C25	C	0.07628	0.87126	0.60047
H26	H	0.20309	0.29982	0.6833
H27	H	0.05109	0.55429	0.80921
H28	H	0.92694	0.6793	0.83004
H29	H	0.33209	0.15783	0.29113
H30	H	0.11531	0.09775	0.55696
H31	H	0.16942	0.64906	0.3067
H32	H	0.33311	0.65726	0.95571
H33	H	0.27515	0.13056	0.87822
H34	H	0.29364	0.97043	0.70851
H35	H	0.25043	0.46966	0.96228
H36	H	0.37292	0.45509	0.37995
H37	H	0.51847	0.16118	0.60084
H38	H	0.49727	0.07489	0.03669
H39	H	0.1497	0.44948	0.51843
H40	H	0.37823	0.31729	0.9372
H41	H	0.01777	0.39392	0.9985
H42	H	0.61656	0.32842	0.62793
H43	H	0.5733	0.48504	0.58095
H44	H	0.96712	0.29545	0.42005
H45	H	0.80326	0.29522	0.15827
H46	H	0.59832	0.34145	0.97539
H47	H	0.91807	0.41456	0.55644
H48	H	0.80294	0.79991	0.28805
H49	H	0.95477	0.0546	0.16208
H50	H	0.07915	0.1794	0.14048
H51	H	0.67372	0.65789	0.67983
H52	H	0.89076	0.59797	0.41472
H53	H	0.83669	0.14931	0.66419
H54	H	0.67295	0.15744	0.01493
H55	H	0.73094	0.63061	0.09289
H56	H	0.71235	0.47045	0.26264
H57	H	0.75479	0.97009	0.0079
H58	H	0.63301	0.95564	0.58961
H59	H	0.48734	0.66114	0.36958
H60	H	0.50875	0.57484	0.93394
H61	H	0.85652	0.94946	0.45285
H62	H	0.62753	0.81736	0.03343
H63	H	0.98799	0.89378	0.97332
H64	H	0.38929	0.82821	0.34294
H65	H	0.43231	0.9849	0.38953
H66	H	0.03887	0.79529	0.55181
H67	H	0.20282	0.79536	0.81289
H68	H	0.40736	0.84118	-0.00459
H69	H	0.08751	0.91455	0.41522
O70	O	0.19738	0.32515	0.27947
O71	O	0.98882	0.68896	0.97378
O72	O	0.16041	0.11782	0.39627

O73	O	0.24383	0.66911	0.93145
O74	O	0.36361	0.01632	0.67022
O75	O	0.34423	0.51994	0.29938
O76	O	0.50894	0.15034	0.01039
O77	O	0.37427	0.32788	0.52668
O78	O	0.97754	0.53339	0.18013
O79	O	0.53499	0.4637	0.74992
O80	O	0.81222	0.36259	0.24942
O81	O	0.80828	0.82531	0.69185
O82	O	0.01733	0.18904	0.99669
O83	O	0.84554	0.61806	0.57519
O84	O	0.76223	0.16919	0.03945
O85	O	0.64239	0.51634	0.30065
O86	O	0.6621	0.02055	0.66938
O87	O	0.4972	0.65031	0.96009
O88	O	0.63157	0.82799	0.44399
O89	O	0.0286	0.03322	0.79174
O90	O	0.47051	0.96357	0.2204
O91	O	0.19382	0.86265	0.72146

H. TS-glycosylation-cellulose mid chain scission

C2	C	0.99232	0.9583	0.04023
C3	C	0.95053	0.80924	0.95294
C4	C	0.99619	0.84841	0.81397
C5	C	0.93441	0.01186	0.77257
C6	C	0.97901	0.14906	0.87218
C7	C	0.90038	0.3085	0.84561
C8	C	0.55828	0.46602	0.3075
C9	C	0.48982	0.32142	0.23219
C10	C	0.52211	0.34736	0.08974
C11	C	0.46838	0.51304	0.04791
C12	C	0.55265	0.65644	0.12938
C13	C	0.46623	0.8141	0.11665
C14	C	0.94625	0.02655	0.5391
C15	C	0.99014	0.17722	0.45287
C16	C	0.95584	0.14027	0.31132
C17	C	0.00718	0.97178	0.27235
C18	C	0.95891	0.83544	0.3716
C19	C	0.03835	0.67623	0.34404
C20	C	0.41572	0.52947	0.81701
C21	C	0.4571	0.67573	0.725
C22	C	0.37833	0.63718	0.59367
C23	C	0.43871	0.47524	0.55026
C24	C	0.38224	0.33217	0.63992
C25	C	0.46349	0.17545	0.6081
H26	H	0.58173	0.4904	0.5504
H27	H	0.13466	0.99082	0.04891

H28	H	0.80843	0.77975	0.95839
H29	H	0.13671	0.85486	0.799
H30	H	0.79237	0.99566	0.75883
H31	H	0.12246	0.17727	0.87359
H32	H	0.91698	0.38316	0.93386
H33	H	0.76052	0.28106	0.82661
H34	H	0.66252	0.45293	0.377
H35	H	0.3524	0.34515	0.35279
H36	H	0.66165	0.34577	0.0703
H37	H	0.32574	0.50803	0.05114
H38	H	0.68832	0.68115	0.09958
H39	H	0.5007	0.89073	0.2018
H40	H	0.32429	0.78336	0.1126
H41	H	1.0002	0.64713	0.08547
H42	H	0.80089	0.69095	0.75823
H43	H	0.97234	0.51643	0.75048
H44	H	0.501	0.13799	0.35329
H45	H	0.32555	0.23156	-0.01084
H46	H	0.50957	0.01994	0.01576
H47	H	0.80418	0.99278	0.54696
H48	H	0.13045	0.20965	0.4655
H49	H	0.81727	0.14221	0.29105
H50	H	0.14897	0.98237	0.25708
H51	H	0.81623	0.80798	0.37497
H52	H	0.02845	0.60306	0.43316
H53	H	0.17692	0.70741	0.32127
H54	H	0.27875	0.52121	0.84761
H55	H	0.59907	0.68987	0.70906
H56	H	0.23584	0.62748	0.5987
H57	H	0.24053	0.30756	0.64598
H58	H	0.44044	0.09117	0.69009
H59	H	0.60423	0.20762	0.59585
H60	H	0.9306	0.33747	0.58292
H61	H	0.16966	0.27184	0.24063
H62	H	0.98232	0.46718	0.24826
H63	H	0.45363	0.84325	0.86307
H64	H	0.44266	0.72493	0.41988
H65	H	0.37937	0.97713	0.50758
O66	O	0.03746	0.67533	0.99512
O67	O	0.92254	0.71414	0.73319
O68	O	0.01898	0.07254	0.65796
O69	O	0.91433	0.09615	0.99478
O70	O	0.98643	0.3978	0.74057
O71	O	0.5593	0.1755	0.27134
O72	O	0.44306	0.21315	0.01251
O73	O	0.52839	0.56102	0.9213
O74	O	0.55644	0.62265	0.2658
O75	O	0.5274	0.90266	0.00404

O76	O	0.89644	0.30837	0.49238
O77	O	0.04244	0.26994	0.23171
O78	O	0.91932	0.91223	0.15837
O79	O	0.02595	0.88919	0.49405
O80	O	0.95246	0.58226	0.24154
O81	O	0.40345	0.82103	0.77437
O82	O	0.44163	0.76836	0.50793
O83	O	0.3876	0.45296	0.41691
O84	O	0.45509	0.37725	0.76384
O85	O	0.39096	0.09734	0.49342

FS-glycosylation-cellulose mid chain scission

C2	C	0.00276	0.96021	0.04291
C3	C	0.96043	0.81133	0.95506
C4	C	0.00898	0.85019	0.81691
C5	C	0.94361	0.01135	0.77603
C6	C	-0.00882	0.14941	0.87366
C7	C	0.91044	0.3076	0.84511
C8	C	0.59868	0.44173	0.2929
C9	C	0.55688	0.31536	0.21099
C10	C	0.55076	0.34673	0.06935
C11	C	0.48839	0.51397	0.04589
C12	C	0.57271	0.65004	0.13379
C13	C	0.47682	0.80309	0.12564
C14	C	0.94341	0.02186	0.54277
C15	C	-0.02109	0.1727	0.45647
C16	C	0.94372	0.13627	0.31565
C17	C	0.00611	0.97348	0.27562
C18	C	0.96065	0.83521	0.37296
C19	C	0.04462	0.67953	0.34279
C20	C	0.4227	0.53834	0.81835
C21	C	0.46683	0.677	0.72115
C22	C	0.36955	0.64308	0.59625
C23	C	0.40544	0.47513	0.54725
C24	C	0.37653	0.33413	0.64412
C25	C	0.47231	0.18601	0.60782
H26	H	0.54421	0.4895	0.52219
H27	H	0.14453	0.99318	0.05321
H28	H	0.81811	0.785	0.959
H29	H	0.14992	0.8594	0.80379
H30	H	0.80085	-0.00687	0.76632
H31	H	0.13397	0.17728	0.87665
H32	H	0.92523	0.38228	0.93317
H33	H	0.77111	0.27603	0.82587
H34	H	0.65951	0.42198	0.38544
H35	H	0.3816	0.40436	0.36803
H36	H	0.68554	0.35259	0.03471

H37	H	0.34607	0.50151	0.05342
H38	H	0.70776	0.68021	0.10408
H39	H	0.50193	0.87387	0.21467
H40	H	0.33654	0.76448	0.11722
H41	H	0.00695	0.64806	0.08839
H42	H	0.81438	0.70124	0.74796
H43	H	-0.02087	0.51799	0.75213
H44	H	0.50817	0.14483	0.34237
H45	H	0.44619	0.24976	0.91203
H46	H	0.50702	0.01565	0.02987
H47	H	0.80253	-0.01609	0.55469
H48	H	0.1185	0.21094	0.46678
H49	H	0.80498	0.13019	0.29408
H50	H	0.14855	-0.00851	0.26385
H51	H	0.81836	0.80398	0.3762
H52	H	0.03903	0.60552	0.43098
H53	H	0.18239	0.71443	0.31951
H54	H	0.28753	0.53234	0.85238
H55	H	0.60556	0.67476	0.69671
H56	H	0.22964	0.64756	0.61041
H57	H	0.23722	0.29983	0.65733
H58	H	0.45256	0.09517	0.6855
H59	H	0.61158	0.22973	0.6021
H60	H	0.92419	0.33605	0.58529
H61	H	0.14674	0.284	0.26213
H62	H	0.97685	0.46769	0.25152
H63	H	0.48289	0.84142	0.86272
H64	H	0.44317	0.71263	0.41999
H65	H	0.40292	0.98754	0.50172
O66	O	0.04334	0.67518	-0.00259
O67	O	0.9398	0.7154	0.73484
O68	O	0.02096	0.07163	0.65923
O69	O	0.92603	0.09865	0.99681
O70	O	-0.00804	0.39902	0.74027
O71	O	0.54277	0.15499	0.24872
O72	O	0.44532	0.21835	0.00422
O73	O	0.53902	0.57362	0.91951
O74	O	0.5774	0.60393	0.26791
O75	O	0.53611	0.90176	0.01758
O76	O	0.88165	0.30042	0.49791
O77	O	0.02486	0.26996	0.2377
O78	O	0.92584	0.91286	0.15955
O79	O	0.02625	0.88784	0.4959
O80	O	0.96042	0.58591	0.24039
O81	O	0.43651	0.83023	0.77278
O82	O	0.43415	0.76672	0.50366
O83	O	0.30265	0.43904	0.43514
O84	O	0.45675	0.38197	0.76683

O85	O	0.41836	0.10784	0.48809

I. TS-ring contraction-cellotetraose end chain scission

C2	C	0.81259	0.01402	0.88878
C3	C	0.98587	0.94009	0.84364
C4	C	0.93917	0.04047	0.78649
C5	C	0.76801	0.03073	0.7643
C6	C	0.60341	0.09654	0.81289
C7	C	0.4334	0.08471	0.79236
C8	C	0.76616	0.0363	0.65682
C9	C	0.61501	0.10778	0.61289
C10	C	0.69253	0.00555	0.5536
C11	C	0.87484	0.01149	0.52999
C12	C	0.01616	0.94794	0.57754
C13	C	0.1961	0.95997	0.55864
C14	C	0.93473	0.9996	0.42259
C15	C	0.11852	0.94342	0.38336
C16	C	0.07966	0.04406	0.32551
C17	C	0.92483	0.02851	0.29487
C18	C	0.75193	0.08374	0.34046
C19	C	0.58946	0.07705	0.31318
C20	C	0.93068	0.05004	0.18709
C21	C	0.77618	0.12364	0.14439
C22	C	0.8465	0.03258	0.08341
C23	C	0.03198	0.02823	0.05836
C24	C	0.16772	0.97495	0.10741
C25	C	0.34743	0.98751	0.08851
C26	C	0.05896	0.5069	0.13567
C27	C	0.17435	0.51316	0.1853
C28	C	0.1156	0.45813	0.24533
C29	C	0.90203	0.54583	0.2574
C30	C	0.81197	0.52438	0.20274
C31	C	0.60027	0.60628	0.20983
C32	C	0.83974	0.54327	0.40535
C33	C	0.70372	0.4864	0.42605
C34	C	0.71657	0.55886	0.50036
C35	C	0.91667	0.48855	0.51897
C36	C	0.05484	0.50847	0.47138
C37	C	0.25638	0.39529	0.48248
C38	C	0.88541	0.4986	0.62724
C39	C	0.00705	0.51098	0.67397
C40	C	0.9544	0.4638	0.73649
C41	C	0.7416	0.54791	0.75164
C42	C	0.64108	0.52661	0.69995
C43	C	0.43045	0.61787	0.71239
C44	C	0.67789	0.55359	0.85881
C45	C	0.52861	0.54366	0.90397

C46	C	0.53247	0.6228	0.964
C47	C	0.72844	0.55299	0.98559
C48	C	0.8762	0.5374	0.93416
C49	C	0.07538	0.42953	0.94894
H50	H	0.01358	0.81054	0.83308
H51	H	0.90108	0.17234	0.7977
H52	H	0.80535	0.89887	0.75385
H53	H	0.5671	0.22828	0.82379
H54	H	0.46876	0.95502	0.77984
H55	H	0.39312	0.15917	0.75212
H56	H	0.25997	0.2425	0.85797
H57	H	0.79887	0.9038	0.66401
H58	H	0.58336	0.23943	0.60552
H59	H	0.72426	0.87529	0.56381
H60	H	0.84494	0.14228	0.52093
H61	H	0.04731	0.8166	0.5863
H62	H	0.16978	0.09156	0.55795
H63	H	0.24677	0.90786	0.51303
H64	H	0.34928	0.20812	0.64586
H65	H	0.56155	0.14353	0.48677
H66	H	0.88452	0.13362	0.43358
H67	H	0.17592	0.80908	0.37171
H68	H	0.0297	0.17672	0.33825
H69	H	0.97053	0.89716	0.28126
H70	H	0.71106	0.21393	0.35519
H71	H	0.62479	0.94692	0.30093
H72	H	0.56947	0.14721	0.27176
H73	H	0.32239	0.01086	0.39177
H74	H	0.30925	0.05336	0.2991
H75	H	0.40982	0.22672	0.3814
H76	H	0.97281	0.91484	0.1917
H77	H	0.74285	0.25631	0.13912
H78	H	0.86583	0.9031	0.08858
H79	H	0.00583	0.15515	0.04415
H80	H	0.20342	0.8432	0.11721
H81	H	0.317	0.12065	0.08832
H82	H	0.39914	0.93432	0.0429
H83	H	0.5061	0.22324	0.17146
H84	H	0.53933	0.96806	0.14335
H85	H	0.08946	0.37545	0.12576
H86	H	0.15047	0.64376	0.19074
H87	H	0.1589	0.32248	0.24263
H88	H	0.85692	0.68005	0.26601
H89	H	0.86334	0.39014	0.1928
H90	H	0.54255	0.73832	0.22386
H91	H	0.54877	0.54154	0.24318
H92	H	0.42912	0.48869	0.15761
H93	H	0.22012	0.42533	0.3236

H94	H	0.53358	0.68525	0.12942
H95	H	0.79913	0.67519	0.3958
H96	H	0.77105	0.35162	0.43569
H97	H	0.64679	0.69575	0.50065
H98	H	0.96365	0.35389	0.52571
H99	H	0.02736	0.63979	0.46638
H100	H	0.2632	0.2752	0.49734
H101	H	0.2926	0.45159	0.51965
H102	H	0.91202	0.36749	0.6195
H103	H	0.98191	0.64246	0.67667
H104	H	0.00357	0.32713	0.73657
H105	H	0.69667	0.68233	0.75977
H106	H	0.68301	0.39297	0.69159
H107	H	0.3862	0.74694	0.72789
H108	H	0.3828	0.55575	0.74765
H109	H	0.65523	0.6847	0.85366
H110	H	0.56427	0.41102	0.91028
H111	H	0.48879	0.75705	0.95689
H112	H	0.76062	0.42886	0.00428
H113	H	0.85875	0.66414	0.92368
H114	H	0.08948	0.30436	0.96024
H115	H	0.10694	0.48347	0.9876
H116	H	0.2442	0.50139	0.89521
H117	H	0.76299	0.99296	0.97517
H118	H	0.1857	0.02089	0.85527
H119	H	0.05613	0.01257	0.70369
H120	H	0.3848	0.94841	0.6138
H121	H	0.58769	0.1396	0.062
H122	H	0.03482	0.92395	0.97854
H123	H	0.22292	0.5363	0.07018
H124	H	0.71375	0.51876	0.31589
H125	H	0.54071	0.57072	0.56772
H126	H	0.44225	0.45221	0.42417
H127	H	0.26113	0.48721	0.655
H128	H	0.03274	0.47135	0.8167
H129	H	0.32798	0.72013	0.63694
H130	H	0.29058	0.74069	0.88024
H131	H	0.29254	0.71359	0.01199
H132	H	0.83513	0.62778	0.04947
H133	H	0.77327	0.14752	0.89808
O134	O	0.85042	0.92402	0.94134
O135	O	0.14386	0.9342	0.87001
O136	O	0.09684	0.97486	0.74362
O137	O	0.71006	0.12581	0.711
O138	O	0.66021	0.99879	0.8651
O139	O	0.28103	0.13645	0.83715
O140	O	0.4517	0.09399	0.6367
O141	O	0.55897	0.05272	0.511

O142	O	0.95667	0.91221	0.47592
O143	O	0.93278	0.04713	0.63188
O144	O	0.33506	0.87256	0.59893
O145	O	0.24055	0.97589	0.41752
O146	O	0.24389	0.9916	0.28547
O147	O	0.87336	0.13114	0.2431
O148	O	0.79825	0.97804	0.39112
O149	O	0.41852	0.13966	0.35108
O150	O	0.61183	0.108	0.16607
O151	O	0.70939	0.11474	0.04117
O152	O	0.12091	0.91186	0.00963
O153	O	0.08477	0.0751	0.1608
O154	O	0.48187	0.89896	0.12886
O155	O	0.08942	0.58467	0.0835
O156	O	0.36487	0.4134	0.16586
O157	O	0.20631	0.4989	0.28993
O158	O	0.85007	0.47334	0.30919
O159	O	0.86738	0.60046	0.15319
O160	O	0.53386	0.59204	0.1542
O161	O	0.53622	0.54962	0.40763
O162	O	0.61131	0.49247	0.53429
O163	O	0.92449	0.56579	0.57374
O164	O	0.01624	0.44727	0.41608
O165	O	0.38695	0.36241	0.43174
O166	O	0.19838	0.41138	0.65505
O167	O	0.04899	0.51357	0.77696
O168	O	0.68114	0.48186	0.80363
O169	O	0.69371	0.59598	0.64738
O170	O	0.34174	0.61832	0.65952
O171	O	0.34882	0.61557	0.88284
O172	O	0.4055	0.60505	0.00918
O173	O	0.71809	0.66812	0.03073
O174	O	0.85478	0.4586	0.88169
O175	O	0.20609	0.40805	0.89882

FS-ring contraction-cellotetraose end chain scission

C2	C	0.81036	0.01297	0.88481
C3	C	0.98088	0.92868	0.83927
C4	C	0.93694	0.0252	0.78129
C5	C	0.7557	0.0308	0.76121
C6	C	0.59455	0.10227	0.81107
C7	C	0.419	0.09674	0.79234
C8	C	0.75991	0.0436	0.65369
C9	C	0.61112	0.11913	0.60904
C10	C	0.69119	0.022	0.54959
C11	C	0.87503	0.02669	0.52829
C12	C	0.01318	0.95936	0.57628

C13	C	0.19455	0.96933	0.55903
C14	C	0.93441	0.00569	0.42045
C15	C	0.11708	0.93868	0.38089
C16	C	0.08308	0.02954	0.32114
C17	C	0.92998	0.00978	0.29149
C18	C	0.75445	0.06404	0.33596
C19	C	0.61117	0.026	0.30946
C20	C	0.92931	0.04024	0.18362
C21	C	0.77448	0.12085	0.14125
C22	C	0.843	0.03579	0.07917
C23	C	0.0248	0.03943	0.05508
C24	C	0.16292	0.97851	0.10344
C25	C	0.33999	0.99568	0.08629
C26	C	0.07946	0.51565	0.13571
C27	C	0.18584	0.5193	0.18859
C28	C	0.12404	0.46121	0.24711
C29	C	0.9118	0.53743	0.25616
C30	C	0.82894	0.52054	0.19916
C31	C	0.61779	0.60362	0.20713
C32	C	0.73193	0.60583	0.45014
C33	C	0.63939	0.5111	0.42389
C34	C	0.72316	0.58777	0.51928
C35	C	0.93248	0.4984	0.53094
C36	C	0.03728	0.5222	0.47447
C37	C	0.22797	0.37774	0.46105
C38	C	0.93319	0.49582	0.63603
C39	C	0.04098	0.51333	0.68592
C40	C	0.97485	0.46381	0.74587
C41	C	0.76063	0.54487	0.75646
C42	C	0.67421	0.52325	0.70112
C43	C	0.4638	0.61362	0.70647
C44	C	0.68397	0.54491	0.86214
C45	C	0.53087	0.53553	0.90566
C46	C	0.5249	0.62803	0.96383
C47	C	0.71615	0.56087	0.98904
C48	C	0.87391	0.53322	0.93975
C49	C	0.06641	0.42477	0.95966
H50	H	-0.00011	0.80093	0.83052
H51	H	0.91358	0.1543	0.79067
H52	H	0.78109	0.90229	0.75037
H53	H	0.56442	0.23255	0.82168
H54	H	0.45195	0.97175	0.77465
H55	H	0.36868	0.18486	0.75595
H56	H	0.25746	0.23112	0.86491
H57	H	0.79393	0.91037	0.65897
H58	H	0.58146	0.25052	0.60291
H59	H	0.72239	0.89068	0.5581
H60	H	0.84759	0.15627	0.51891

H61	H	0.0426	0.82825	0.58418
H62	H	0.17012	0.10005	0.55587
H63	H	0.25148	0.90986	0.51459
H64	H	0.35427	0.21947	0.64848
H65	H	0.62088	0.03667	0.46723
H66	H	0.88666	0.14052	0.42879
H67	H	0.16724	0.80399	0.37208
H68	H	0.03461	0.16383	0.33072
H69	H	0.98029	0.87826	0.27744
H70	H	0.6987	0.20004	0.34399
H71	H	0.65911	0.89029	0.3084
H72	H	0.59859	0.0695	0.2633
H73	H	0.32962	-0.0049	0.38634
H74	H	0.31749	0.02738	0.29384
H75	H	0.39966	0.20899	0.36085
H76	H	0.97205	0.90476	0.18572
H77	H	0.74579	0.2528	0.13785
H78	H	0.8663	0.90485	0.08212
H79	H	-0.00575	0.16977	0.04473
H80	H	0.19975	0.84531	0.10987
H81	H	0.30811	0.1289	0.08796
H82	H	0.39528	0.94581	0.04051
H83	H	0.50609	0.22828	0.16991
H84	H	0.53284	0.97348	0.14128
H85	H	0.11731	0.38446	0.12297
H86	H	0.16098	0.64926	0.19623
H87	H	0.17772	0.32412	0.24478
H88	H	0.85997	0.6713	0.26723
H89	H	0.88084	0.38731	0.18739
H90	H	0.56336	0.73323	0.22371
H91	H	0.5675	0.53609	0.23966
H92	H	0.43885	0.49799	0.15992
H93	H	0.17944	0.46894	0.33169
H94	H	0.51446	0.71272	0.13397
H95	H	0.665	0.73727	0.43764
H96	H	0.71971	0.37397	0.42499
H97	H	0.65542	0.71062	0.54179
H98	H	0.96751	0.36503	0.53562
H99	H	0.04633	0.64133	0.47732
H100	H	0.21563	0.26025	0.46244
H101	H	0.32053	0.37436	0.49497
H102	H	0.96184	0.36354	0.62972
H103	H	0.01463	0.64478	0.68991
H104	H	0.02517	0.32697	0.74443
H105	H	0.71123	0.67906	0.76605
H106	H	0.71931	0.38948	0.69197
H107	H	0.41349	0.74537	0.71936
H108	H	0.40481	0.55672	0.7405

H109	H	0.66243	0.6757	0.85782
H110	H	0.57084	0.40364	0.91498
H111	H	0.4853	0.75956	0.95287
H112	H	0.74044	0.44231	0.01073
H113	H	0.86328	0.65692	0.92767
H114	H	0.07296	0.30366	0.9732
H115	H	0.08891	0.48589	0.99831
H116	H	0.24446	0.48332	0.90496
H117	H	0.75601	0.99905	0.97136
H118	H	0.18084	0.00751	0.85258
H119	H	0.05487	-0.00395	0.69861
H120	H	0.37596	0.96661	0.61517
H121	H	0.58366	0.13932	0.05892
H122	H	0.02448	0.93932	0.97458
H123	H	0.24395	0.5519	0.07144
H124	H	0.72519	0.50806	0.31121
H125	H	0.56679	0.52786	0.57841
H126	H	0.37405	0.45751	0.40133
H127	H	0.29329	0.48832	0.65933
H128	H	0.03037	0.46679	0.82884
H129	H	0.35596	0.7162	0.63118
H130	H	0.29462	0.71946	0.87637
H131	H	0.27846	0.73187	0.00797
H132	H	0.76919	0.63029	0.06693
H133	H	0.77788	0.14563	0.89195
O134	O	0.84582	0.92784	0.93844
O135	O	0.1461	0.9144	0.86295
O136	O	0.09053	0.94537	0.73761
O137	O	0.69851	0.12933	0.7085
O138	O	0.65275	0.0031	0.86285
O139	O	0.27639	0.13233	0.83981
O140	O	0.44547	0.10758	0.631
O141	O	0.55908	0.08747	0.50652
O142	O	0.95648	0.92423	0.47486
O143	O	0.92701	0.05724	0.63071
O144	O	0.32388	0.88993	0.60265
O145	O	0.24297	0.9696	0.41383
O146	O	0.24725	0.96813	0.28135
O147	O	0.87189	0.11518	0.24064
O148	O	0.79498	0.98001	0.39182
O149	O	0.43312	0.09623	0.34271
O150	O	0.60609	0.11074	0.16166
O151	O	0.70321	0.12109	0.03801
O152	O	0.11441	0.93429	0.00346
O153	O	0.08198	0.06934	0.15879
O154	O	0.47192	0.90628	0.12745
O155	O	0.11192	0.60253	0.08699
O156	O	0.37846	0.4212	0.17163

O157	O	0.20121	0.51241	0.29287
O158	O	0.86056	0.45581	0.30461
O159	O	0.88385	0.60141	0.15074
O160	O	0.54454	0.6006	0.15163
O161	O	0.4892	0.5753	0.40207
O162	O	0.62305	0.49404	0.53692
O163	O	0.98216	0.55573	0.58262
O164	O	-0.07623	0.52693	0.42747
O165	O	0.31008	0.38369	0.40197
O166	O	0.23501	0.41283	0.67268
O167	O	0.05774	0.51132	0.79072
O168	O	0.69388	0.47507	0.80589
O169	O	0.73826	0.59281	0.6513
O170	O	0.39772	0.6029	0.64938
O171	O	0.35542	0.59583	0.88188
O172	O	0.38956	0.62213	0.00815
O173	O	0.70844	0.68209	0.03117
O174	O	0.85802	0.45013	0.88729
O175	O	0.21109	0.38874	0.91263

J. TS- ring contraction -cellotetraose mid chain scission

C2	C	0.80938	0.01676	0.88865
C3	C	0.98301	0.94409	0.84352
C4	C	0.93432	0.04654	0.78694
C5	C	0.76642	0.03333	0.76383
C6	C	0.60071	0.09905	0.81216
C7	C	0.43207	0.08695	0.79096
C8	C	0.76736	0.03839	0.65614
C9	C	0.61579	0.11054	0.61235
C10	C	0.69441	0.00935	0.55271
C11	C	0.87637	0.01634	0.52933
C12	C	0.01833	0.95411	0.57687
C13	C	0.194	0.97313	0.55683
C14	C	0.94263	0.00112	0.4216
C15	C	0.12297	0.9297	0.37944
C16	C	0.08509	0.03821	0.32349
C17	C	0.9269	0.02746	0.29312
C18	C	0.75487	0.0817	0.33883
C19	C	0.59878	0.06184	0.31191
C20	C	0.92871	0.05526	0.18591
C21	C	0.77422	0.13343	0.14338
C22	C	0.84424	0.03955	0.08286
C23	C	0.02986	0.03454	0.05767
C24	C	0.16655	0.98038	0.10649
C25	C	0.3448	0.99536	0.08736
C26	C	0.05907	0.51782	0.14105
C27	C	0.18026	0.52622	0.18831

C28	C	0.13072	0.46704	0.24878
C29	C	0.91749	0.5539	0.26418
C30	C	0.81706	0.5391	0.21132
C31	C	0.60608	0.62724	0.2218
C32	C	0.85334	0.54906	0.37099
C33	C	0.70872	0.52591	0.41499
C34	C	0.71737	0.58061	0.47896
C35	C	0.91973	0.49375	0.49521
C36	C	0.05606	0.51449	0.44765
C37	C	0.25557	0.40983	0.46329
C38	C	0.85874	0.49144	0.64336
C39	C	0.02158	0.49725	0.66212
C40	C	0.94354	0.44663	0.73782
C41	C	0.73106	0.538	0.75577
C42	C	0.61351	0.53368	0.70635
C43	C	0.40426	0.63524	0.71737
C44	C	0.67846	0.54664	0.86265
C45	C	0.52667	0.54468	0.90838
C46	C	0.53357	0.62633	0.96735
C47	C	0.73043	0.55335	0.98848
C48	C	0.87743	0.53369	0.93617
C49	C	0.07685	0.42838	0.95106
H50	H	0.01216	0.81424	0.83283
H51	H	0.89065	0.1784	0.7997
H52	H	0.80511	0.90119	0.75336
H53	H	0.56444	0.23092	0.82289
H54	H	0.46588	0.95615	0.78086
H55	H	0.39912	0.15444	0.74899
H56	H	0.2669	0.24172	0.85946
H57	H	0.80211	0.90537	0.6632
H58	H	0.58317	0.24268	0.60544
H59	H	0.72573	0.87868	0.56196
H60	H	0.84465	0.14761	0.52004
H61	H	0.05449	0.82165	0.58518
H62	H	0.16197	0.1062	0.55862
H63	H	0.23642	0.92815	0.51016
H64	H	0.34283	0.21326	0.63933
H65	H	0.56809	0.14869	0.48626
H66	H	0.90041	0.13511	0.43105
H67	H	0.15443	0.80096	0.36616
H68	H	0.03742	0.16929	0.33828
H69	H	0.97243	0.8969	0.27841
H70	H	0.70798	0.21456	0.35086
H71	H	0.64159	0.92974	0.30108
H72	H	0.57392	0.12991	0.26997
H73	H	0.32969	0.99736	0.38836
H74	H	0.31258	0.04916	0.29635
H75	H	0.40452	0.22725	0.36951

H76	H	0.96822	0.92023	0.18947
H77	H	0.74696	0.26473	0.1379
H78	H	0.8633	0.91035	0.08888
H79	H	0.00404	0.16148	0.04357
H80	H	0.20348	0.84811	0.11569
H81	H	0.31156	0.12908	0.08624
H82	H	0.39749	0.94021	0.04205
H83	H	0.50407	0.24339	0.17033
H84	H	0.5302	0.98533	0.14359
H85	H	0.08551	0.38647	0.13307
H86	H	0.15242	0.65773	0.19419
H87	H	0.17395	0.33126	0.24519
H88	H	0.87515	0.68702	0.27412
H89	H	0.86125	0.406	0.20093
H90	H	0.55694	0.75859	0.23546
H91	H	0.55678	0.56654	0.25712
H92	H	0.435	0.50919	0.16542
H93	H	0.19636	0.46979	0.33066
H94	H	0.52339	0.71378	0.14295
H95	H	0.82625	0.68177	0.36919
H96	H	0.74876	0.39117	0.41497
H97	H	0.66864	0.71705	0.48104
H98	H	0.95751	0.35915	0.49829
H99	H	0.02482	0.64726	0.44463
H100	H	0.26953	0.28638	0.47685
H101	H	0.28452	0.46866	0.50134
H102	H	0.87566	0.36749	0.62939
H103	H	0.01138	0.61941	0.67634
H104	H	0.99773	0.31036	0.73639
H105	H	0.69754	0.66983	0.76476
H106	H	0.64681	0.40494	0.6928
H107	H	0.36959	0.75847	0.7372
H108	H	0.35265	0.56885	0.7499
H109	H	0.66	0.676	0.85554
H110	H	0.55782	0.41355	0.91619
H111	H	0.49381	0.75952	0.95901
H112	H	0.75999	0.42975	0.00726
H113	H	0.85988	0.65954	0.92397
H114	H	0.09316	0.3029	0.96282
H115	H	0.10761	0.4841	0.98946
H116	H	0.2444	0.50172	0.89783
H117	H	0.76078	0.99484	0.97496
H118	H	0.18061	0.02661	0.85443
H119	H	0.05079	0.01705	0.7038
H120	H	0.38919	0.96012	0.60909
H121	H	0.58613	0.14542	0.06143
H122	H	0.03109	0.92981	0.9781
H123	H	0.22061	0.5491	0.07569

H124	H	0.45582	0.72275	0.40462
H125	H	0.54502	0.61619	0.5515
H126	H	0.42515	0.47714	0.40864
H127	H	0.05715	0.48585	0.56665
H128	H	0.07786	0.43019	0.8079
H129	H	0.32894	0.73863	0.64042
H130	H	0.29149	0.74276	0.88298
H131	H	0.29063	0.72124	0.01329
H132	H	0.8436	0.62567	0.05096
H133	H	0.76969	0.15016	0.8982
O134	O	0.84716	0.92585	0.94094
O135	O	0.14084	0.9396	0.86974
O136	O	0.092	0.98946	0.74429
O137	O	0.71043	0.12785	0.71042
O138	O	0.65688	0.00179	0.86458
O139	O	0.27219	0.14902	0.83354
O140	O	0.45293	0.09754	0.63616
O141	O	0.55975	0.05984	0.51003
O142	O	0.96181	0.91662	0.47524
O143	O	0.93349	0.05128	0.63153
O144	O	0.34406	0.88166	0.59274
O145	O	0.27789	0.92502	0.40835
O146	O	0.24619	0.98801	0.2828
O147	O	0.87348	0.13336	0.24255
O148	O	0.80042	0.98423	0.39155
O149	O	0.42892	0.11827	0.35042
O150	O	0.60547	0.12517	0.16476
O151	O	0.70774	0.11949	0.04031
O152	O	0.11795	0.91858	0.00878
O153	O	0.08417	0.07884	0.16023
O154	O	0.48065	0.91134	0.12785
O155	O	0.08645	0.59002	0.08702
O156	O	0.36974	0.43284	0.1662
O157	O	0.22977	0.5043	0.2913
O158	O	0.85486	0.48471	0.31485
O159	O	0.86964	0.61418	0.16075
O160	O	0.52833	0.61862	0.16784
O161	O	0.52683	0.60065	0.39513
O162	O	0.59969	0.53401	0.51843
O163	O	0.93439	0.55889	0.55117
O164	O	0.03629	0.45255	0.39121
O165	O	0.39201	0.38137	0.41415
O166	O	0.18028	0.39005	0.63464
O167	O	0.04226	0.50167	0.77306
O168	O	0.67644	0.47214	0.80844
O169	O	0.68596	0.60751	0.65715
O170	O	0.31698	0.64869	0.66406
O171	O	0.34678	0.61863	0.88705

O172	O	0.40476	0.61396	0.01299
O173	O	0.72506	0.66744	0.03304
O174	O	0.85393	0.45047	0.88543
O175	O	0.20784	0.40749	0.90086

FS- ring contraction -cellotetraose mid chain scission

C2	C	0.80727	0.00205	0.88655
C3	C	0.98159	0.92457	0.84213
C4	C	0.93546	0.02214	0.78461
C5	C	0.76865	0.00939	0.76077
C6	C	0.60202	0.07871	0.80917
C7	C	0.43061	0.06876	0.78949
C8	C	0.78105	0.02511	0.65232
C9	C	0.63288	0.10698	0.60829
C10	C	0.70909	0.02253	0.54675
C11	C	0.89083	0.03179	0.52669
C12	C	0.03276	0.96034	0.5737
C13	C	0.20341	0.98857	0.55597
C14	C	0.9536	0.01501	0.41884
C15	C	0.12977	0.93826	0.37543
C16	C	0.09001	0.04311	0.3188
C17	C	0.9302	0.03027	0.29043
C18	C	0.75823	0.08515	0.33664
C19	C	0.60935	0.0502	0.31199
C20	C	0.92828	0.06105	0.18336
C21	C	0.77308	0.13796	0.14102
C22	C	0.84439	0.04549	0.08028
C23	C	0.02775	0.0443	0.0552
C24	C	0.16447	0.99123	0.10419
C25	C	0.3432	0.00535	0.08593
C26	C	0.06056	0.51471	0.13998
C27	C	0.18055	0.52626	0.18702
C28	C	0.13059	0.46834	0.24781
C29	C	0.91753	0.55223	0.263
C30	C	0.81681	0.53835	0.21007
C31	C	0.60632	0.62879	0.22034
C32	C	0.85355	0.54685	0.36957
C33	C	0.70653	0.53031	0.41388
C34	C	0.71194	0.59613	0.47617
C35	C	0.9123	0.52144	0.49479
C36	C	0.05427	0.52276	0.44486
C37	C	0.25485	0.41769	0.45879
C38	C	0.92899	0.42036	0.6859
C39	C	0.06123	0.48323	0.65689
C40	C	0.90847	0.44065	0.75507
C41	C	0.69365	0.53233	0.7683
C42	C	0.61496	0.51485	0.71088

C43	C	0.42336	0.65456	0.70581
C44	C	0.63006	0.54441	0.87196
C45	C	0.49323	0.54121	0.9226
C46	C	0.51996	0.62638	0.97764
C47	C	0.72262	0.55235	0.99327
C48	C	0.85232	0.5317	0.93587
C49	C	0.05836	0.43178	0.94223
H50	H	0.00902	0.79473	0.8328
H51	H	0.8889	0.15488	0.79671
H52	H	0.80518	0.8783	0.74974
H53	H	0.56843	0.21035	0.81881
H54	H	0.46193	0.93922	0.77858
H55	H	0.39255	0.13929	0.74824
H56	H	0.24956	0.23754	0.85155
H57	H	0.81477	0.8915	0.65604
H58	H	0.59768	0.24064	0.60638
H59	H	0.74152	0.8897	0.55072
H60	H	0.86079	0.1628	0.51857
H61	H	0.07368	0.82551	0.57633
H62	H	0.17099	0.11832	0.56747
H63	H	0.23471	0.97022	0.50723
H64	H	0.36141	0.19667	0.62874
H65	H	0.62818	0.0596	0.46529
H66	H	0.91341	0.14869	0.42686
H67	H	0.15646	0.80995	0.36357
H68	H	0.04439	0.17473	0.33201
H69	H	0.97688	0.89969	0.27575
H70	H	0.70516	0.22024	0.34528
H71	H	0.65455	0.91496	0.30984
H72	H	0.59301	0.09629	0.26616
H73	H	0.33674	0.0061	0.38317
H74	H	0.31779	0.04985	0.28838
H75	H	0.41158	0.23143	0.36551
H76	H	0.97208	0.92546	0.18621
H77	H	0.74294	0.26998	0.13595
H78	H	0.86744	0.91516	0.08612
H79	H	0.00008	0.17148	0.04103
H80	H	0.20181	0.85913	0.11347
H81	H	0.31268	0.1384	0.08661
H82	H	0.3948	0.95463	0.04
H83	H	0.50398	0.24431	0.16899
H84	H	0.53343	-0.01413	0.14119
H85	H	0.0863	0.38349	0.13346
H86	H	0.15192	0.65788	0.19245
H87	H	0.1778	0.3321	0.24475
H88	H	0.8738	0.68519	0.27328
H89	H	0.8595	0.40577	0.19973
H90	H	0.5595	0.75988	0.23375

H91	H	0.55501	0.5701	0.25584
H92	H	0.43524	0.51015	0.16446
H93	H	0.2045	0.46835	0.32924
H94	H	0.52278	0.71507	0.14124
H95	H	0.83004	0.67836	0.36695
H96	H	0.74391	0.39666	0.41711
H97	H	0.66005	0.73289	0.47482
H98	H	0.9494	0.39115	0.50692
H99	H	0.02871	0.65275	0.43699
H100	H	0.27235	0.29399	0.47309
H101	H	0.29318	0.47427	0.49524
H102	H	0.97542	0.2892	0.67236
H103	H	0.02179	0.6175	0.66328
H104	H	-0.03444	0.31833	0.7755
H105	H	0.65901	0.66492	0.7759
H106	H	0.61183	0.39326	0.70817
H107	H	0.43131	0.77436	0.70737
H108	H	0.33563	0.65254	0.74608
H109	H	0.60958	0.67458	0.86553
H110	H	0.52434	0.41116	0.93246
H111	H	0.48323	0.75704	0.96584
H112	H	0.75734	0.43019	0.01387
H113	H	0.82685	0.65822	0.92183
H114	H	0.08827	0.30331	0.95445
H115	H	0.10261	0.48821	0.97708
H116	H	0.22379	0.50221	0.89034
H117	H	0.75742	0.98863	0.97332
H118	H	0.18004	0.00732	0.85267
H119	H	0.05724	-0.00446	0.70258
H120	H	0.41893	0.94591	0.60218
H121	H	0.58653	0.14699	0.05925
H122	H	0.02962	0.93194	0.97721
H123	H	0.22126	0.54986	0.07406
H124	H	0.45622	0.72642	0.40115
H125	H	0.54558	0.63706	0.54973
H126	H	0.4238	0.48266	0.4031
H127	H	0.03709	0.56066	0.55974
H128	H	0.03849	0.49865	0.8148
H129	H	0.34368	0.72847	0.62719
H130	H	0.26473	0.73616	0.89309
H131	H	0.27974	0.72955	0.02254
H132	H	0.85535	0.62435	0.04899
H133	H	0.76741	0.13608	0.89419
O134	O	0.84372	0.91653	0.94005
O135	O	0.13959	0.92078	0.86782
O136	O	0.09518	0.96369	0.74324
O137	O	0.71618	0.10716	0.70778
O138	O	0.6565	0.98432	0.86236

O139	O	0.27768	0.12584	0.83432
O140	O	0.47121	0.08677	0.63011
O141	O	0.57104	0.10037	0.50596
O142	O	0.97793	0.93239	0.47252
O143	O	0.94868	0.04072	0.63129
O144	O	0.36363	0.8773	0.58453
O145	O	0.28783	0.93086	0.40292
O146	O	0.24848	0.98935	0.27692
O147	O	0.87077	0.13688	0.2403
O148	O	0.80502	-0.00215	0.39181
O149	O	0.43345	0.12153	0.34709
O150	O	0.60646	0.12654	0.16251
O151	O	0.70718	0.12238	0.03771
O152	O	0.11748	0.92778	0.00648
O153	O	0.08069	0.08939	0.15791
O154	O	0.4778	0.91603	0.12612
O155	O	0.08781	0.58229	0.08485
O156	O	0.37057	0.43312	0.16576
O157	O	0.2267	0.51032	0.29003
O158	O	0.85555	0.48186	0.31347
O159	O	0.87081	0.61233	0.15951
O160	O	0.52788	0.62054	0.16645
O161	O	0.52634	0.60375	0.39284
O162	O	0.59421	0.5543	0.51675
O163	O	0.91313	0.6153	0.54567
O164	O	0.03294	0.44969	0.39102
O165	O	0.38016	0.39306	0.40663
O166	O	0.20406	0.3951	0.62552
O167	O	0.00275	0.53281	0.77389
O168	O	0.61312	0.47807	0.81818
O169	O	0.74935	0.52208	0.66523
O170	O	0.34041	0.64091	0.65397
O171	O	0.30504	0.62007	0.90853
O172	O	0.39659	0.62739	0.02761
O173	O	0.7324	0.66842	0.03367
O174	O	0.81342	0.44691	0.88903
O175	O	0.16199	0.42578	0.88594

K. TS- ring contraction -cellobiose end-mid chain scission

C2	C	0.25828	0.29235	0.51335
C3	C	0.04403	0.59457	0.98258
C4	C	0.27223	0.17611	0.47718
C5	C	0.16988	0.61593	0.10511
C6	C	0.33863	0.13102	0.71994
C7	C	0.23065	0.51124	0.15897
C8	C	0.45901	0.18803	0.77173
C9	C	0.14983	0.43705	0.31458

C10	C	0.43993	0.3051	0.77333
C11	C	0.01746	0.43663	0.21212
C12	C	0.55935	0.36463	0.78398
C13	C	0.93206	0.38471	0.4062
C14	C	0.7391	0.76269	0.47048
C15	C	0.96109	0.11677	0.0091
C16	C	0.72747	0.65958	0.56118
C17	C	0.83228	0.12344	0.89406
C18	C	0.66742	0.62223	0.24932
C19	C	0.77909	0.01524	0.86507
C20	C	0.5477	0.68024	0.20125
C21	C	0.86792	0.9369	0.74848
C22	C	0.56965	0.79689	0.20533
C23	C	0.9995	0.94649	0.84702
C24	C	0.45386	0.86067	0.2067
C25	C	0.08627	0.8859	0.67234
H26	H	0.20741	0.31088	0.69543
H27	H	0.05542	0.54317	0.80886
H28	H	0.90685	0.64702	0.76843
H29	H	0.32987	0.1646	0.30347
H30	H	0.11561	0.11163	0.58718
H31	H	0.15847	0.65719	0.29407
H32	H	0.32964	0.66246	0.95243
H33	H	0.27983	0.13909	0.89408
H34	H	0.30094	0.97766	0.73827
H35	H	0.24659	0.47547	0.96292
H36	H	0.37083	0.46465	0.37838
H37	H	0.52154	0.16799	0.61028
H38	H	0.50335	0.08322	0.04421
H39	H	0.1528	0.45993	0.52454
H40	H	0.38349	0.32665	0.94377
H41	H	0.01378	0.39524	0.02125
H42	H	0.62216	0.33481	0.63414
H43	H	0.57592	0.48952	0.56797
H44	H	0.96952	0.30969	0.4659
H45	H	0.80441	0.3081	0.19779
H46	H	0.60196	0.35399	0.97964
H47	H	0.92392	0.43365	0.58185
H48	H	0.81584	0.78698	0.34805
H49	H	0.95976	0.08118	0.20794
H50	H	0.07929	0.21001	0.15303
H51	H	0.64329	0.65105	0.67679
H52	H	0.88786	0.78809	0.86388
H53	H	0.83651	0.15989	0.69688
H54	H	0.67282	0.1725	0.03968
H55	H	0.73753	0.63528	0.10011
H56	H	0.72231	0.47505	0.27341
H57	H	0.75606	0.98838	0.06654

H58	H	0.6443	0.95716	0.64277
H59	H	0.48489	0.65973	0.36134
H60	H	0.50425	0.57944	0.91695
H61	H	0.86625	0.94723	0.53112
H62	H	0.62778	0.81994	0.0399
H63	H	0.007	0.91754	0.05253
H64	H	0.39269	0.83226	0.3616
H65	H	0.43861	0.98964	0.4094
H66	H	0.04794	0.80936	0.63248
H67	H	0.2152	0.80272	0.85132
H68	H	0.40823	0.8493	0.014
H69	H	0.09525	0.92745	0.48362
O70	O	0.19956	0.33353	0.29028
O71	O	0.97869	0.6803	0.90453
O72	O	0.15881	0.12755	0.4215
O73	O	0.24103	0.67606	0.92582
O74	O	0.36761	0.02475	0.6841
O75	O	0.34313	0.52871	0.2924
O76	O	0.51215	0.15878	0.02097
O77	O	0.37803	0.33531	0.53237
O78	O	0.97611	0.53967	0.17814
O79	O	0.53771	0.47123	0.73881
O80	O	0.81143	0.3727	0.30101
O81	O	0.82109	0.83653	0.81163
O82	O	0.01504	0.21226	0.01428
O83	O	0.82107	0.6011	0.62869
O84	O	0.76181	0.18415	0.07037
O85	O	0.64599	0.51838	0.28381
O86	O	0.67214	0.02453	0.70526
O87	O	0.49269	0.65468	0.952
O88	O	0.63599	0.81933	0.45438
O89	O	0.03474	0.0521	0.84109
O90	O	0.48067	0.96655	0.24588
O91	O	0.20374	0.87563	0.79157

FS- ring contraction -cellobiose end-mid chain scission

C2	C	0.25862	0.30184	0.54036
C3	C	0.05612	0.61734	0.03957
C4	C	0.27384	0.18586	0.49897
C5	C	0.1867	0.62693	0.13786
C6	C	0.33567	0.14032	0.74746
C7	C	0.24008	0.51893	0.17506
C8	C	0.45696	0.19592	0.79482
C9	C	0.15662	0.44896	0.33699
C10	C	0.44053	0.31286	0.80351
C11	C	0.02444	0.4533	0.23441
C12	C	0.56215	0.36892	0.80934

C13	C	0.93521	0.39855	0.41384
C14	C	0.74548	0.70591	0.30227
C15	C	0.96695	0.13251	0.99541
C16	C	0.75436	0.69296	0.59486
C17	C	0.8449	0.14998	0.85588
C18	C	0.66187	0.6228	0.17823
C19	C	0.78698	0.04818	0.77618
C20	C	0.53891	0.67787	0.14882
C21	C	0.87782	0.97513	0.64529
C22	C	0.56525	0.79323	0.16092
C23	C	0.99582	0.96441	0.80496
C24	C	0.48362	0.84771	0.35483
C25	C	0.09127	0.90042	0.6643
H26	H	0.20595	0.31875	0.72065
H27	H	0.05343	0.57877	0.84413
H28	H	0.9365	0.70851	0.89676
H29	H	0.33593	0.17615	0.33185
H30	H	0.11633	0.11916	0.58927
H31	H	0.18672	0.66593	0.3318
H32	H	0.33811	0.67019	0.93747
H33	H	0.27562	0.15074	0.91825
H34	H	0.29647	0.98581	0.77451
H35	H	0.24792	0.48343	0.97622
H36	H	0.37725	0.46386	0.39099
H37	H	0.51703	0.17726	0.62848
H38	H	0.50633	0.08841	0.05069
H39	H	0.16042	0.47359	0.5455
H40	H	0.38616	0.33484	0.97648
H41	H	0.01985	0.41783	0.03592
H42	H	0.62304	0.33562	0.6611
H43	H	0.58425	0.49563	0.5876
H44	H	0.97226	0.32359	0.47376
H45	H	0.81191	0.3221	0.18889
H46	H	0.60425	0.35878	0.00563
H47	H	0.92277	0.44584	0.59139
H48	H	0.83783	0.70221	0.22463
H49	H	0.95229	0.09389	0.18685
H50	H	0.08628	0.21478	0.17437
H51	H	0.6846	0.73331	0.7128
H52	H	0.76935	0.876	0.45864
H53	H	0.86064	0.19523	0.67478
H54	H	0.6846	0.18487	0.02407
H55	H	0.6977	0.60371	0.98422
H56	H	0.72188	0.48244	0.29092
H57	H	0.75383	0.00906	0.95609
H58	H	0.64159	0.01115	0.54628
H59	H	0.48106	0.65411	0.31397
H60	H	0.49124	0.57842	0.87148

H61	H	0.90058	0.00727	0.45003
H62	H	0.55351	0.82858	0.96478
H63	H	0.97789	0.92998	0.00017
H64	H	0.49305	0.81171	0.55164
H65	H	0.45212	0.98718	0.48816
H66	H	0.05277	0.82487	0.61707
H67	H	0.21153	0.81689	0.87599
H68	H	0.38866	0.83603	0.28686
H69	H	0.1151	0.93846	0.4773
O70	O	0.20231	0.34443	0.31642
O71	O	0.0056	0.71525	0.02131
O72	O	0.16229	0.1382	0.42754
O73	O	0.2487	0.68787	0.94784
O74	O	0.36386	0.03359	0.7216
O75	O	0.35648	0.52777	0.29552
O76	O	0.51507	0.1634	0.03729
O77	O	0.37792	0.34518	0.56585
O78	O	0.98692	0.55832	0.22268
O79	O	0.54631	0.47538	0.75859
O80	O	0.81755	0.38652	0.29443
O81	O	0.82449	0.87684	0.61493
O82	O	0.02685	0.22495	0.02707
O83	O	0.83164	0.63765	0.69865
O84	O	0.77068	0.20753	0.03278
O85	O	0.65249	0.53069	0.32548
O86	O	0.68895	0.07241	0.60093
O87	O	0.47909	0.65417	0.90413
O88	O	0.69348	0.80355	0.22957
O89	O	0.04463	0.06635	0.84154
O90	O	0.51215	0.95482	0.36565
O91	O	0.19958	0.89011	0.82249

L. TS- ring contraction -cellulose mid chain scission

C2	C	0.01424	0.96477	0.06403
C3	C	0.97298	0.81739	0.97481
C4	C	0.03685	0.85449	0.83908
C5	C	0.97591	0.01673	0.79498
C6	C	0.02681	0.15543	0.89146
C7	C	0.95427	0.31572	0.85746
C8	C	0.51103	0.4345	0.2706
C9	C	0.43106	0.29386	0.20195
C10	C	0.58813	0.38478	0.06974
C11	C	0.51963	0.54241	0.03097
C12	C	0.54818	0.66997	0.13747
C13	C	0.45394	0.82015	0.11583
C14	C	0.96314	0.02962	0.5639
C15	C	0.9914	0.1798	0.47542

C16	C	0.92548	0.13901	0.34043
C17	C	0.99685	0.98235	0.29469
C18	C	0.95852	0.84201	0.39192
C19	C	0.03711	0.68563	0.3566
C20	C	0.49203	0.56505	0.80675
C21	C	0.52124	0.69779	0.70459
C22	C	0.42904	0.63906	0.58034
C23	C	0.48243	0.46924	0.54702
C24	C	0.44685	0.34681	0.65728
C25	C	0.50845	0.18062	0.63139
H26	H	0.62243	0.48131	0.52478
H27	H	0.15519	0.98792	0.08372
H28	H	0.83024	0.796	0.97124
H29	H	0.17869	0.86375	0.83257
H30	H	0.83303	0.00102	0.78647
H31	H	0.17012	0.1777	0.89668
H32	H	0.95342	0.38923	0.946
H33	H	0.81991	0.2875	0.82412
H34	H	0.63954	0.43058	0.31325
H35	H	0.3124	0.32055	0.14795
H36	H	0.72269	0.39803	0.10356
H37	H	0.37831	0.51758	0.01628
H38	H	0.68601	0.70321	0.15926
H39	H	0.46435	0.89683	0.2027
H40	H	0.3165	0.77675	0.09826
H41	H	0.99623	0.64922	0.10918
H42	H	0.85312	0.68861	0.77783
H43	H	0.03709	0.52546	0.77006
H44	H	0.39294	0.27813	0.44152
H45	H	0.54469	0.29767	0.89628
H46	H	0.53659	0.0323	0.03212
H47	H	0.82288	0.99573	0.58265
H48	H	0.13252	0.21128	0.47041
H49	H	0.78286	0.12147	0.33729
H50	H	0.13926	0.00751	0.28381
H51	H	0.81638	0.81217	0.40175
H52	H	0.04406	0.61365	0.44549
H53	H	0.16963	0.71764	0.31964
H54	H	0.35273	0.5456	0.83151
H55	H	0.661	0.72044	0.68108
H56	H	0.28763	0.62857	0.59596
H57	H	0.30785	0.33222	0.68126
H58	H	0.48287	0.10229	0.71649
H59	H	0.64861	0.19882	0.61179
H60	H	0.96954	0.34777	0.60802
H61	H	0.09497	0.27229	0.22908
H62	H	0.95006	0.47262	0.2749
H63	H	0.49293	0.85933	0.84402

H64	H	0.45444	0.70909	0.39804
H65	H	0.4337	0.99579	0.50918
O66	O	0.04463	0.6768	0.02159
O67	O	0.97469	0.71905	0.75562
O68	O	0.05212	0.07404	0.67691
O69	O	0.95449	0.1098	0.01382
O70	O	0.05612	0.40771	0.76083
O71	O	0.4522	0.14633	0.23057
O72	O	0.5559	0.25323	0.98508
O73	O	0.59261	0.61338	0.91321
O74	O	0.46092	0.58751	0.24876
O75	O	0.52488	0.9147	0.00874
O76	O	0.91061	0.31358	0.52539
O77	O	0.97482	0.27547	0.25522
O78	O	0.92108	0.9242	0.17631
O79	O	0.03555	0.8927	0.51172
O80	O	0.93315	0.59076	0.2633
O81	O	0.45841	0.84136	0.75175
O82	O	0.47862	0.7597	0.48326
O83	O	0.3853	0.40122	0.43773
O84	O	0.54648	0.4118	0.7655
O85	O	0.41452	0.11119	0.52261

FS- ring contraction -cellulose mid chain scission

C2	C	0.02437	0.96347	0.07641
C3	C	0.98319	0.81996	0.98446
C4	C	0.04241	0.85617	0.84754
C5	C	0.98571	0.02128	0.80513
C6	C	0.04255	0.15894	0.90172
C7	C	0.97245	0.32173	0.8719
C8	C	0.54448	0.41454	0.21096
C9	C	0.3766	0.30372	0.22141
C10	C	0.60615	0.41688	0.06984
C11	C	0.52965	0.56838	0.0217
C12	C	0.56678	0.68788	0.13173
C13	C	0.45941	0.83109	0.13191
C14	C	0.96511	0.02829	0.57394
C15	C	0.98372	0.17703	0.483
C16	C	0.90764	0.12668	0.35272
C17	C	0.99152	0.97686	0.30743
C18	C	0.95837	0.8356	0.40371
C19	C	0.04141	0.68113	0.36984
C20	C	0.50026	0.56511	0.79695
C21	C	0.5292	0.69014	0.68989
C22	C	0.43564	0.62672	0.56834
C23	C	0.4815	0.4538	0.53811
C24	C	0.45584	0.34129	0.65596

C25	C	0.51497	0.17166	0.63966
H26	H	0.61735	0.46061	0.50487
H27	H	0.16315	0.98546	0.10043
H28	H	0.84031	0.80027	0.98096
H29	H	0.18343	0.86013	0.83704
H30	H	0.84281	0.00926	0.79916
H31	H	0.18547	0.17713	0.90768
H32	H	0.98725	0.39742	0.95967
H33	H	0.83355	0.29574	0.84968
H34	H	0.64085	0.37299	0.2768
H35	H	0.25652	0.36416	0.21219
H36	H	0.74841	0.43982	0.06594
H37	H	0.38794	0.53978	0.01215
H38	H	0.70496	0.73191	0.13895
H39	H	0.4903	0.90839	0.21698
H40	H	0.32187	0.78107	0.13585
H41	H	0.00882	0.65105	0.11921
H42	H	0.85185	0.68907	0.80095
H43	H	0.03869	0.52686	0.77542
H44	H	0.3834	0.26303	0.44436
H45	H	0.556	0.29792	0.90926
H46	H	0.51544	0.04243	0.03754
H47	H	0.82669	0.99213	0.59695
H48	H	0.12289	0.21481	0.47094
H49	H	0.76604	0.09501	0.36112
H50	H	0.13206	0.01065	0.29869
H51	H	0.81748	0.80251	0.41702
H52	H	0.03834	0.60488	0.45711
H53	H	0.1776	0.71537	0.34256
H54	H	0.36128	0.54533	0.82222
H55	H	0.66895	0.71248	0.6674
H56	H	0.29469	0.61863	0.58566
H57	H	0.3178	0.33104	0.6824
H58	H	0.45143	0.0905	0.71323
H59	H	0.65617	0.18437	0.65353
H60	H	0.96528	0.34547	0.61494
H61	H	0.93558	0.21873	0.17497
H62	H	0.95234	0.47117	0.28329
H63	H	0.49736	0.85448	0.82411
H64	H	0.48705	0.68127	0.38592
H65	H	0.45403	0.9865	0.51623
O66	O	0.05286	0.67806	0.02974
O67	O	0.96835	0.72177	0.76727
O68	O	0.05862	0.0763	0.68517
O69	O	0.96905	0.11262	0.02527
O70	O	0.06127	0.40989	0.76798
O71	O	0.37286	0.1544	0.23069
O72	O	0.54556	0.27053	0.00229

O73	O	0.59875	0.62838	0.90166
O74	O	0.51655	0.58245	0.24048
O75	O	0.49217	0.92513	0.01602
O76	O	0.90182	0.30893	0.53497
O77	O	0.94284	0.26139	0.26414
O78	O	0.92244	0.92364	0.18469
O79	O	0.03888	0.89203	0.52178
O80	O	0.94938	0.59048	0.26827
O81	O	0.465	0.83636	0.73273
O82	O	0.48262	0.74244	0.46797
O83	O	0.3642	0.38132	0.44239
O84	O	0.55764	0.4114	0.76309
O85	O	0.47367	0.107	0.5141